

8-2012

## Targeting AKT/mTOR Signaling Pathways During Murine Skin Tumor Promotion and the Impact of Dietary Energy Balance Manipulation

Laura A. Checkley

Follow this and additional works at: [https://digitalcommons.library.tmc.edu/utgsbs\\_dissertations](https://digitalcommons.library.tmc.edu/utgsbs_dissertations)



Part of the [Laboratory and Basic Science Research Commons](#), and the [Nutrition Commons](#)

### Recommended Citation

Checkley, Laura A., "Targeting AKT/mTOR Signaling Pathways During Murine Skin Tumor Promotion and the Impact of Dietary Energy Balance Manipulation" (2012). *The University of Texas MD Anderson Cancer Center UTHealth Graduate School of Biomedical Sciences Dissertations and Theses (Open Access)*. 290. [https://digitalcommons.library.tmc.edu/utgsbs\\_dissertations/290](https://digitalcommons.library.tmc.edu/utgsbs_dissertations/290)

This Dissertation (PhD) is brought to you for free and open access by the The University of Texas MD Anderson Cancer Center UTHealth Graduate School of Biomedical Sciences at DigitalCommons@TMC. It has been accepted for inclusion in The University of Texas MD Anderson Cancer Center UTHealth Graduate School of Biomedical Sciences Dissertations and Theses (Open Access) by an authorized administrator of DigitalCommons@TMC. For more information, please contact [digitalcommons@library.tmc.edu](mailto:digitalcommons@library.tmc.edu).

TARGETING AKT/mTOR SIGNALING PATHWAYS DURING MURINE SKIN TUMOR  
PROMOTION AND THE IMPACT OF DIETARY ENERGY BALANCE MANIPULATION

By

Laura Allyson Checkley, B.S.

APPROVED:

---

John DiGiovanni, Ph.D.  
Supervisory Professor

---

Ellen Richie, Ph.D.

---

Gary Johanning, Ph.D.

---

Karen Vasquez, Ph.D.

---

Rick Wood, Ph.D.

APPROVED:

---

Dean, The University of Texas  
Graduate School of Biomedical Sciences at Houston

TARGETING AKT/mTOR SIGNALING PATHWAYS DURING MURINE SKIN TUMOR  
PROMOTION AND THE IMPACT OF DIETARY ENERGY BALANCE MANIPULATION

A

DISSERTATION

Presented to the Faculty of  
The University of Texas  
Health Science Center at Houston  
and  
The University of Texas  
M.D. Anderson Cancer Center  
Graduate School of Biomedical Sciences

in Partial Fulfillment

of the Requirements

for the Degree of

DOCTOR OF PHILOSOPHY

By

Laura Allyson Checkley, B.S.  
Houston, TX

August, 2012

## **Dedication**

I dedicate this to my wonderful husband TJ who has stood by my side for the past four and a half years. You have kept me motivated and encouraged through the ups and downs of graduate school. I appreciate all the rides you have given me to the lab, animal facility, and library, food on days in the lab when I didn't have time to get lunch and your infinite ability to listen. Thanks for all your love and support.

## **Acknowledgements**

First and foremost, I would like to express my deepest gratitude to my mentor, Dr. John DiGiovanni for taking me on as a graduate student and allowing me the opportunity to work on such an exciting project. Throughout my time in graduate school, he has given me so many wonderful opportunities to work on manuscripts, attend meetings and present our work. He has been a true inspiration to me and encouraged me in my scientific endeavors. I would not be where I am today without him.

I would also like to thank my committee members, both past and present, Dr. Ellen Richie, Dr. Gary Johanning, Dr. Karen Vasquez, Dr. Rick Wood, Dr. Stephen Hursting, and Dr. Sue Fischer for all their helpful scientific suggestions and all of the time they dedicated to attend my meetings. I would also like to thank Becky Brooks, Lauren Pascale, and Linda Beltran for all of their help with the administrative aspects of graduate school.

Special thanks to the members of the DiGiovanni Lab. I am very grateful for the training provided by Steve Carbajal and Tricia Moore in the early stages of my graduate studies. In addition, I offer much thanks to lab member Okkyung Rho. She has provided me with many valuable discussions regarding my research and offered many helpful suggestions in addition to being a wonderful friend. I would also like to thank my “support team” in the lab, Ron Bozeman and Dharanija Rao, two of my GSBS fellow graduate students and desk mates. Throughout the ups and downs of lab life and graduate school they have provided help when needed with experiments as well as much needed break time and laughs. I would also like to thank Jiyeon Cho, Everardo Macias, Alex McClellan, and Jorge Blando for their technical support in the lab and friendship. I have enjoyed the days spent in the lab with this great group of scientists.

# TARGETING AKT/mTOR SIGNALING PATHWAYS DURING MURINE SKIN TUMOR PROMOTION AND THE IMPACT OF DIETARY ENERGY BALANCE MANIPULATION

Publication Number: \_\_\_\_\_

Allyson Checkley, B.S.

Supervisory Professor: John DiGiovanni, Ph.D.

The prevalence of obesity has continued to rise over the last several decades in the United States lending to overall increases in risk for chronic diseases including many types of cancer. In contrast, reduction in energy consumption via calorie restriction (CR) has been shown to be a potent inhibitor of carcinogenesis across a broad range of species and tumor types. Previous data has demonstrated differential signaling through Akt and mTOR via the IGF-1R and other growth factor receptors across the diet-induced obesity (DIO)/CR spectrum. Furthermore, mTORC1 is known to be regulated directly via nutrient availability, supporting its role in the link between epithelial carcinogenesis and diet-induced obesity. In an effort to better understand the importance of mTORC1 in the context of both positive and negative energy balance during epithelial carcinogenesis, the use of specific pharmacological inhibitors, rapamycin (mTORC1 inhibitor) and metformin (AMPK activator) was employed to target mTORC1 or various components of this pathway during skin tumor promotion. Two-stage skin carcinogenesis studies demonstrated that mTORC1 inhibition via rapamycin, metformin or combination treatments greatly inhibited skin tumor development in normal, overweight and obese mice. Furthermore, mechanisms by which these chemopreventive agents may be exerting their anti-tumor effects were explored. In addition, the effect of these compounds on the epidermal proliferative response was analyzed and drastic decreases in epidermal hyperproliferation and hyperplasia were found. Rapamycin also inhibited dermal inflammatory cell infiltration in a dose-dependent

manner. Both compounds also blocked or attenuated TPA-induced signaling through epidermal mTORC1 as well as several downstream targets. In addition, inhibition of this pathway by metformin appeared to be, at least in part, dependent on AMPK activation in the skin.

Overall, the data indicate that pharmacological strategies targeting this pathway offset the tumor-enhancing effects of DIO and may serve as possible CR mimetics. They suggest that mTORC1 contributes significantly to the process of skin tumor promotion, specifically during dietary energy balance effects. Exploiting the mechanistic information underlying dietary energy balance responsive pathways will help translate decades of research into effective strategies for prevention of epithelial carcinogenesis.

## Table of Contents

Approval Page .....	i
Title Page.....	ii
Dedication .....	iii
Acknowledgements .....	iv
Abstract.....	v
Table of Contents.....	vii
List of Illustrations .....	x
List of Tables.....	xiii
List of Abbreviations.....	xiv
<b>Chapter 1: Introduction and Background.....</b>	<b>1</b>
1.1 Dietary energy balance and cancer .....	1
1.2 Mechanisms of energy balance effects on carcinogenesis .....	2
1.3 PI3K/Akt/mTOR signaling pathway .....	9
1.4 Calorie restriction mimetics: Targeting mTORC1 .....	15
1.4.1 Rapamycin .....	15
1.4.2 Metformin .....	16
1.5 Two-stage murine model of skin carcinogenesis and PI3K/Akt/mTOR pathway .....	21
1.6 Hypothesis and Specific Aims .....	25
<b>Chapter 2: Materials and Methods .....</b>	<b>27</b>



<b>Chapter 3: Topical Rapamycin Potently Inhibits Skin Tumor Promotion by TPA in Normal Weight, Overweight, and Obese Mice.....</b>	<b>35</b>
3.1 Effect of rapamycin on skin tumor promotion in normal weight mice.....	36
3.2 Effect of rapamycin on skin tumor promotion in overweight and obese mice .....	40
<b>Chapter 4: Metformin Given in the Drinking Water Attenuates Skin Tumor Promotion in Overweight and Obese Mice .....</b>	<b>47</b>
4.1 Metformin administered via the drinking water attenuates TPA skin tumor promotion in overweight mice .....	49
4.2 Metformin administered via the drinking water potently inhibits skin tumor promotion by TPA in obese mice .....	52
4.3 Metformin and rapamycin reduce skin tumor size in overweight and obese mice .....	57
<b>Chapter 5: Mechanisms Associated with the Inhibitory Effects of Rapamycin and Metformin on Skin Tumor Promotion by TPA .....</b>	<b>59</b>
5.1 Rapamycin inhibits TPA-induced epidermal hyperproliferation .....	60
5.2 Rapamycin reduces TPA-induced inflammation in mouse skin.....	62
5.3 Rapamycin inhibits TPA-induced activation of mTORC1 and downstream signaling in mouse epidermis .....	67
5.4 Metformin attenuates TPA-induced epidermal hyperproliferation.....	77
5.5 Metformin activates epidermal AMPK and attenuates TPA-induced signaling through mTORC1 .....	79
5.6 Effect of metformin on body weight, serum hormones, and glucose tolerance .....	85
<b>Chapter 6: Summary, Significance and Future Studies .....</b>	<b>90</b>

References .....	96
Vita .....	114

## List of Illustrations

### Chapter 1

Figure 1-1 Differential effect of DIO and CR on globally active circulating proteins.....	6
Figure 1-2 Summary of dietary energy balance manipulation on epithelial growth factor signaling.....	8
Figure 1-3 Mammalian Target of Rapamycin (mTOR) signaling schematic .....	11
Figure 1-4 Schematic of mTOR/AMPK mediated regulation of ULK1 in response to nutrient availability .....	14
Figure 1-5 Schematic of LKB1/AMPK signaling.....	18
Figure 1-6 Schematic of two-stage murine model of skin carcinogenesis.....	23

### Chapter 2- *No illustrations*

### Chapter 3

Figure 3-1 Effect of rapamycin treatment on skin tumor promotion by TPA in normal weight mice .....	38
Figure 3-2 Confirmation of rapamycin's potent inhibitory effects on skin tumor promotion by TPA .....	39
Figure 3-3 Weight gain of mice during two-stage skin carcinogenesis experiments with topical rapamycin treatment .....	40
Figure 3-4 Effect of rapamycin treatment on skin tumor promotion by TPA in overweight/control mice .....	42
Figure 3-5 Rapamycin decreases squamous cell carcinoma development in overweight/control mice .....	43

Figure 3-6 Effect of rapamycin treatment on skin tumor promotion by TPA in obese mice .....	46
---	----

## Chapter 4

Figure 4-1 Metformin alone and in combination with rapamycin attenuates skin tumor promotion in overweight mice.....	49
Figure 4-2 Metformin decreases the number of SCCs and does not alter the rate of malignant conversion in overweight mice .....	50
Figure 4-3 Metformin and rapamycin did not significantly alter weight gain in mice on control/overweight or obesity inducing diets .....	53
Figure 4-4 Metformin given in the drinking water is a potent inhibitor of skin tumor promotion by TPA in obese mice .....	54
Figure 4-5 Summary of effect of metformin and rapamycin on skin tumor promotion in overweight and obese mice.....	55
Figure 4-6 Metformin and rapamycin treatment reduced the size of skin tumors in both overweight and obese mice.....	57

## Chapter 5

Figure 5-1 Rapamycin inhibits TPA-induced epidermal hyperplasia in a dose-dependent manner.....	60
Figure 5-2 Visual representation of the inhibition of TPA-induced dermal inflammation by rapamycin.....	62
Figure 5-3 Quantitative analysis of the effect of rapamycin on TPA-induced dermal inflammation.....	63
Figure 5-4 Rapamycin inhibits TPA-induced expression of COX-2 in epidermis .....	64
Figure 5-5 Rapamycin inhibits TPA-induced signaling through mTORC1 .....	67
Figure 5-6 Multiple treatments with rapamycin at higher doses prevent mTOR	

Complex I formation .....	68
Figure 5-7 Effect of rapamycin on the induction of autophagy in the epidermis using a multiple treatment protocol .....	73
Figure 5-8 Summary of the impact of rapamycin treatment on Akt/mTOR phosphorylation in mouse epidermis following TPA treatment.....	74
Figure 5-9 Metformin inhibits TPA-induced hyperplasia and hyperproliferation .....	76
Figure 5-10 Metformin activates epidermal AMPK and attenuates TPA-induced activation of mTOR and downstream targets .....	80
Figure 5-11 Combination treatments of metformin and rapamycin are more effective than either agent alone at inhibiting TPA-induced mTORC1 signaling in the epidermis .....	82
Figure 5-12 Effect of metformin and diet on energy balance related serum hormones .....	85
Figure 5-13 Effect of metformin and diet on glucose tolerance .....	87

## List of Tables

Table 1 List of antibodies used.....	28
Table 2 Nutritional composition of diets used .....	29

## List of Abbreviations

°C	degrees Celsius
µg	microgram
µl	microliter
µm	micromole
4E-BP1	eukaryotic initiation factor 4E binding protein
ACC	acetyl co-A carboxylase
AKT	Protein Kinase B
AMPK	5' adenosine monophosphate-activated protein kinase
ATGs	autophagy related genes
ATP	adenosine triphosphate
BK5	bovine keratin 5
BrdU	bromodeoxyuridine
CR	calorie restriction
DIO	diet-induced obesity
DMBA	7,12-Dimethylbenz(a)anthracene
EGFR	epidermal growth factor receptor
FASN	fatty acid synthase
GEMMs	genetically engineered mouse models
IF	Immunofluorescence
IGF-1	insulin-like growth factor 1
IGF-1R	insulin-like growth factor 1 receptor
IHC	immunohistochemistry
IL-6	interleukin-6
IP	immunoprecipitation

IR	insulin receptor
IRS-1	insulin receptor substrate 1
LKB1	liver kinase B1
MCP-1	monocyte chemo-attractant
mTOR	mammalian Target of Rapamycin
mTORC1	mammalian Target of Rapamycin Complex 1
mTORC2	mammalian Target of Rapamycin Complex 2
Ob	obesity gene
ObR	transmembrane leptin receptor
PDCD4	Programmed Cell Death Receptor 4
PI3K	phosphoinositide -3-kinase
PIP3	phosphatidylinositol (3,4,5)-triphosphate
PKC	Protein Kinase C
PRAS40	proline-rich akt substrate of 40 kDa
pS6	ribosomal protein S6
p70S6K	ribosomal S6 kinase
RTKs	receptor tyrosine kinases
SCCs	squamous cell carcinomas
SDS-PAGE	sodium dodecyl sulfate polyacrylamide gel electrophoresis
Ser	serine
Thr	threonine
TNF- $\alpha$	tumor necrosis factor-alpha
TPA	12-O-tetradecanoylphorbol-13-acetate
TSC	tuberous sclerosis complex
Tyr	tyrosine



ULK1/2	unc-51-like kinase 1/2
WAT	white adipose tissue
WT	wild-type

## Chapter 1: Introduction and Background

### 1.1 Dietary energy balance and cancer

*Dietary energy balance* refers to the relationship between calories consumed and calories expended. A positive state of energy balance occurs when the ratio of calories consumed is higher than those expended, and a negative state of energy balance occurs when more calories are expended than consumed. A chronic state of positive energy balance leads to overweight and obesity and is associated with “metabolic syndrome” or a cascade of metabolic disorders leading to the development of cardiovascular disease, type II diabetes as well as many types of human cancer. Estimates from the Cancer Prevention Study II, suggest that 14% of all cancer deaths in men, and 20% of all cancer deaths in women can be attributed to excess body weight, and this is relevant for a range of cancer types (1). Obesity has risen drastically over the past several decades in the United States and, according to 2010 estimates from the Centers for Disease Control and Prevention, more than one third (35.7%) of US adults and a startling 17% of children and adolescents are obese (2). In addition, many animal models also support this association between obesity and cancer. Chronic consumption of an *ad libitum* high fat diet, in which 45-60% of Kcal are from fat, leads to diet-induced obesity (DIO) and is associated with many chronic diseases including type II diabetes and many types of cancer in rodents, some of which include pancreas, breast, colon, liver, ovarian and lung (3-6). In addition, two-stage murine skin carcinogenesis model studies have also demonstrated a role for a high-fat diet in accelerating the rate of tumor development during epithelial carcinogenesis, and when the high fat diet was administered in an isocaloric manner, (diet high in corn-oil but isocaloric) papilloma multiplicity and incidence in SENCAR mice were significantly increased (7). However, these studies did not specifically evaluate the effects of DIO (weight gain and adiposity) on susceptibility to tumorigenesis, and effects and mechanisms underlying positive energy balance are thus less well studied.

On the opposite spectrum, negative energy balance, achieved by calorie restriction (CR) has been shown to universally inhibit carcinogenesis and other chronic diseases across species, as well as extend lifespan (8). CR is an experimental mode in which total energy intake is restricted. Typically, test subjects receive a 15-40% reduction in calories (fat and/or carbohydrates) as compared to an *ad libitum* control fed group but still maintain isonutrient conditions (9). Consistently, CR has been shown to be a potent inhibitor of carcinogenesis in animal models and acts broadly with respect to type of tumor affected as well as mode of induction.

## **1.2 Mechanisms of energy balance effects on carcinogenesis**

CR is considered to be one of the most potent dietary manipulations used to suppress the carcinogenic process, and many key studies in animal models have supported this notion. With more and more of the US population's accession to obesity, it is becoming ever more important to translate knowledge from animal models into human chemoprevention strategies. In order to achieve this, understanding the underlying mechanisms responsible for the differential effects of CR and DIO on tumorigenesis is critical. Current studies have shown that these effects are multifaceted and thus are achieved through the combined effects of numerous cellular and biochemical processes, some of which affect hormones and growth factor signaling as well as inflammation.

### *Globally Active Circulating Proteins*

It is thought that a primary mechanism of action responsible for dietary energy balance effects on tumorigenesis is through variations in serum-related hormones and growth factors that regulate many physiological processes. Some of these include but are not limited to appetite, energy expenditure and metabolism, and thermoregulation. Recent evidence from the literature suggests that primary mediators include insulin, insulin-like

growth factor-1(IGF-1), and glucocorticoids as well as the adipokines, leptin and adiponectin (Figure 1-1) (10).

CR has been shown to reduce circulating insulin levels, while obesity increases them. During conditions of chronic hyperinsulinemia and insulin resistance in particular, insulin has been shown to increase cancer risk at several organ sites (11). Additionally, it is unclear if increases in tumorigenesis can be primarily attributed to the direct effects of insulin receptor activation and subsequent downstream signaling, or if indirect effects on IGF-1 synthesis or other hormones are primarily responsible. Circulating levels of IGF-1 are determined by hepatic synthesis which is regulated by variations in overall insulin and growth factor levels due to variations in energy and nutrient intake. High circulating levels of insulin also decrease the availability of IGF binding protein-1, subsequently providing more bioavailable IGF-1. There is also recent evidence of crosstalk between the insulin receptor and many hormonal pathways thus further complicating its role in energy balance effects (12, 13).

Consistently, *in vitro* studies have provided evidence that IGF-1 enhances cellular growth in a variety of cancer cell lines (14). In addition, it has been identified as a cell cycle progression factor through its activation of the phosphoinositide-3-kinase (PI3K)/Akt signal transduction pathway and subsequent stimulation of G1 to S phase progression (15, 16). This is also supported *in vivo* as studies using LID (reduced circulating IGF-1) mice showed reductions in tumor burden in both an orthotopic model of pancreatic cancer (17) as well as in a two-stage chemical skin carcinogenesis model (18). It is important to note that in each of these studies, while there was a 75% reduction in circulating IGF-1, insulin levels remained high, thus making it hard to discern the primary mediator of energy balance effects.

Adipokines, which are cytokines secreted from adipocytes, have also been identified

as mediators in energy balance effects. Leptin, a 16 kDa adipocyte derived cytokine regulates metabolism and satiety by acting in the hypothalamus to send a cascade of neuroendocrine signals (19). Leptin is differentially regulated by DIO and CR, and levels strongly correlate to overall body weight and fat mass. In normal weight individuals, increases in leptin result in decreased appetite while an obese state has consistently been shown to increase overall circulating levels of leptin to a point of causing leptin resistance (20-22). It is thought that this resistance causes the exogenous leptin to lose its ability to prevent weight gain (22). In addition, this rise in circulating leptin is associated with increased cancer risk for many types of cancer most notably colorectal and prostate cancer with limited data supporting a role for leptin in breast and endometrial cancers (23-25). *In vivo* studies have shown that leptin may increase tumor invasion and support angiogenesis (26), and *in vitro* studies have shown leptin to increase proliferation of neoplastic but not “normal” cells (27). Leptin is a product derived from the *Ob* gene, and its major actions are mediated primarily through the transmembrane leptin receptor (ObR) whereby the Janus Kinase 2/signal transducer and activator of transcription 3 (Jak-STAT) signaling cascade is subsequently activated. These pathways have been shown to be critical signaling pathways during tumor development (19, 28). There is also further evidence that the importance of leptin during energy balance modulation and cancer development could also be due to the ratio of leptin to adiponectin in contrast to the independent effect of leptin as they act in opposition of one another to influence carcinogenesis (29, 30). Adiponectin is a 28 kDa adipokine insulin sensitizer that plays a key role in glucose and lipid metabolism. Concentrations of adiponectin increase as overall weight declines and decrease in obese and diabetic states as well as other conditions classified as “metabolic syndrome”(31). Metabolic syndrome is the name given to a set of risk factors which include insulin resistance, hyperglycemia, excess body weight around the waist, high blood pressure, high triglycerides, and low HDL cholesterol levels that collectively lead to increased heart

disease, type II diabetes and stroke. Extreme weight loss through CR and surgery has been shown to reverse these effects (10). Although the role of adiponectin in cancer is not well characterized, recent data suggest that levels of adiponectin may inversely correlate with cancer development (27, 29, 32, 33). Possible mechanisms include adiponectin mediated activation of AMP-activated protein kinase (AMPK) and subsequent inhibition of mTORC1 signaling as well as its attenuation of Stat signaling (10).

Previous CR studies have also suggested a possible role for adrenal glucocorticoids in mediating some of the anti-cancer effects of CR. Marked increases in corticosterone have been observed in rodents undergoing CR  $\geq 30\%$ , and this increase was associated with a decrease in tumor development in the two-stage skin carcinogenesis model (34). There are several proposed mechanisms by which corticosterone may be exerting anti-tumor effects which include reductions in inflammation, inhibition of cell cycle progression via p27 activation and inhibition of PKC and subsequent ERK signaling (34, 35). Adrenalectomy studies further complicate the role of corticosterone during CR, as removal of the adrenal gland abolished the anti-cancer effects of CR during skin tumor promotion in mice; in contrast, adrenalectomy had no impact on CR mediated tumor growth inhibition in rats in a chemically induced model of mammary carcinogenesis (35, 36). Additionally, studies in a rat mammary carcinogenesis model also showed that supplementation of corticosterone in a non-CR state inhibits tumorigenesis, but also results in dose-dependent reductions in circulating IGF-1 levels (37).

Chronic inflammation is associated with cancer development, and more recently, obesity (38). Increases in white adipose tissue (WAT) cause increased flux in the number of circulating inflammatory cytokines as well as at the local or tissue level, some of which include interleukin-6 (IL-6), tumor necrosis factor-alpha (TNF- $\alpha$ ), monocyte chemoattractant (MCP-1) as well as C-reactive protein (39). A cascade of events then occurs, beginning with increased macrophage infiltration and further adipose-derived increases in

inflammatory cytokines. This is followed by increased signaling through inflammatory pathways such as NF- $\kappa$ B, STAT3, and JNK leading to a low-grade but chronic inflammatory state giving rise to a tumorigenic environment (40).

**Figure 1-1**

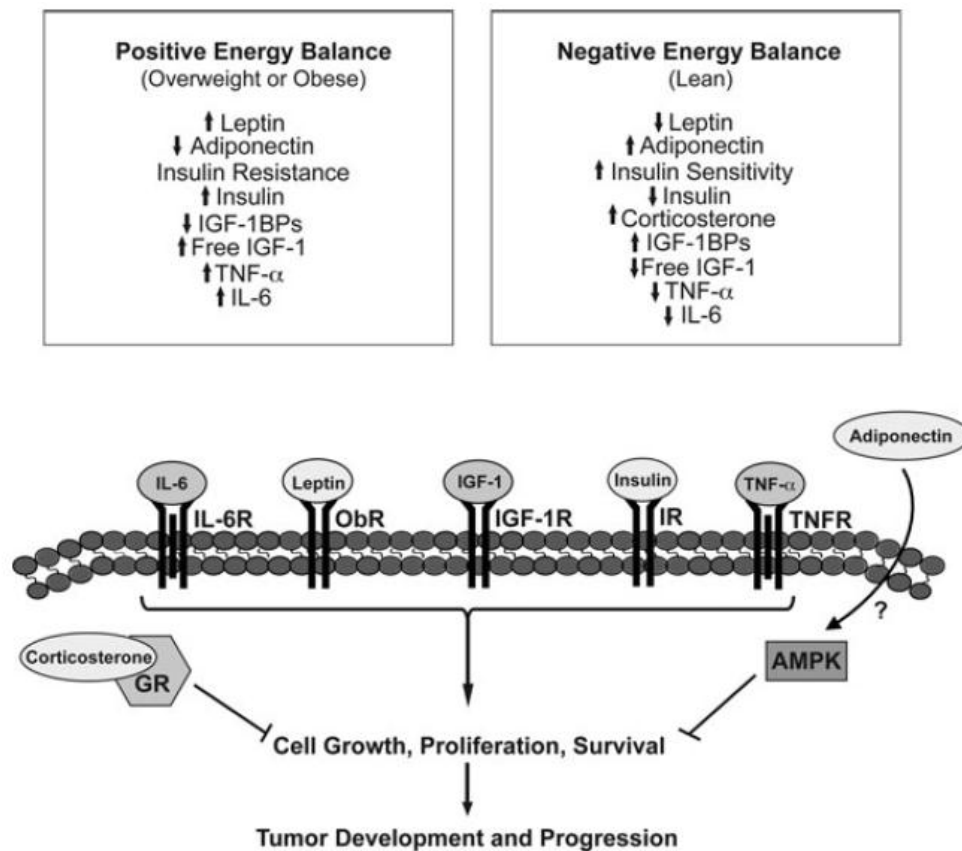


**Figure 1-1 Differential effect of DIO and CR on globally active circulating proteins**  
DIO or positive energy balance increases circulating levels of leptin, IGF-1, TNF- $\alpha$  and IL-6 and decreases levels of adiponectin. The opposite effect is seen with CR or negative energy balance and increases in corticosterone and adiponectin occur. Changes in circulating levels of these serum hormones and cytokines affect activation of corresponding receptors leading to differential effects on cellular growth, proliferation and survival. Reprinted by permission from Wiley and Sons: [Annals of the New York Academy of Science] (10), copyright 2011

There is also recent evidence to suggest that differential signaling through the PI3K/Akt/mTOR pathway across the DIO/CR spectrum may provide a potential mechanism by which dietary energy balance modulates tumorigenesis (Figure 1-2). An *ad libitum* diet or consumption of a high fat diet inhibits the TSC complex, and subsequently activates mTORC1 enabling an increase in cellular growth and proliferation. Recent data suggest that this occurs through increases in ATP, glucose and amino acids caused by high energy conditions. In contrast, nutrient deprivation via CR has been shown to inhibit mTORC1. It is thought that one mechanism through which this may occur is through the LKB1/AMPK pathway. When ATP/AMP ratios become low, AMPK is activated and phosphorylated by LKB1 and subsequently mTORC1 is inhibited. In addition, this activation reduces energy expenditure by the cell thus limiting stress inspired apoptosis (41). It should be noted however that this mechanism appears to be tissue specific as CR was found to activate AMPK in liver, skeletal muscle, and fat tissue but did not appear to be differentially activated by DIO or CR in skin epidermis or dorsolateral prostate (42, 43). Recent studies have also shown CR to reduce IGF-1R activation and subsequently downstream activity (Akt, mTORC1 and downstream substrates) in a variety of epithelial tissues including skin epidermis, liver and prostate while DIO increased activation in both steady-state conditions as well as after TPA treatment (43). Furthermore in this study, dietary energy balance modulation was also found to differentially modulate epidermal growth factor receptor (EGFR) contributing to the observed differences in Akt and mTORC1 status with DIO and CR. Another study found similar decreases in serum IGF-1 levels and decreased protein activation of mTOR and p70S6K in mammary tumors and mammary fat pads using MMTV-TGF- $\alpha$  mice undergoing intermittent calorie restriction (ICR) (44). Studies in LID mice also show reductions in TPA-induced epidermal activation of Akt and mTORC1 comparable to those undergoing CR thus further supporting the role of IGF-1 in mediating dietary energy balance effects (18).



**Figure 1-2**

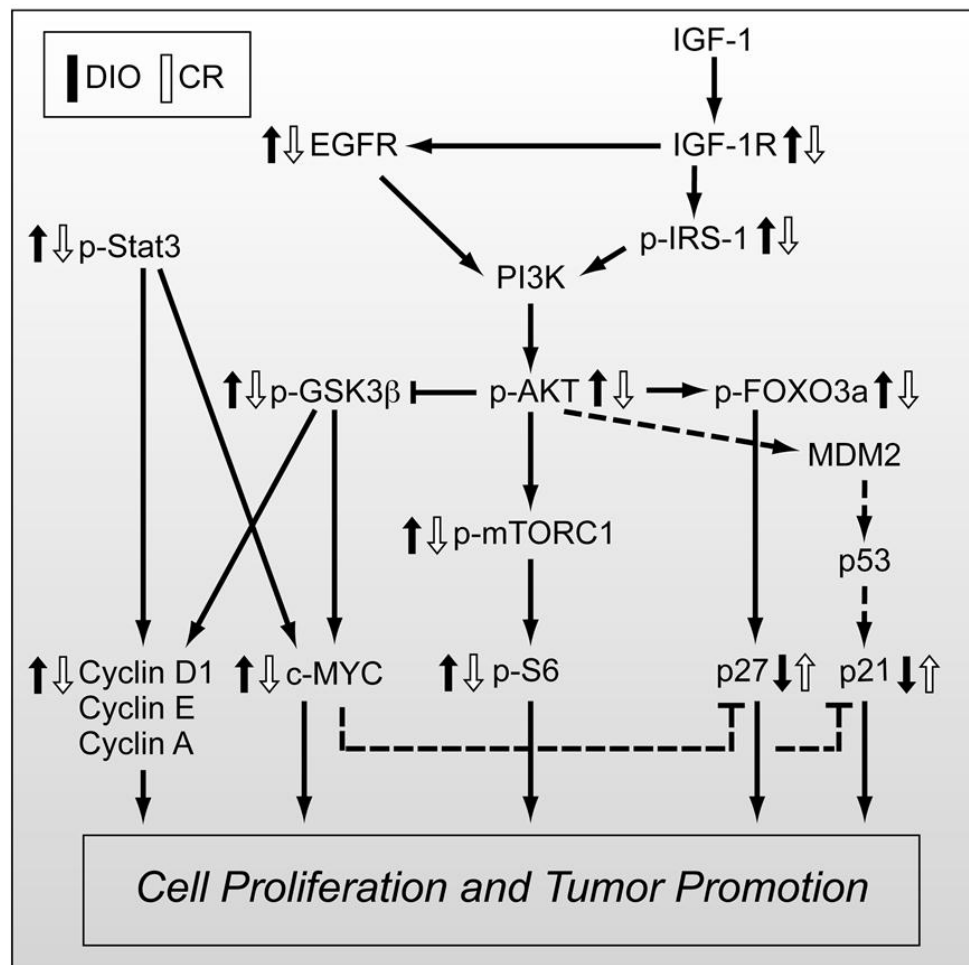


**Figure 1-2 Summary of dietary energy balance manipulation on epithelial growth factor signaling.** Illustration representing the proposed mechanism by which dietary energy balance (calorie restriction and diet-induced obesity) modulates susceptibility to skin tumor promotion. DIO increases while CR decreases circulating levels of IGF-1 which in turn differentially regulate activation of IGF-1R and subsequently EGFR due to potential receptor crosstalk. Akt, mTOR and other downstream targets including cell cycle regulatory proteins such as cyclin D1, cyclin E and cyclin A are differential regulated. Dotted lines represent potential changes supported by preliminary data. Black arrows represent changes in epidermal signaling in obese mice, and white arrows indicate changes seen in epidermis of CR mice.

Additional studies have used A-ZIP/F-1 mice, which lack WAT and display low levels of adipokines but are still insulin resistant and diabetic to enable a distinction to be made from the effects of adiposity (leptin, adiponectin, etc.) and various hormonal factors and signaling pathways that have been linked to obesity and tumorigenesis. These mice were found to remain highly susceptible to tumor development in both the two-stage skin carcinogenesis model as well as in the C3(1)/T-Ag transgenic mouse mammary model in the absence of obesity thus further supporting the hypothesis that insulin, IGF-1 and downstream signaling pathways as well as inflammation are the primary mediators in the link between obesity and cancer (45).

### **1.3 PI3K/Akt/mTOR signaling pathway**

It is well established that the PI3K/Akt/mTOR signaling pathway is a major element of IGF-1 and insulin responses that are involved in cellular metabolism and growth and that this pathway may be a major contributor to IGF-1's effects on tumorigenesis (15, 46, 47).

Evidence from the literature also suggests that this pathway is one of the most commonly altered pathways found in human tumors (48, 49). Akt has been shown to regulate cell cycle progression and cell survival via phosphorylation of many downstream effectors including Bad, Foxo1, and GSK3 $\beta$  and thus mediates or promotes cellular transformation when signaling is aberrant. IGF-1 and/or insulin bind to the IGF-1R and IR respectively and in turn, these activated receptor tyrosine kinases and Ras, activate PI3K via scaffolding adaptors such as insulin receptor substrate I (IRS-1) or through direct phosphorylation (1-1). PI3K produces phosphatidyl-inositol-3,4,5-triphosphate (PIP3) which is then bound to Akt and PDK1, with Akt representing its primary substrate. PDK1 phosphorylates Akt at T308 which is the activation loop (50).

Elevated levels of Akt activation have also been associated with increases in mammalian target of rapamycin (mTOR) activity. mTOR is a highly conserved

serine/threonine protein kinase that integrates energy sensing and nutrient status to growth factor signaling in order to regulate multiple critical cellular processes including cellular growth and proliferation, protein translation and autophagy (51). mTOR is composed of two distinct complexes, mTORC1 and mTORC2. mTORC1 is composed of mLST8 and raptor and is primarily driven by nutrient status (Figure 1-3). mTORC1 is known to be rapamycin sensitive. External signals such as growth factor signaling via nutrient status and availability regulate activation or repression of tuberous sclerosis complex (TSC) which is the primary regulator of mTORC1 activation. TSC binds to and relieves G-protein Rheb from mTORC1, subsequently inhibiting mTORC1. However, when TSC is phosphorylated it is inactivated, and the released Rheb, in a GTP-bound state can then activate mTORC1. In addition, PRAS40, a proline-rich Akt substrate and binding partner of raptor is a negative regulator of mTORC1 that is released in response to insulin (52).

**Figure 1-3**

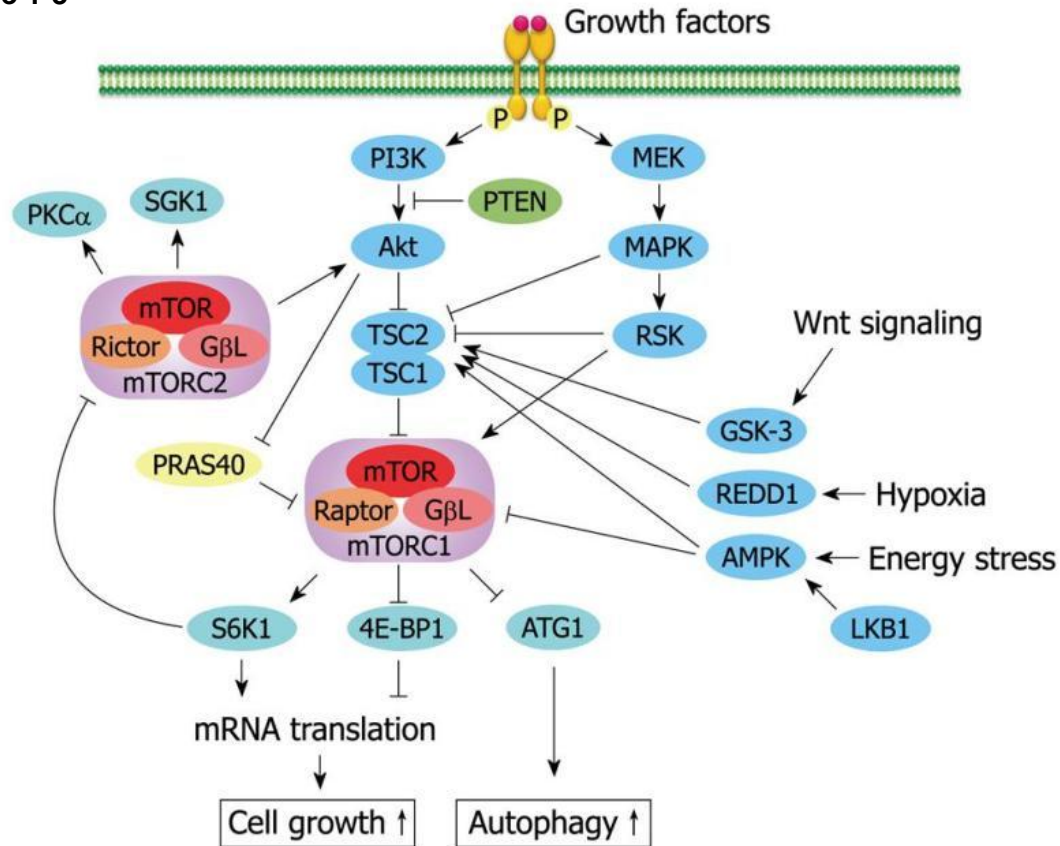


**Figure 1-3 Mammalian Target of Rapamycin (mTOR) signaling schematic.** Illustration representing key regulators of the mTOR signaling pathway. mTOR is a 289 kD protein composed of two functionally distinct complexes: mTORC1 and mTORC2. Growth factors including insulin and IGF-1 and environmental stressors such as hypoxia and energy promote mTORC1 mediated cellular growth and proliferation through downstream targets S6K1 and 4E-BP1 and inhibit the induction of autophagy. mTORC1 is the rapamycin-sensitive complex. mTORC2 is rapamycin insensitive and activated via RTKs by an unknown mechanism. The mTORC1/S6K1 negative feedback loop suppresses activation of mTORC2/Akt. [Reprinted from (53) under the Creative Commons Attribution Non-commercial License]

Primary processes of mTORC1 are carried out by downstream targets, ribosomal S6 kinases (S6Ks, p70S6K) and 4E-binding protein-1 (4E-BP1) which are translational regulators (54). The S6Ks have been shown to increase ribosome biogenesis and lead to increased cellular growth although complete understandings of the mechanisms of action behind this remain unclear. Of particular interest is S6K's negative regulation of insulin signaling through phosphorylation of IRS-1 and subsequent decreases in signaling through Akt/mTOR. Because this signaling pathway is stimulated by nutrients, this negative feedback loop may play a role in obesity related diseases (52). Further downstream of S6K, this will be referred to hence forth as p70S6K, is Programmed Cell Death Receptor 4 (PDCD4). Emerging evidence suggests that transcription as well as translation is greatly influenced by levels of PDCD4 which in turn modulate signaling pathways thus potentiating PDCD4's role as a tumor suppressor (55). During skin tumor promotion, a recent study found tumor promoter TPA to stimulate proteasomal degradation of PDCD4 in mouse epidermis and skin tumors, and levels inversely correlated with tumor response. Both Akt and p70S6K were found to phosphorylate PDCD4 and target it for ubiquitylation via E3-ubiquitin ligase (56). mTORC1 also regulates protein synthesis via the 4E-BPs. The 4E-BPs inhibit protein synthesis by binding to eIF4E to prevent it from interacting with eIF4G1/eIF4G2 and thus inhibit its function in mRNA translation, though it's thought that these translational repressors only affect certain mRNAs (52).

Additional downstream targets of mTORC1 include many autophagy-related genes (ATGs). Macroautophagy is an important component of the cellular stress response, designed to maintain cellular homeostasis. It is a catabolic process that involves the breakdown of a large variety of cellular material and debris via delivery of these cytoplasmic proteins and organelles by specific membranous vesicles known as autophagosomes to lysosomes (57). The process is crucial to maintaining cellular homeostasis by eliminating damaged proteins and organelles, as well as playing a key role in many other physiological

processes including immunity, cellular apoptosis, and metabolism (58, 59). Deregulation of this process has been linked to increases in susceptibility to a variety of diseases including cancer (59, 60). Many alterations have been found in autophagic signaling pathways during various stages of tumorigenesis. However, it is important to note that autophagy's role in cancer is an environment-dependent process. Autophagy maintains cellular homeostasis which can limit the availability of a microenvironment that promotes tumor growth. Particularly, if irregularities are present that decrease autophagic processing such as various disease states, this may give rise to a microenvironment that is able to promote tumorigenesis (58). In contrast, established solid tumors may actually exploit autophagy to stimulate tumor growth and promote metastases (59).

Most pro-autophagic events including initiation and nucleation converge on the mammalian Target of Rapamycin (mTOR) which as aforementioned serves as a critical sensor of energy and nutrient status and a subsequent regulator of protein synthesis. Nutrient rich states cause a complex formation between mTORC1, ULK1/2, FIP200 and mAtg13 due to interactions between raptor and ULK1 (61). ULK1 and ULK2 are mammalian homologs of the yeast autophagy related gene 1 (Atg1) serine/threonine protein kinase critical for autophagic regulation (62). Phosphorylation of ULK1 and Atg13 by mTORC1 prevents the pro-autophagic kinase activity of these proteins (58). This is accompanied by an mTORC1 mediated increase in protein synthesis. Nutrient starvation or treatment with mTOR inhibitors reverses this negative regulation of autophagy and allows for the ULK complex to localize to the newly forming phagophore (58, 62) (Figure 1-4).

mTORC2 associates with rictor, mLST8 and SIN1 and is activated by RTKs that respond to stimuli that have yet to be elucidated and overall understanding of its functions are greatly limited (15, 51). It is thought to be rapamycin-insensitive, and it primarily targets Akt for phosphorylation at serine 473 (51). Finding specific inhibitors of mTORC2 kinase activity will aid greatly in the understanding of control and cellular function of mTORC2.

**Figure 1-4**

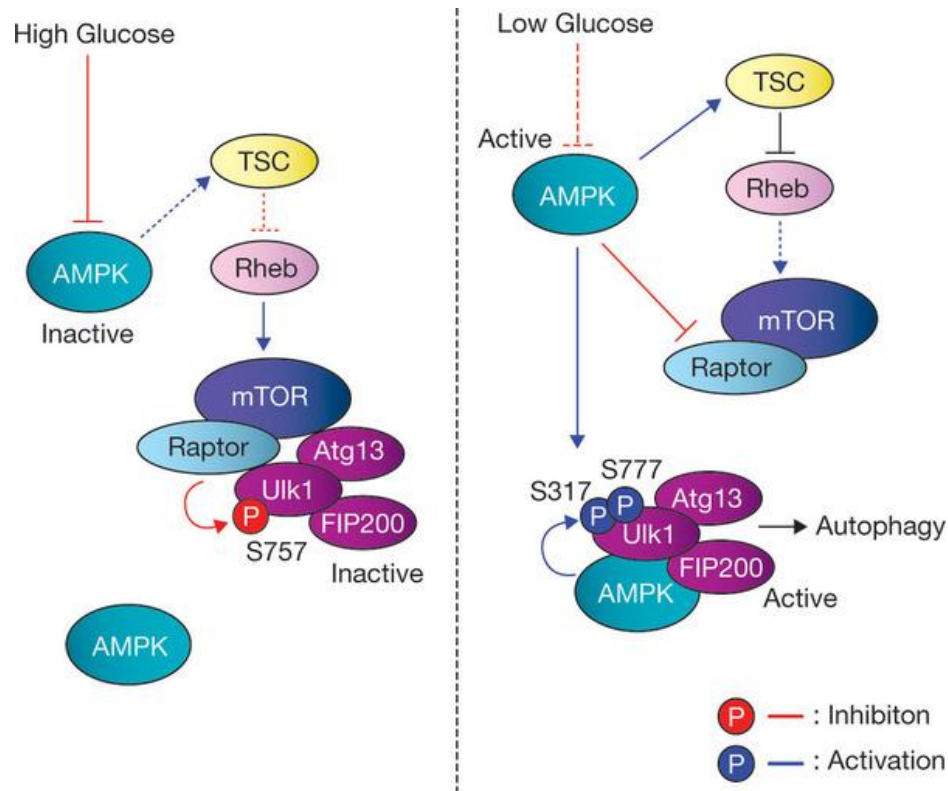


**Figure 1-4 Schematic of mTOR/AMPK mediated regulation of ULK1 in response to nutrient availability.** Under glucose rich conditions, AMPK is inactivated and mTOR is activated. Activated mTORC1 phosphorylates ULK1 on Serine 757 disturbing its interaction with AMPK and subsequent activation. When nutrient availability is limited, AMPK remains activated and thus phosphorylates TSC and inactivates mTORC1. Subsequently, AMPK can phosphorylate ULK1 on Serine 317 and Serine 777 thereby initiating autophagy through its activation. Reprinted by permission from Macmillan Publishers Ltd: [Nature Cell Biology] (63), copyright 2011

#### **1.4 Calorie restriction mimetics: Targeting mTORC1**

A new chemopreventive approach may lie in the identification or development of natural or synthetic agents to appropriately “mimic” the protective effects generated by CR as previous findings regarding CR and anti-cancer properties are vast. Drastic lifestyle changes which include long-term CR are difficult for the general population to maintain. As discussed earlier, much data supports the hypothesis that the IGF-1R and Akt/mTOR pathways are important mediators in CR effects during tumorigenesis thus making them front line targets for mimetic drug development. Current drugs under development have targeted IGF-1 with small-molecule inhibitors (64) as well as with anti-sense inhibitor approaches (65) and anti-IGF-1 antibodies (66). In addition retinoids and flavonoids which are widely used as chemopreventive agents have also demonstrated inhibition of the IGF-1 pathway (67-69). More recent studies have begun to explore further downstream of IGF-1 with Akt and mTOR inhibitors as potential CR mimetics. As previously discussed, mTOR, a target of Akt, has been shown to be a key component in mediating some of the effects of aberrant Akt signaling that occur during tumorigenesis (70, 71).

##### **1.4.1 Rapamycin**

Rapamycin is a macrolide found in the soil originating as a product from the bacterium *Streptomyces hygroscopicus*. Rapamycin is a powerful immunosuppressant, and it is primarily used to prevent organ transplant rejection, especially in kidney transplant patients. However, its anti-proliferative properties have also generated a large amount of interest in rapamycin as an anti-cancer or chemopreventive agent. Additionally, rapamycin has been shown to extend lifespan in mice thus exerting similar effects to CR (72). Importantly, rapamycin is a well-established mTORC1 inhibitor. It has been shown to exert this effect by binding to its intracellular receptor, immunophilin FKBP12, forming an inhibitory complex. This in turn, destabilizes mTORC1 by binding to a C-terminus region on mTOR thus



preventing mTOR interaction with raptor (73-75). mTORC2 is thought to be “rapamycin-insensitive” as acute treatment has shown no effect on mTORC2 substrates, however chronic treatment *in vitro* did demonstrate possible mTORC2 inhibition via decreases in AKT/PKB which is a primary downstream target of mTORC2 (76).

Rapamycin has been shown to suppress tumorigenesis in a variety of tumor model systems. It was found to inhibit growth of mammary lesions, both pre-malignant and malignant transplanted from Tg (*MMTV-PYV-mT*) mice (77). In addition, in a xenograft model of highly metastatic human hepatocellular carcinoma, rapamycin was found to inhibit primary tumor growth as well as metastasis (78). Rapamycin, administered in the diet also inhibited tumor growth in primary skin tumors induced by chronic exposure to UV (79) as well as induced regression of late-stage skin tumors in the chemically-induced two-stage model of skin carcinogenesis in mice (80). Chemopreventive properties of rapamycin were demonstrated in A/J mice with carcinogen induced lung cancer as these mice displayed marked decreases in tumor size and multiplicity (81, 82). Furthermore, several transgenic mouse models including a head and neck SCC mouse model based on a K-ras<sup>G12D</sup> and p53 loss in the oral epithelium (83) as well as an erbB2-dependent breast cancer mouse model (84) have demonstrated rapamycin’s potent anti-cancer properties through decreases in tumor growth, angiogenesis and survival.

#### **1.4.2 Metformin**

Metformin is a biguanide derived from guanidine, the active ingredient in *Galega officinalis* (goat’s rue). It is the most commonly prescribed oral hypoglycemic agent today with over 120 million users worldwide (85). Its primary use is in the treatment of diabetes mellitus type 2 whereby it inhibits hepatic glucose production and induces an overall reduction in insulin resistance. This also stimulates glucose uptake in peripheral tissues thereby reducing overall circulating blood glucose levels. Primary mediators in these insulin and

glucose lowering effects include AMPK activation via activation of liver-kinase B1 (LKB1). This activation occurs through metformin's primary mechanism of action whereby it interferes with respiratory complex I in the mitochondria reducing overall adenosine triphosphate levels (ATP) (86). AMPK is a central energy and nutrient sensor that responds to variations in the ratio of AMP to ATP. Nutrient deprivation leads to activation of AMPK and subsequent inhibition of energy consumption and related processes such as protein translation regulated via mTOR and its various downstream targets, and fatty acid synthesis via acetyl CoA Carboxylase (ACC) and fatty acid synthase (FASN) (Figure 1-5). Activation of AMPK helps partially reverse the metabolic deregulation present in type II diabetes.

**Figure 1-5**

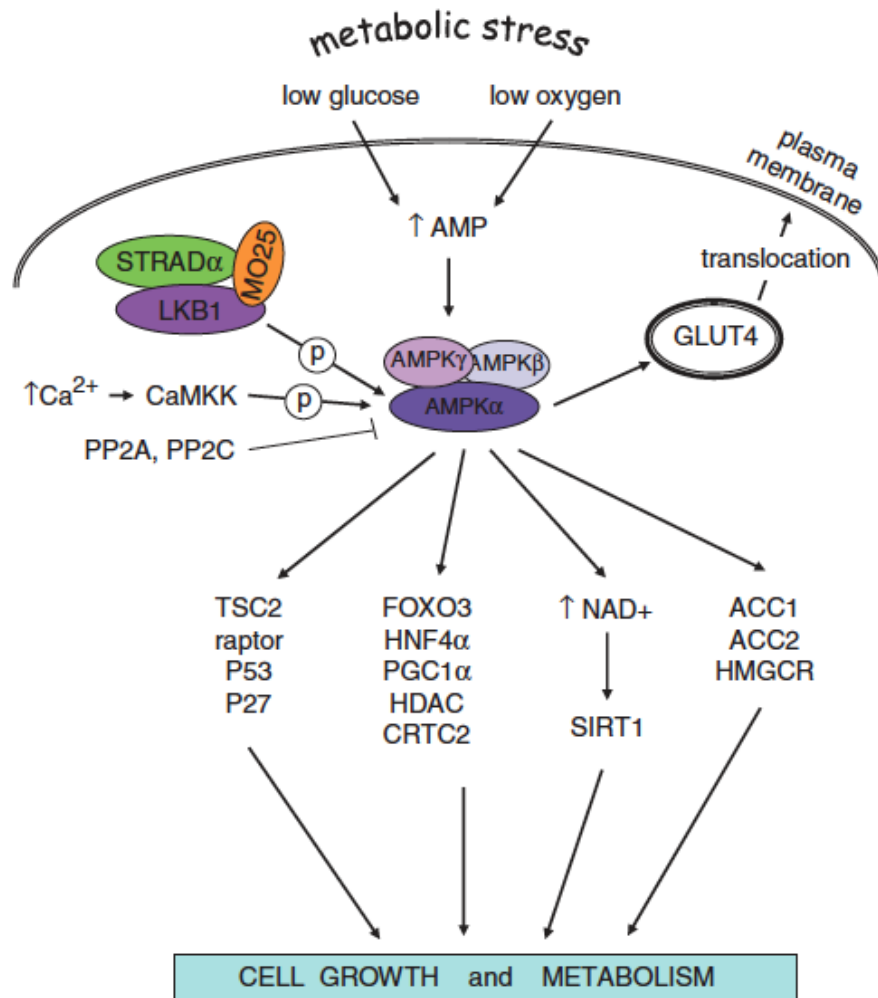


**Figure 1-5 Schematic of LKB1/AMPK signaling.** Various downstream effectors mediate LKB1/AMPK's regulation of cellular growth and metabolism. Metabolic stress induces increases in cellular AMP thus forming the AMPK $\alpha$  complex which can then be activated by LKB1. The AMPK complex can also be phosphorylated by calcium/calmodulin-dependent protein kinase (CaMKK). PP2A and PP2C inhibit its phosphorylation. Activation of AMPK causes translocation of GLUT4 to the plasma membrane whereby it stimulates glucose uptake and regulates downstream signaling involved in cellular gene transcription and cellular metabolism. Reprinted by permission from Macmillan Publishers Ltd: [Oncogene] (87), copyright 2011

There is increasing evidence from case-control and prospective cohort studies that type II diabetes is associated with increased cancer risk; however, there remains large overlap in cause since there are various other cancer risk factors associated with type II diabetes such as obesity, sedentary lifestyle, and a high-fat diet (88). With the elucidation of AMPK's role in metabolism, as well as all the metabolic abnormalities linked with increased cancer risk, there is great interest in pursuing metformin as an anti-cancer/chemopreventive agent. Population-based studies have provided evidence that patients with type II diabetes treated with metformin have reduced cancer incidence as well as reduced mortality than patients receiving other types of diabetes treatment (89, 90). In addition, this appears to be true for a variety of solid tumor types. Recent epidemiological studies show a reduced incidence of colorectal cancer in diabetic patients receiving metformin (91). Patients taking metformin with pancreatic cancer and colorectal cancer displayed a 30% improvement in overall survival (91, 92). A retrospective study showed that breast cancer patients taking metformin in addition to systemic therapy, displayed an increase in the overall effectiveness of the chemotherapy (93).

In addition, the possible anti-tumorigenic properties of metformin have been supported in a variety of *in vitro* and *in vivo* experimental systems. Several studies in cancer cell lines have provided evidence that metformin inhibits neoplastic growth (94, 95). In A/J mice exposed to a tobacco carcinogen 4- (methylnitrosamino)-1-(3-pyridyl)-1-butanone (NNK), both oral and intraperitoneal administration of metformin reduced lung tumor burden. With oral administration there were modest decreases in mTOR activity in lung tumor tissue, however upon IP injection, signaling through the IGF-1R/IR was decreased as well as mTOR, Akt and ERK, in an AMPK independent fashion (96). In HER-2/neu mice, metformin treatment via the drinking water (100 mg/kg bw per day) reduced the size and incidence of mammary adenocarcinomas as well as prolonged lifespan (97). Metformin administered in a basal powdered diet form (250 mg/kg bw per day) in APC<sup>min/+</sup>

mice was shown to reduce polyp growth as well as activate AMPK and reduce signaling through mTOR in tumor tissue (98). Since most epidemiological studies have been obtained from type II diabetic populations which present metabolic disorders including obesity, hyperglycemia and hyperinsulinemia, a few studies have explored metformin's effect in mice receiving a high-energy vs. normal control diet on tumor growth. One study found that oral administration via the drinking water (50 mg/kg bw per day) blocked the stimulatory effect of a high-energy diet on growth of an *in vivo* model of colon carcinomas using MC38 carcinoma cells. Metformin attenuated high-energy associated effects on tumor growth including a reduction in insulin levels, a reduction in Akt activation in the tumor tissue, and a reduction in expression of Fatty Acid Synthase (FASN) in tumor tissue (99). This same group also showed that in a lewis lung LLC1 carcinoma cancer model in C57BL/6J mice, the effect of a high-energy diet on lung tumor growth was greatly attenuated with oral administration of metformin and was associated with reduced signaling through the IR. Both the high-energy and control groups of mice displayed activation of AMPK in tumor tissue, but only the high-energy group displayed significant reductions in tumor growth suggesting AMPK independent mechanisms (100).

Thus the potential anti-tumorigenic properties of metformin may be attributed to both "direct" and "indirect" mechanisms. Indirect mechanisms of action include overall reductions in systemic insulinemia, bringing both glucose and insulin to physiologically normal plasma levels. This could attenuate signaling through the insulin receptor and attenuate growth of insulin responsive tumors. A primary "direct" class of proposed mechanisms requires activation of LKB1 and downstream target AMPK in neoplastic cells. A simplified model of this mechanism involves activation of this pathway and a subsequent suppression of protein synthesis through inhibition of mTOR, though the downstream effectors of AMPK are vast, and AMPK mediates many inhibitory effects on multiple signaling pathways. An

interesting question lies in whether or not non-diabetic patients will have the same reduction in cancer risk as their diabetic counterparts with metformin treatment.

### **1.5 Two-stage murine model of skin carcinogenesis and PI3K/Akt/mTOR pathway**

The multistage or “two-stage” model of chemical carcinogenesis in mouse skin is a well-established *in vivo* tumor model system used to evaluate the consecutive or step-wise process that gives rise to tumor development in the skin (Figure 1-6). Many epithelial cancers (e.g. colon, breast, prostate) found in humans result from a multistage process (101) making it relevant to address tumor development in a sequential, stage-oriented manner. Strengths of the model include its ability to distinguish between initiation, promotion, and progression phases of tumor development as well as the convenient ability to visualize tumor growth throughout the lifespan of the mouse. Due to a highly reproducible tumor response, the model is particularly useful for studying the effects of dietary energy balance manipulation as well as pharmacological intervention via various chemopreventive agents (both synthetic and natural) on tumor development. These pharmacological inhibitors can also be used to determine the importance of specific signaling pathways during each stage. The model may also be super-imposed on genetically engineered mouse models (GEMMs) to help identify proto-oncogenes and tumor suppressor genes as well as to determine susceptibility.

This multistage process begins with an irreversible single sub-carcinogenic topical dose of a mutagenic agent. While a large range of “initiating” agents are used, currently the most common agent employed is the polycyclic aromatic hydrocarbon 7-12-dimethylbenz[a]anthracene (DMBA). This stage is referred to as the “initiation” stage and gives rise to genetic lesions found in both follicular and interfollicular stem cells in the skin (102, 103). The *Hras1* gene has been found to be the primary target gene during this stage, although there is evidence for mutations in *Kras* as well after exposure to DMBA and

initiating agent *N*-methyl-*N'*-nitro-*N*-nitrosoguanidine (MNNG) (101). Following the initiation stage, promotion then occurs through clonal expansion of the mutated population of cells via repeated topical application of chemical agents that cause overall increases in proliferation and result in epidermal hyperplasia. In addition, initiated cells are thought to have a growth advantage allowing for their selective expansion (104, 105). Common tumor promoting agents include phorbol ester compounds of which the most frequently used is 12-*O*-tetradecanoylphorbol-13-acetate (TPA). TPA activates Protein Kinase C (PKC) which mediates signaling through the Epidermal Growth Factor Receptor (EGFR) and has been shown to induce cellular proliferation through activation of the Akt signaling cascade (106). Promoting agents can also stimulate a host of pathways including PKC leading to increases in cellular growth and proliferation through stimulation of EGFR and may also influence inflammatory cell infiltration and oxidative stress. Repeated application of tumor promoting agents eventually results in exophytic growths on the skin referred to as “papillomas” which consist of a stromal core and are surrounded by hyperplastic tissue. Promoting agents are usually applied two or more times per week and must be consistent as promotion at this stage can be reversible causing papillomas to regress if treatment is not maintained. Although timing is dependent upon the strain of the mouse used, papillomas can generally be seen after 10 weeks of promotion. Eventually these benign outgrowths may progress to the highly vascularized, downward invading malignant squamous cell carcinomas (SCCs) as early as 20 weeks after promotion due to the additional accumulation of genetic alterations which include trisomies of chromosomes 6 and 7 and mutations in *p53* in these small tumors (101).

While this model has several advantages over “complete” skin tumor models in which a single carcinogen is used or continuous UV exposure is applied, there are a few limitations to this model system that must be addressed. In this protocol, the mice present a *Hras* driven model of tumorigenesis, whereas *p53* appears to be the most important

target gene in non-melanoma skin cancer in humans (107). Primary gene targets of this model system appear to be more relevant to other human epithelial cancers some of which include cancers of the lung, pancreas and colon (108). Additionally, there is no direct human equivalent for a “papilloma.” However, SCCs that arise from malignant conversion histologically favor those seen in humans as they are highly vascularized and invasive (101). And lastly, this model has very low rates of metastasis, making it only useful for studying primary tumors (109).

**Figure 1-6**

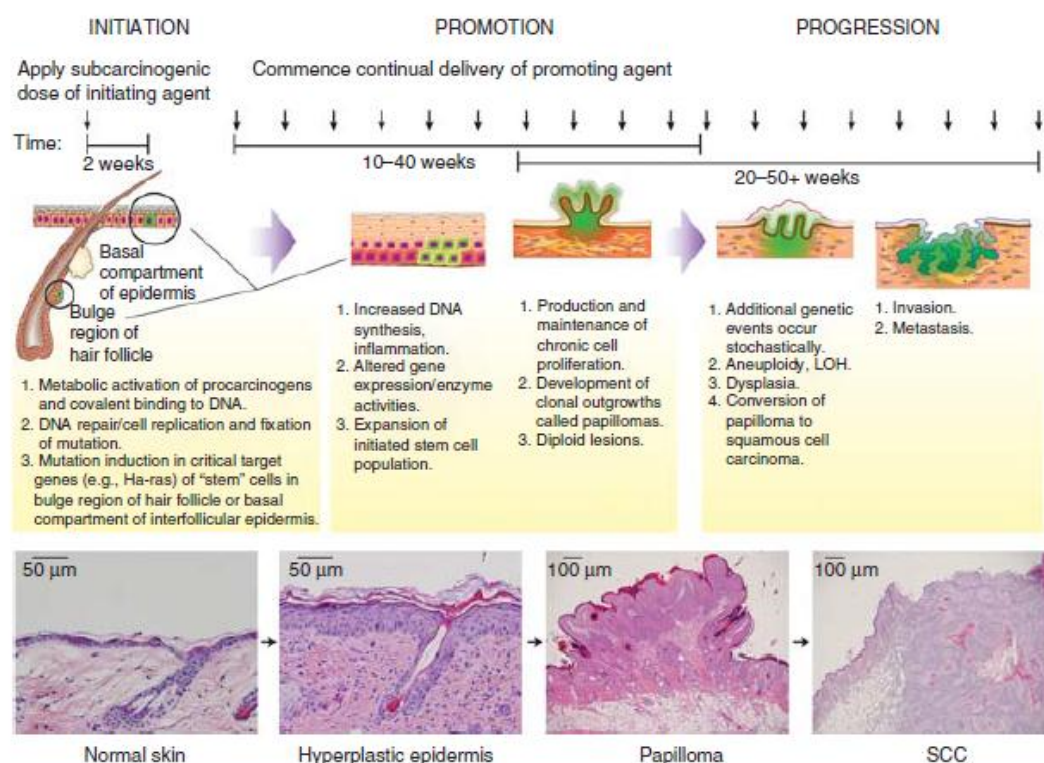


**Figure 1-6 Schematic of two-stage murine model of skin carcinogenesis.** Initiation occurs with a single, topical sub-carcinogenic dose of a mutagenic agent followed by repeated topical applications of a promoting agent two weeks after initiation. Promotion continues for the entirety of the study. Papillomas begin to develop 6-12 weeks after promotion begins and a small fraction eventually converts to SCCs beginning approximately 20 weeks after promotion. This panel shows representative H&E stains of normal epidermis followed by hyperplastic epidermis, a papilloma and a SCC. Reprinted by permission from Macmillan Publishers Ltd: [Nature Protocols] (101), copyright 2009



There is much evidence to suggest that signaling downstream of IGF-1R and various other growth factor receptors to Akt and mTOR are primary mediators of tumor promotion during epithelial carcinogenesis in mouse skin. In the BK5.IGF-1 transgenic mouse model in which the bovine keratin 5 (BK5) promoter drives IGF-1 overexpression in the epidermis, increased susceptibility to two-stage skin carcinogenesis, and spontaneous tumor formation occurred. This was also associated with increased signaling through PI3K/Akt and progression through the cell cycle as seen through upregulation of cell cycle regulatory proteins in the epidermis (110, 111). The PI3K inhibitor LY294002 inhibited the observed changes in this signaling pathway in the epidermis, and furthermore, it inhibited skin tumor promotion in a dose dependent manner upon topical application (110). These IGF-1 transgenic mouse studies support the role of PI3K and Akt in IGF-1's role during skin tumorigenesis. Additional studies further support a role for Akt during skin carcinogenesis. Segrelles et al., reported that epidermal Akt activation was sustained through the duration of the two-stage protocol in mouse skin (112). Additional studies have further confirmed the importance of Akt signaling and cellular proliferation during skin tumor promotion using transgenic mice that overexpress Akt1<sup>wt</sup> or Akt1<sup>myr</sup> in the epidermis under control of the BK5 promoter and found that deregulation of Akt expression and subsequent alterations in related signaling pathways significantly heightened tumor response and resulted in the generation of spontaneous tumors in both transgenic mouse models (113). The Akt1<sup>myr</sup> mice have a permanently activated form of Akt through a myristoylation sequence located in the basal layer of the epidermis while the Akt1<sup>wt</sup> mice express wildtype Akt in the basal layer of the epidermis (113). In addition to enhanced tumorigenesis through activation of the IGF-1/PI3K/Akt pathway, a marked increase in downstream target mTORC1 was also observed in these mice in response to TPA treatment (106, 113). These data suggest that mTORC1 activation may represent an important downstream Akt target and event during skin tumor promotion.

## 1.6 Hypothesis and Specific Aims

The overall goal of this project was to determine the contribution of mTORC1 to epithelial carcinogenesis, specifically during skin tumor promotion using the two-stage model of epithelial carcinogenesis in mouse skin across a range of weight phenotypes. Previous published work from our lab has demonstrated that deregulation and overexpression of Akt in the epidermis leads to enhanced susceptibility to chemical carcinogenesis in mouse skin and generation of spontaneous tumors. Aberrant Akt activity in the epidermis also leads to activation of many downstream effectors of Akt including GSK3 $\beta$ , Bad, and mTORC1 (113). In addition, published data from our lab have shown that DIO and CR differentially modulate the activity of Akt and mTOR in several tissues including the epidermis, and liver-specific IGF-1 deficiency (LID), which results in decreased circulating levels of IGF-1, has been shown to inhibit skin tumor promotion by TPA in mice (18, 43). These data suggest that the differential effects of DIO/CR on Akt and mTOR signaling pathways are mediated partially through IGF-1 and insulin responses. While previous data have shown aberrant activation of Akt during skin tumor promotion and differential regulation of this pathway across the DIO/CR spectrum, specific studies have not been completed to evaluate the independent impact of mTORC1 during tumorigenesis across the spectrum of dietary energy balance in the two-stage model of epithelial carcinogenesis. In this project, we used pharmacological approaches to target mTORC1 in this well-characterized model to test our **hypothesis that mTORC1 signaling plays an important role in tumor promotion and plays an important role in dietary energy balance effects on tumor promotion. mTORC1 is a key target for preventing/controlling obesity related cancers. Selectively targeting mTORC1 will offset the tumor-enhancing effects of obesity and produce calorie restriction mimetic effects.**

**Specific Aim 1: To determine the effect of rapamycin in control, overweight, and obese mice during TPA skin tumor promotion.** Two-stage skin carcinogenesis experiments were completed to examine the impact of mTORC1 inhibition via rapamycin on skin tumor promotion across a range of weight phenotypes via dietary manipulation to test the hypotheses that pharmacological strategies targeting mTORC1 can inhibit skin tumor promotion and offset the effects of overweight and obesity. The findings in this aim will support future translational studies targeting this pathway for the prevention and control of human epithelial cancers.

**Specific Aim 2: To determine the impact of metformin on skin tumor promotion by TPA.** The effects of AMPK activation and mTORC1 inhibition via anti-diabetic drug metformin on skin tumor promotion were evaluated during two-stage skin carcinogenesis experiments. Metformin was administered via the drinking water during the skin tumor promotion stage to overweight and obese mice either alone or in combination with rapamycin. The goal of this aim was to find an agent that could be administered either alone or in combination with rapamycin to target the mTORC1 pathway without dose limiting toxic effects such as drastic deregulation of carbohydrate metabolism. The findings in this aim are significant as they provide evidence that metformin may be more effective in an obese rather than a normal weight population.

**Specific Aim 3: To determine the mechanisms for the effects of rapamycin and metformin on skin tumor promotion by TPA.** The effects of both compounds on TPA-induced epidermal hyperproliferation and inflammation were evaluated as well as TPA-induced epidermal signaling through the Akt/mTORC1 pathway as well as other relevant pathways. In addition, the effects of metformin on circulating serum levels of energy balance related hormones and glucose tolerance were evaluated.

## Chapter 2: Materials and Methods

### *Antibodies, Chemicals and Reagents*

A complete list of antibodies used is located in Table 1. Antibodies were supplied from BD Biosciences (San Diego, CA), CalBioChem (EMD Millipore) (Darmstadt, Germany), Cayman Chemical Co. (Ann Arbor, MI), and Cell Signaling Technologies (Danvers, MA). Chemiluminescence detection kits were purchased from Pierce (Rockford, IL). 7,12-dimethylbenz(a)anthracene (DMBA), Bromodeoxyuridine (BrdU), Metformin (1-1-Dimethylbiguanide hydrochloride), proteinase inhibitor cocktails, phosphatase inhibitor cocktails, anti-actin as well as anti-mouse and anti-rabbit secondary antibodies were purchased from Sigma-Aldrich (St. Louis, MO). TPA was purchased from Alexis Biochemicals (Plymouth Meeting, PA). Rapamycin was purchased from LC Laboratories (Woburn, MA) (114).

### *Mouse Housing and Animal Care*

All housing and mouse procedures were carried out in accordance with the guidelines established by the Institutional Animal Care and Use Committee. Mice were fed *ad libitum* and group housed for the duration of these studies.

### *Dietary Regimens*

For preliminary studies, to achieve a normal weight range, mice were placed on a regular chow diet. For dietary energy balance studies, diets were purchased in pellet form from Research Diets, Inc. (New Brunswick, NJ) (Table 2). Upon arrival, mice were placed on the semipurified control diet (10 kcal% fat, # D12450B) for a one week equilibrium period after which they were randomized into one of two dietary treatment groups: control/overweight (10 kcal% fat), fed *ad libitum*, or DIO (60 kcal% fat, # D12492), fed *ad libitum*. The precise compositions of these diets are found in table 2. Before treatment protocols began, mice

remained on diet for 8 weeks, or until statistically significant weight differences between the groups were achieved.

**Table 1**

Protein	Company	Catalog #
4E-BP1 (Ser65), phospho	Cell Signaling Technologies	9451
4E-BP1 (Thr37/46), phospho	Cell Signaling Technologies	2855
Acetyl-CoA Carboxylase	Cell Signaling Technologies	3662
Acetyl-CoA Carboxylase (Ser79), phospho	Cell Signaling Technologies	3661
Akt	Cell Signaling Technologies	9272
Akt (Thr308) (D9E)XP®, phospho	Cell Signaling Technologies	4056
Akt (Ser473) (D9E)XP®, phospho	Cell Signaling Technologies	4060
AMPK $\alpha$	Cell Signaling Technologies	2532
AMPK $\alpha$ (Thr172), phospho	Cell Signaling Technologies	2531
Beclin-1	Cell Signaling Technologies	3738
COX-2	Cayman Chemicals	160126
LC3B XP®	Cell Signaling Technologies	3868
LKB1	Cell Signaling Technologies	3050
mTOR	Cell Signaling Technologies	2971
mTOR (Ser2448), phospho	Cell Signaling Technologies	2976
NF $\kappa$ B p65	Cell Signaling Technologies	3034
NF $\kappa$ B p65 (Ser536), phospho	Cell Signaling Technologies	3033
p27/kip1	BD Biosciences	610242
p70S6K	Cell Signaling Technologies	9202
p70S6K (Thr389), phospho	Cell Signaling Technologies	9234
PDCD4 XP®	Cell Signaling Technologies	9535
PRAS40 XP®	Cell Signaling Technologies	2691
PRAS40 (Thr246)	Cell Signaling Technologies	2997
S6 Ribosomal Protein (Ser235/236), phospho	Cell Signaling Technologies	2211
S6 Ribosomal Protein (Ser240/244), phospho	Cell Signaling Technologies	2215
ULK1 (Ser555), phospho	Cell Signaling Technologies	5869
ULK1 (Ser757), phospho	Cell Signaling Technologies	6888

**Table 1 List of Antibodies Used**

**Table 2**

Research diets	D12450B Control		D12492 DIO	
	gram% (kcal%)		gram% (kcal%)	
Protein	19.2	(20)	26.2	(20)
Carbohydrate	67.3	(70)	26.3	(20)
Fat	4.3	(10)	34.9	(60)
kcal/g	3.85		5.24	
<b>Ingredient</b>	gram%		gram%	
Casein, 80 Mesh	200		200	
L-Cystine	3		3	
Corn Starch	315		0	
Maltodextrin 10	35		125	
Sucrose	350		68.8	
Cellulose, BW200	50		50	
Soybean Oil	25		25	
Lard	20		245	
Mineral Mix S10026	10		10	
DiCalcium Phosphate	13		13	
Calcium Carbonate	5.5		5.5	
Potassium Citrate, 1 H <sub>2</sub> O	16.5		16.5	
Vitamin Mix V10001	10		10	
Choline Bitartrate	2		2	
FD&C Yellow Dye #5	0.05		0.05	

**Table 2 Nutritional composition of diets used.** Distribution of protein, carbohydrate, fat and ingredient content across the two dietary groups used in dietary energy balance studies. Adapted from Research Diets Inc. product information, 2006.

### *Treatment Regimens*

Female FVB/N mice 6-8 weeks of age were obtained from the National Cancer Institute and group housed for the duration of the study in all experiments. For normal weight mice, treatment protocols began immediately. For dietary energy balance studies, treatments began after 7-8 weeks on various diets. In order to evaluate various protein markers and signaling in the epidermis, groups of 5-6 mice each were dorsally shaved and treated twice weekly for two weeks (i.e. 4 treatments total) with acetone vehicle (0.2 ml), 6.8 nmol of TPA, or various doses of pharmacological inhibitors, rapamycin or metformin. Similar single treatment experiments were also conducted. Rapamycin was dissolved in 0.2 ml of acetone vehicle at doses ranging between 1000 nmol and 2 nmol. For metformin treatment experiments, metformin was administered via the drinking water at the start of the two-week treatment period at doses of 50, 250 or 350 mg/kg body weight per day. It was assumed that each mouse consumed approximately 5 ml of water per day. The metformin treated water was replaced twice weekly and adjusted for changes in body weight every two weeks. Mice were sacrificed 6 hours after final acetone or TPA treatment and pooled epidermal protein lysates were prepared. To histologically evaluate short term markers of skin tumor promotion including epidermal hyperplasia and labeling index (LI), as well as immune cell infiltration, the dorsal skin of mice was shaved and treated. BrdU was administered via i.p. injection (100  $\mu$ g/g body weight) in 0.9% NaCl 30 min prior to sacrifice. Mice were sacrificed 48 hours after the last treatment. Dorsal skin samples were fixed in 10% neutral buffered formalin, stored in 70% ethanol, embedded in paraffin and then sectioned. Sections were cut and stained with H&E, anti-BrdU, or antibodies against LY6G, S100A9, or CD3. Epidermal thickness and labeling index were determined as described previously (115). Dermal immune cell infiltration was determined by the number of positive stained cells per 200  $\mu$ m<sup>2</sup> field (24 fields per slide) (114).

### *Two-Stage Skin Carcinogenesis (Normal Weight)*

Groups of 15-20 female FVB/N mice between 7-9 weeks of age on a regular chow diet were used. 48 hours prior to initiation, the dorsal skins of mice were shaved. Mice were initiated with either a topical application of 25 nmol of DMBA dissolved in 0.2 ml acetone applied to the dorsal skin, or received 0.2 ml vehicle (acetone). Two-weeks after initiation, mice received treatment with various doses of rapamycin administered topically (2 nmol-200 nmol) in 0.2 ml acetone or vehicle (acetone) 30 min prior to promotion with 6.8 nmol of TPA in 0.2 ml acetone. This treatment protocol was continued twice weekly until tumor multiplicity plateaued ( i.e.25 weeks). For regression tumor studies, groups of mice did not receive inhibitor treatment for 15 weeks, in which time skin tumors were generated. Mice were then treated with various doses of topical rapamycin (20 nmol and 100 nmol) with or without continued TPA treatment. Tumor incidence (percentage of mice with papillomas), tumor multiplicity (average number of papillomas per mouse), and mouse weight were recorded weekly for the entirety of the studies (114).

### *Two-Stage Skin Carcinogenesis (Overweight and Obese)*

For diet based tumor studies, mice were initiated with 25 nmol of DMBA or acetone as previously described and were placed on a 10 kcal% fat diet for a two-week equilibrium period and then either continued on this diet, or were placed on the DIO diet (60 kcal % fat), fed *ad libitum*. After 6-8 weeks on the experimental diets mice began treatment with various doses of topical rapamycin dissolved in 0.2 ml acetone or began metformin treatment administered in the drinking water. This was followed by promotion for 25 weeks with 6.8 nmol of TPA twice weekly. Tumor multiplicity, tumor incidence, and mouse weight were recorded each week for the duration of the study. To evaluate the effect of inhibitors on progression (conversion of papillomas to squamous cell carcinomas) treatment protocols



were continued until week 50. During this time carcinoma number and conversion ratios were recorded. Counts were verified histologically by a blinded pathologist.

#### *Preparation of Epidermal Lysates*

Upon sacrifice, a depilatory agent was applied to mouse dorsal skin for 30 s and removed under cool, gently running water. The skin was then excised, and the epidermal layer was removed by scraping with a razor blade into prepared lysis buffer (50 mM Tris-HCl pH 7.4, 150 mM NaCl, 1 mM EDTA, 1 mM sodium orthovanadate, 1% NP-40, phosphatase inhibitor cocktail 1 and 2, proteinase inhibitor cocktail) and then homogenized using an 18-gauge needle. Epidermal scrapings were pooled from 3-6 mice to generate an epidermal protein lysate. These lysates were spun at 14,000 RPM for 15 min, and supernatant was removed. This process was repeated, and the collected supernatant was snap frozen in liquid nitrogen and stored at -80°C until analysis (114).

#### *Western Blot Analysis and Immunoprecipitation*

Protein concentration was determined using the DC (detergent compatible) protein assay from Bio Rad (Lowry). For western blot analysis, 50-75 µg of protein lysate per lane was used. Epidermal protein lysate was electrophoresed in 4-15% SDS-PAGE gels and then transferred onto nitrocellulose membranes (BioRad, Hercules, CA). The criterion precast gel system was utilized (BioRad, Hercules, CA). Membranes were blocked for 1 h in 5% bovine serum albumin (BSA) in TBS with 1% tween (TTBS) and incubated overnight at 4°C with designated antibodies found in Table 1. The membranes were then washed 3 times for 10 min each in TTBS prior to incubation with secondary antibodies for 1 h at room temperature. Additional washes (3 washes, 10 min each) were done to remove unbound secondary antibody, and protein bands were then visualized using a chemiluminescence detection kit (Pierce ECL Western Blotting Substrate, Rockford, IL) (114). For experiments

requiring quantitation, film was scanned manually and densitometry was performed using AlphaView Software: Protein Simple (Santa Clara, CA). Westerns were normalized by dividing the phosphorylated protein density by the total protein density or total actin, and the acetone control was set to 1. For co-immunoprecipitation experiments, epidermal lysates were prepared from CHAPS lysis buffer (30 mM Tris-Cl, pH 7.5, 150 mM NaCl, 1% CHAPS) and were precipitated with raptor (cell signaling) antibody using Dynabead Protein G IP kit (Invitrogen, Carlsbad, CA), and blots were probed for mTOR and raptor (Cell Signaling, Danvers, MA).

#### *Serum Analysis*

Blood was collected from individual mice immediately following CO<sub>2</sub> asphyxiation via cardiac puncture (7-8 mice per treatment/diet group). Blood was allowed to sit at RT for 2 hours and then spun at 7,500 rpm for 7 min. Supernatant was collected and spun again under the same conditions. Serum was then collected and flash frozen in liquid nitrogen and stored at -80° until analysis. Serum levels of insulin and leptin were measured using a 10 µl sample with a Milliplex MAP Mouse Serum Adipokine panel multiplex Luminex Assay (Millipore, Darmstadt, Germany). Serum adiponectin levels were measured using a 10 µl sample with a Milliplex MAP Mouse Serum single plex Luminex Assay (Millipore, Darmstadt, Germany).

#### *Glucose Tolerance Test*

Glucose tolerance tests were performed at week 20 during a diet based tumor study from a randomly selected subset of mice from each treatment/diet group (n=10). Mice were fasted for 12 hours and 20% glucose (2 g/kg body weight via IP) was administered. Blood samples were taken from the tails, and glucose levels were determined at baseline, 30, 60, 90, and

120 min after injections of glucose using the Ascencia Elite XL 3901G Glucose Analyzer from Bayer Corporation (Pittsburgh, PA).

### *Statistical Analyses*

Labeling index (% BrdU positive cells), epidermal thickness ( $\mu\text{m}$ ), and dermal immune cell infiltration (positive cells per field) were presented as the mean  $\pm$  the standard error of the mean, and mean differences were analyzed with the Mann-Whitney *U*-test. To determine minimal sample size for two-stage skin carcinogenesis and diet studies, power calculations were completed using GraphPad Statmate (Lo Jolla, CA). To compare tumor incidence in all two-stage studies, the  $\chi^2$  test was used. For comparison of tumor multiplicity in two-stage studies, the Mann-Whitney *U*-test was again used. Differences in serum levels were analyzed using the Mann-Whitney *U*-test. GraphPad prism was used for all tests unless otherwise noted, and significance was set at  $P < 0.05$  in all cases.

### **Chapter 3-Rapamycin Potently Inhibits Skin Tumor Promotion by TPA in Normal Weight, Overweight, and Obese Mice**

As previously discussed in the Introduction, earlier work from our lab as well as others, suggest that signaling through the PI3K/Akt/mTOR pathway plays a crucial role during epithelial carcinogenesis, specifically during skin tumor promotion by 12-O-tetradecanoylphorbol-13-acetate. During this process, activation of epidermal Akt occurs as well as many downstream Akt effectors including mTORC1. In addition, differential signaling through this pathway across the CR/DIO spectrum has been revealed in a variety of epithelial tissues further supporting the hypothesis that pathways activated in diabetic and high IGF-1 states (such as in DIO) may be the key targets for preventing obesity-driven cancers. While it is clear that deregulated Akt signaling is associated with development and progression of many types of human cancers, Akt's downstream effectors mediating much of these effects has not been as well defined. Because of mTORC1's central role in linking energy and nutrient status to growth factor signaling and subsequent protein synthesis, it was hypothesized that mTORC1 plays a primary role during skin tumor promotion, and its activation and/or repression might be a key mediator between dietary energy balance effects during skin tumorigenesis. In addition, it was hypothesized that pharmacological disruption of mTORC1 may block the harmful effects of DIO and a high-energy diet as well as replicate the benefits associated with CR. In order to address this question, initial experiments were carried out to assess the ability of established mTORC1 inhibitor, rapamycin to block skin tumor promotion by TPA. These experiments utilized female wild-type mice (FVB/N) that were either a normal weight (regular chow diet), overweight (10 kcal% fat), or obese (DIO, 60 kcal% fat). FVB/N mice were chosen as an appropriate strain for these studies. Using an inbred strain helps reduce variability in tumor development. In addition, this strain of mice is moderately sensitive to TPA as a skin tumor promoting agent, typically reaching between 20-100% tumor incidence and up to 11.8 papillomas per mouse

when using DMBA (19.5 to 390 nmol) and TPA (0.8 to 8.0 nmol) (101). In all cases, female mice were used to reduce aggressive behavior and allow for group housing.

### **3-1 Effect of rapamycin on skin tumor promotion in normal weight mice**

Two-stage skin carcinogenesis experiments in FVB/N mice were completed to assess inhibitory effects of rapamycin on skin tumor promotion in normal weight mice. These studies were designed to establish baseline effects of rapamycin on skin tumor promotion as well as provide appropriate doses of rapamycin to be applied topically for use in subsequent dietary energy balance studies.

Groups of female FVB/N mice 7-8 weeks of age were initiated with 25 nmol of DMBA, and then 2 weeks later, treated topically with various doses of rapamycin (5-200 nmol) or acetone vehicle followed 30 min later by 6.8 nmol of TPA. All treatments were given twice weekly for the duration of the experiment (25 weeks). Tumor incidence (percentage of mice with papillomas) and tumor multiplicity were measured weekly for each group. As shown in Figure 3-1A, rapamycin exerted a powerful anti-promoting effect. Treatment groups receiving topical application of 200, 100, or 50 nmol of rapamycin 30 minutes prior to application of TPA, had complete inhibition of papilloma development (Figure 3-1A). In addition, there was also a significant reduction in papilloma development in the groups receiving 20 nmol and 5 nmol doses of rapamycin compared to the DMBA-TPA only control group. In this regard, at week 25 a 92% inhibition of papilloma development was observed in the group receiving 20 nmol of rapamycin prior to TPA, and a 49% inhibition of papilloma development was observed in the group receiving 5 nmol of rapamycin prior to TPA ( $P < 0.05$ , Mann-Whitney  $U$ ) (see again Figure 3-1A). No papillomas developed in the groups initiated with DMBA followed by twice weekly treatments with either acetone or 200 nmol of rapamycin. In addition, we did not observe a significant number of SCCs in any of the groups at the end of the tumor experiment, consistent with previous studies from our laboratory that used an even higher initiating dose of DMBA (116). These studies showed that most SCCs developed in FVB/N mice after 25 weeks of promotion.

Tumor latency was also affected in groups treated with 20 nmol and 5 nmol of rapamycin prior to treatment with TPA. The time to 50% incidence of papillomas in the TPA promotion control group was 10-11 weeks versus 16-17 weeks in the 5 nmol rapamycin treated group (Figure 3-1B). Mice in the 20 nmol rapamycin pretreated group reached only 32% tumor incidence as determined at week 25 (Figure 3-1B). Differences in tumor latency were statistically significant ( $P < 0.05$ ,  $\chi^2$  test). These data clearly show that rapamycin was a potent inhibitor of TPA skin tumor promotion, dramatically reducing both tumor multiplicity and tumor incidence and altering latency in a dose-dependent manner.

On the basis of the data in Figures 3-1A and 3-1B showing that rapamycin dramatically inhibited the promotion of skin tumors, an experiment was conducted to determine whether topical treatments of rapamycin would inhibit growth of existing

papillomas generated by the two-stage protocol. For this experiment, female FVB/N mice 7-8 weeks of age were initiated with 25 nmol of DMBA and promotion was begun two weeks later with 6.8 nmol of TPA. Promotion was continued twice-weekly for 15 weeks. At week 15, mice were randomized into groups that received topical applications of 100 nmol or 20 nmol of rapamycin alone, acetone alone, or rapamycin treatments (100 nmol and 20 nmol) 30 minutes prior to continued promotion with 6.8 nmol of TPA. All treatments continued until week 25. Tumor multiplicity and tumor incidence were determined each week. As shown in Figure 3-1C, topical treatment of rapamycin induced regression or inhibited growth of existing skin tumors. All groups receiving acetone or a dose of rapamycin with or without continued promotion with 6.8 nmol of TPA had statistically significant reductions in tumor multiplicity compared to the group that continued with just 6.8 nmol TPA treatments alone ( $P < 0.05$ , Mann Whitney  $U$ ). At week 25 there was a 48% reduction of papilloma development in the acetone treated group compared to the 6.8 nmol treated group (Figure 3-1C). There was a 74% inhibition in the group receiving 100 nmol of rapamycin alone and a 67% inhibition in the group receiving 100 nmol of rapamycin prior to 6.8 nmol of TPA (Figure 3-1C). There was a 75% inhibition of papillomas in the group receiving 20 nmol of rapamycin alone and a 49% inhibition in the mice receiving 20 nmol of rapamycin prior to treatment with 6.8 nmol of TPA (Figure 3-1C). There were no statistically significant differences in tumor incidence (data not shown). These data indicate that, in addition to dramatically preventing the formation of skin tumors, topically applied rapamycin inhibited growth and/or induced regression of existing papillomas even in the presence of continued TPA treatment. [Reprinted from (114)]

The experiment in Figure 3-1A and B was repeated using similar doses of rapamycin and promoted with 6.8 nmol of TPA for 23 weeks (Figure 3-2A). Results were close to those found in Figures 3-1A and 3-1B. Time to 50% incidence was 10-11 weeks in the TPA control group versus 15-16 weeks in the 5 nmol rapamycin treatment group (Figure 3-2C). There was an 85% inhibition of papilloma development in the 5 nmol rapamycin treatment group and complete inhibition at 200, 100, and 50 nmol of rapamycin (Figure 3-2B). Mouse weight gain was recorded every two weeks for the duration of the study to monitor for any possible toxicity present with rapamycin treatment. Topical rapamycin treatment had no effect on body weight gain in any of the experimental treatment groups for the duration of the study (Figure 3-3).

**Figure 3-1**

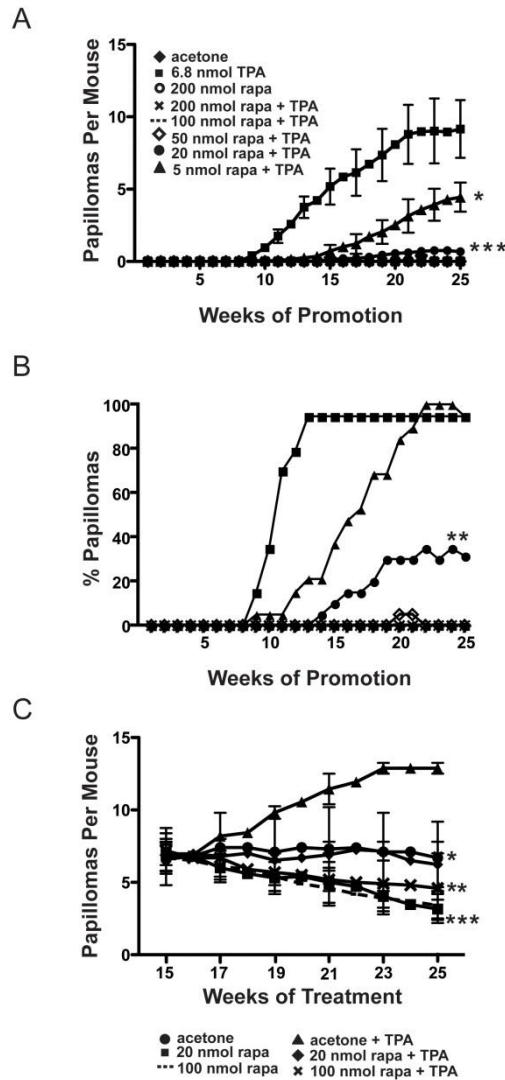


**Figure 3-1 Effect of rapamycin treatment on skin tumor promotion by TPA in normal weight mice.** Female FVB/N mice 7-8 weeks of age were initiated with 25 nmol of DMBA. Two weeks following initiation, mice were treated topically twice weekly with various rapamycin doses or acetone, followed by promotion with 6.8 nmol TPA for 25 weeks. **A)** Tumor multiplicity: Differences in the average number of papillomas per mouse at 25 weeks between 20 nmol (●), 5 nmol (▲) rapamycin treated groups and the corresponding 6.8 nmol TPA (■) treated group were statistically significant (\* $P < 0.05$ , \*\*\* $P < 0.001$ , respectively, Mann-Whitney  $U$ ). **B)** Differences in tumor incidence at 25 weeks between the 20 nmol (●) rapamycin group and the 6.8 nmol TPA (■) group were statistically significant (\*\* $P < 0.01$ ,  $\chi^2$ -test). **C)** Female FVB/N mice 7-8 weeks of age were initiated with 25 nmol of DMBA and two weeks following initiation, promotion began with 6.8 nmol of TPA. After 15 weeks of promotion, mice were randomized to receive either 100 or 20 nmol of rapamycin or acetone either alone or followed by treatment with 6.8 nmol TPA. Differences in tumor multiplicity were statistically significant between the rapamycin treated groups and TPA treated group. Acetone (●) and 20 nmol rapamycin + TPA (◇) groups (\* $P < 0.05$ ), 100 nmol rapamycin + TPA (×) (\*\* $P < 0.01$ ), 20 nmol rapamycin (■) and 100 nmol rapamycin (---) (\*\*\* $P < 0.0001$ ; Mann-Whitney  $U$ ). [Reprinted from (114)]

Figure 3-2

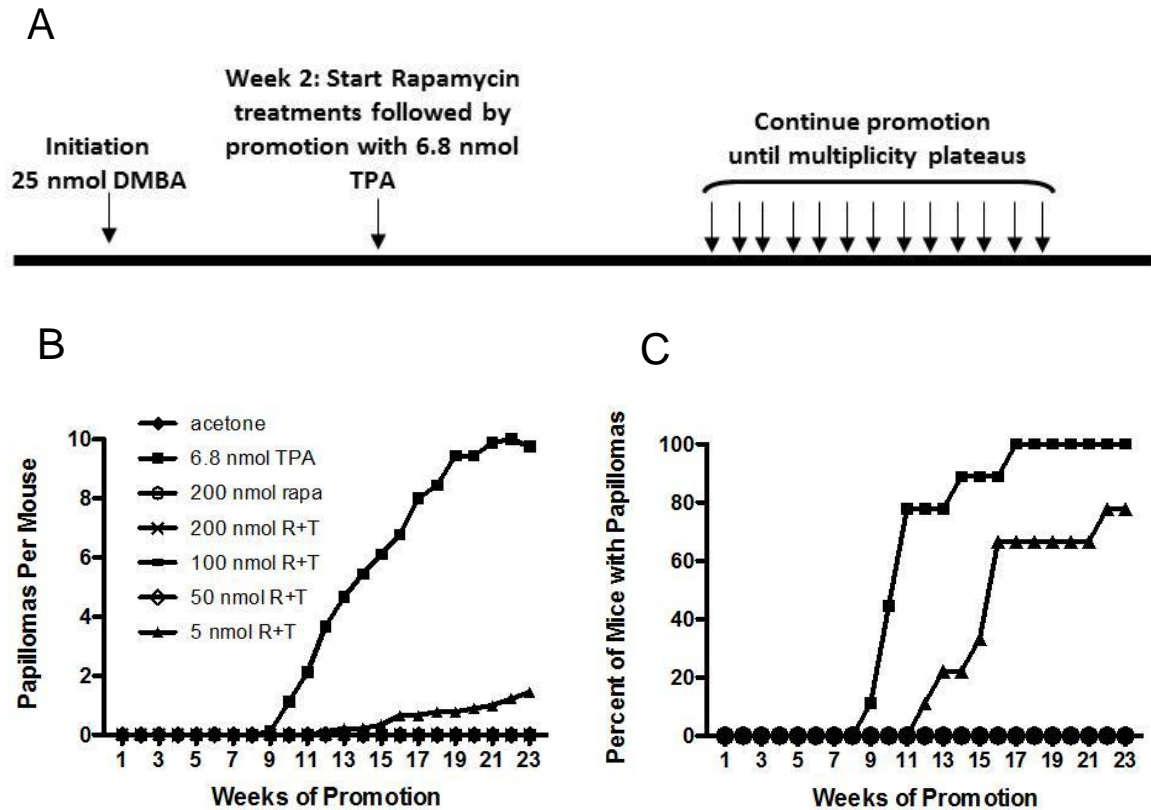


**Figure 3-2 Confirmation of rapamycin' s potent inhibitory effects on skin tumor promotion by TPA.** A two-stage skin carcinogenesis study was repeated to confirm the previous potent reductions seen after topical administration of rapamycin on tumor development. **A)** Treatment protocol: Mice were initiated with 25 nmol of DMBA. Treatment with rapamycin and promotion with TPA began two weeks later. Treatment protocols continued for 23 weeks. **B)** Tumor multiplicity: Differences in the average number of papillomas per mouse at week 23. **C)** Tumor Incidence: Differences in the percent of mice with papillomas at week 23.



**Figure 3-3**

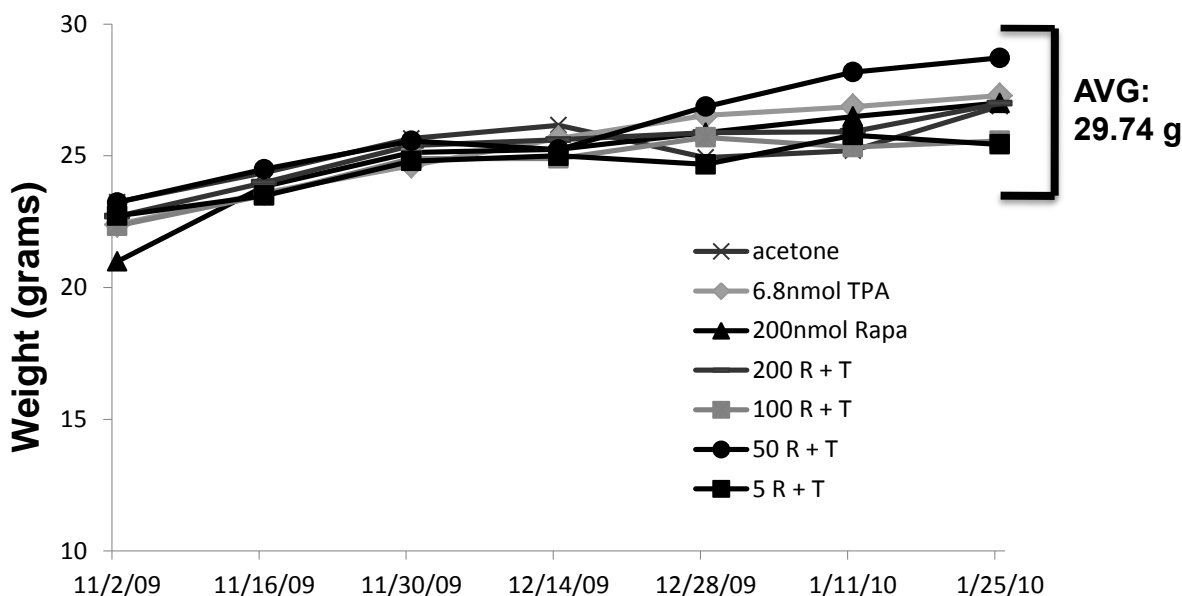


**Figure 3-3 Weight gain of mice during two-stage skin carcinogenesis experiments with topical rapamycin treatment.** There were no significant differences in weight gain across the various acetone, TPA and rapamycin treatment groups for the duration of the 23 week study.

### 3.2 Effect of rapamycin on skin tumor promotion in overweight and obese mice

The previous experiments provided substantial evidence supporting mTORC1's contribution to the process of skin tumor promotion, as rapamycin exerted a powerful anti-promoting effect. Therefore, the ability of rapamycin to reverse the effects of overweight and obesity on tumor development and augment the anticancer benefits of CR in the two-stage model of murine skin carcinogenesis was examined. Inhibition of tumor development with rapamycin in these dietary manipulated groups would also complement previous data from our lab supporting mTORC1's importance in dietary energy balance effects during skin tumorigenesis. For these experiments female FVB/N mice 7-8 weeks of age were initiated with 25 nmol of DMBA. After a two week equilibrium period on control diet, they either continued on this control diet (10 kcal % fat ) fed *ad libitum* or began DIO via the high fat diet (60 kcal % fat) fed *ad libitum* for the duration of the studies. While Research Diets

DI2450B semipurified diet is noted as a “control” diet, previous studies in our lab as well as others (117) have noted that this diet leads to overweight female FVB/N mice as well as C57BL/6nCr based on appropriately corresponding Body Mass Index.

Promotion during these two-stage studies began after 6 weeks on each experimental diet, after which differences in body weights between the two diet groups had reached statistical significance (Figure 3-4D). Mice were treated topically with 20 nmol or 5 nmol of rapamycin 30 min prior to promotion with 6.8 nmol of TPA. All treatments were administered twice weekly for the duration of the experiment. Tumor incidence (percentage of mice with papillomas) and tumor multiplicity (average number of papillomas per mouse) were measured weekly for each group. As shown in Figure 3-4B, rapamycin potently inhibited skin tumor promotion by TPA in the overweight mice. In this regard, groups receiving 5 nmol of topical rapamycin treatment prior to TPA, displayed an 88% reduction in papilloma development at week 25 as compared to the DMBA-TPA control group ( $P < 0.05$ ; Mann –Whitney  $U$ ). In addition, the 20 nmol rapamycin treatment + TPA group had a 97% reduction in papilloma development ( $P < 0.05$ ; Mann –Whitney  $U$ ). The 20 nmol rapamycin treatment + TPA group only resulted in 23% incidence, and the 5 nmol rapamycin treatment + TPA group reached just 43% incidence (Figure 3-4C). Additionally, this diet group was carried out to the progression phase of skin carcinogenesis. Carcinomas were counted weekly, and the average number of carcinomas and conversion ratios were recorded. Treatment protocols continued as previously conducted during promotion and continued until week 50. However, it should be noted that in contrast to papilloma development, the development of SCCs during progression will likely cause mice to die. Thus, for this portion of the tumor study SCC multiplicity and incidence were calculated cumulatively. All SCCs from the tumor bearing mice were carried forward even after sacrifice. As expected, rapamycin inhibited the conversion of papillomas to squamous cell carcinomas in a dose

dependent manner corresponding to decreases in papillomas during skin tumor promotion (Figure 3-5). Carcinoma development was verified histologically by a blinded pathologist.

Figure 3-4

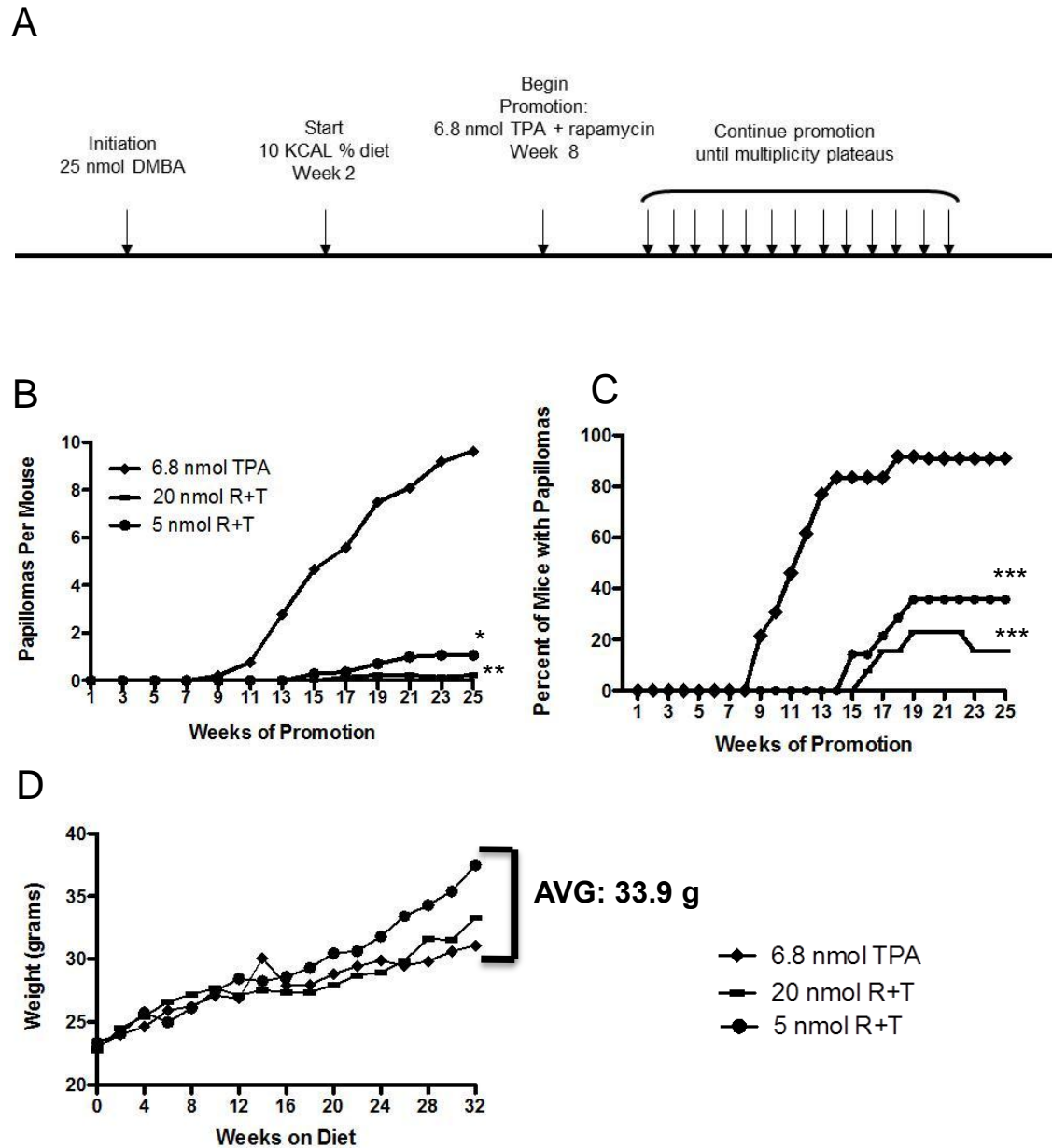


**Figure 3-4 Effect of rapamycin treatment on skin tumor promotion by TPA in overweight/control mice.** Female FVB/N mice 7-8 weeks of age were initiated with 25 nmol of DMBA. **A)** Treatment protocol: At week 2, mice were placed on the 10 kcal% fat diet, fed *ad libitum*. After 6 weeks on diet to allow for weight gain, topical rapamycin treatment began followed 30 min later by promotion with 6.8 nmol TPA. Treatment protocol was continued for 25 weeks. **B)** Tumor multiplicity: Differences in the average number of papillomas per mouse at 25 weeks between 20 nmol (-), 5 nmol (●) rapamycin treated groups and the corresponding 6.8 nmol TPA (♦) were statistically significant, (\*\* $P<0.01$ , \* $P<0.05$ , respectively, Mann-Whitney  $U$ ). **C)** Differences in tumor incidence at 25 weeks between 20 nmol (-), 5 nmol (●) rapamycin group and the 6.8 nmol TPA (♦) group were statistically significant (\*\* $P<0.001$ ,  $\chi^2$ -test). **D)** There were no statistically significant differences in weight gain between any of the treatment groups.

**Figure 3-5**

Treatment Group	Total Number of Mice <sup>1</sup>	Average Papillomas Per Mouse <sup>1</sup>	Carcinoma Incidence (%)	Carcinomas per Mouse	Conversion Ratio <sup>2</sup>
6.8 nmol TPA	11	9.54	100.0	2.44	0.26
5 nmol R+T	13	1.14 <sup>a</sup>	46.2	0.53 <sup>a</sup>	0.46
20 nmol R+T	13	0.31 <sup>a</sup>	7.7	0.08 <sup>a</sup>	0.26

**Figure 3-5 Rapamycin decreases squamous cell carcinoma development in control/overweight mice (10 kcal % fat).** <sup>1</sup>Data taken at 27 weeks of promotion with 6.8 nmol TPA after which the papilloma response had reached a plateau. <sup>2</sup>Ratio of the average number of SCCs at 49 weeks to average number of papillomas at 27 weeks  
<sup>a</sup>Denotes significantly different from DMBA/TPA control;  $P<0.05$ , Mann Whitney  $U$ ).

In the obese mice, there were dramatic decreases in papilloma development and tumor burden. In a similar protocol with the exception of the high-fat diet in place of control/overweight diet, (Figure 3-6A), two-stage studies revealed potent inhibition of tumor development in the obese mice. In addition, rapamycin appeared to be slightly more effective in the obese mice with a 98% inhibition of tumor development in the 20 nmol rapamycin + TPA treatment group and a 94% inhibition in the 5 nmol rapamycin + TPA treatment group as compared to the DMBA-TPA control group (Figure 3-6B). In terms of tumor incidence, there were also dramatic responses as the 20 nmol rapamycin treatment group was just under 7% incidence at week 25, and the 5 nmol rapamycin treatment group was just under 29% incidence (Figure 3-6C).

Rapamycin caused no significant decreases in overall body weight throughout the duration of the study. There were however significant differences in overall body weight between the overweight ( $33.9 \pm 1.90$ ) and obese mice ( $44.9 \pm 0.84$ ) as expected ( $P < 0.05$ , Mann Whitney *U*), (Figure 3-4D and 3-6D).

The results presented in this chapter support previous findings that mTORC1 plays an important role in skin tumor promotion. Data from previous two-stage carcinogenesis experiments in our lab using transgenic Akt and IGF-I mice, overexpressing these proteins in the epidermis support the hypothesis that Akt levels elevated in the epidermis increase susceptibility to epithelial carcinogenesis. These mice displayed heightened epidermal hyperproliferation as well as increases in mTORC1 activation in response to TPA treatment (111, 113, 118). Lu and colleagues reported that activation of mTORC1 activator, Rheb led to spontaneous skin tumor development in a DMBA-induced tumorigenesis model (119) lending to additional overall support of this hypothesis. In addition, this data also support a role for mTORC1 activation in the link between obesity and epithelial carcinogenesis consistent with previous data. In terms of dietary energy balance, Moore and colleagues demonstrated that dietary energy balance modulation results in differential signaling

through the cell surface receptors, IGF-1R and EGFR and downstream substrates. In a variety of epithelial tissues, DIO enhanced, while CR reduced signaling through these receptors and downstream to Akt and mTOR (43). Another study showed that LID mice with a 75% reduction in circulating levels of IGF-1 reduced skin tumor development in the two-stage model of skin carcinogenesis and reduced activation of Akt and mTOR (18).

Overall, these findings show that rapamycin on a molar basis, is one of the most effective inhibitors of skin tumor promotion to date. When rapamycin is topically applied to mouse skin prior to promotion with TPA, it potently inhibits this stage in a dose-dependent manner as well as inhibits growth of existing skin tumors. In addition, rapamycin appears to reverse the effects of overweight and obesity on skin tumorigenesis and may be more effective in these dietary energy balance groups.

**Figure 3-6**

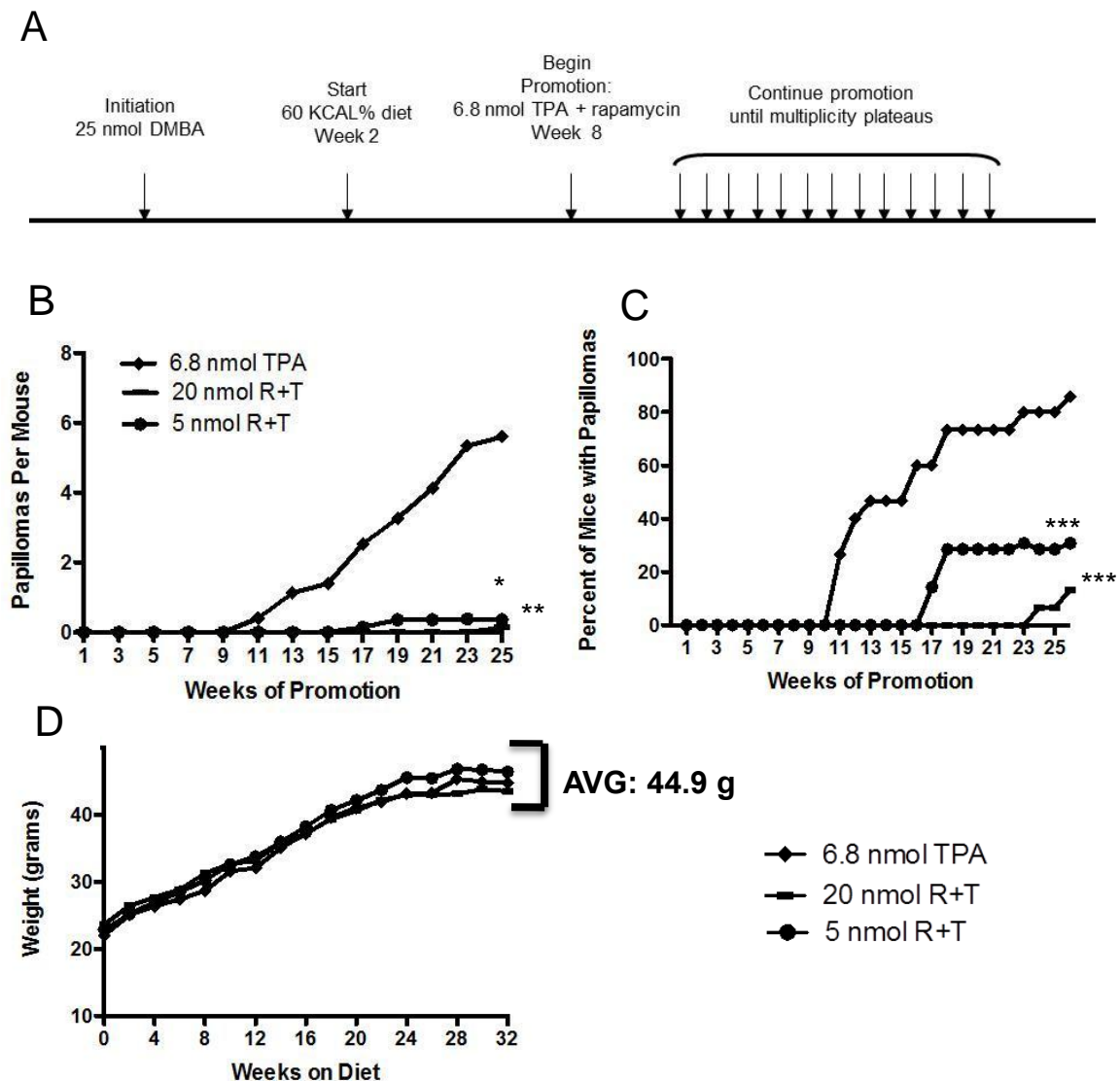


**Figure 3-6 Effect of rapamycin treatment on skin tumor promotion by TPA in obese mice.** Female FVB/N mice 7-8 weeks of age were initiated with 25 nmol of DMBA. **A)** Treatment protocol: At week 2, mice were placed on the high fat diet, DIO (60 kcal% fat diet, fed *ad libitum*). After 6 weeks on diet, topical rapamycin treatment began followed 30 min later by promotion with 6.8 nmol TPA. Treatment protocol was continued for 25 weeks. **B)** Tumor multiplicity: Differences in the average number of papillomas per mouse at 25 weeks between 20 nmol (-), 5 nmol (●) rapamycin treated groups and the corresponding 6.8 nmol TPA (◆) were statistically significant, (\*\* $P < 0.01$ , \* $P < 0.05$ , respectively, Mann-Whitney  $U$ ). **C)** Differences in tumor incidence at 25 weeks between 20 nmol (-), 5 nmol (●) rapamycin group and the 6.8 nmol TPA (◆) group were statistically significant (\*\* $P < 0.001$ ,  $\chi^2$ -test). **D)** There were no statistically significant differences in weight gain between any of the treatment groups.

#### **Chapter 4- Metformin Given in the Drinking Water Attenuates Skin Tumor Promotion in Overweight and Obese Mice**

The class of pharmacological agents targeting PI3K, Akt, and mTOR are not expected to be highly tumor-specific and thus inhibition of this pathway in normal tissue as well as tumor tissue is expected to occur in response to use of these therapies. Thus targeting PI3K or signaling nodes downstream of this pathway has been associated with large systemic effects including deregulation of carbohydrate metabolism and insulin signaling. This can result in hyperglycemia due to decreases in glucose uptake by the muscles and hyperinsulinemia (120). The subsequent insulin resistance that occurs may limit the efficacy of the many PI3K and downstream inhibitors, including mTORC1 inhibitor rapamycin. In addition, treatment with mTORC1 inhibitors such as rapamycin has been associated with inhibition of the p70S6K-IRS-1 negative feedback loop. This mTORC1 dependent feedback loops acts to inhibit activation of the PI3K/Akt pathway as IRS-1's inhibitory sites are bound by mTOR and p70S6K (70, 121). When pharmacological doses of mTORC1 inhibitors are great enough to interrupt this feedback loop, activation of Akt occurs resulting in a limitation of the antineoplastic effects of this class of inhibitors.

In the previous two-stage skin carcinogenesis experiments performed, rapamycin was utilized as a topical treatment applied directly to the epidermis resulting in limited systemic effects. In addition, despite the possibility of negative feedback loop inhibition, all doses of rapamycin used caused significant decreases in tumor development as previously shown in Chapter 3. However, other treatment options were explored targeting this pathway that could be administered orally or in combination with rapamycin without efficacy interference or dose-limiting toxicity. In addition, when using rapamycin, there was a large decrease in inflammation associated with use of TPA possibly accounting for much of rapamycin's anti-cancer effects, thus studies were conducted to explore another mTORC1 inhibitor that might not have such dramatic effects on TPA-induced inflammation making it



easier to attribute decreases in tumor burden to mTORC1 inhibition. The data displaying rapamycin's mechanisms of action are shown and discussed in more detail in Chapter 5. The effect of the type II diabetes drug, metformin administered via the drinking water on skin tumor promotion by TPA was investigated next. Many population based studies have provided evidence that patients with type II diabetes treated with metformin have reduced cancer incidence as well as reduced mortality (89, 90). In addition, a variety of *in vitro* and *in vivo* studies have also supported this association.

As discussed in the Introduction, metformin inhibits gluconeogenesis and thus lowers overall circulating levels of glucose and subsequently insulin, thereby treating diabetes. It does this through activation of the LKB1/AMPK pathway in the liver. In contrast to PI3K and downstream inhibitors, metformin's mode of action should not interfere with efficacy or disrupt normal metabolic function. In fact, it should attenuate the hyperglycemia and insulinemia associated with PI3K/Akt/mTOR inhibitors and contribute to antineoplastic activity either indirectly through its insulin lowering effects or directly through AMPK activation and subsequent mTORC1 inhibition in cancer cells. Metformin treatment has also been associated with decreases in Akt activation in many tumor types lending to its overall efficacy (95, 96). This could further support its promising role as a monotherapy or in combination therapies with the PI3K and downstream class of inhibitors.

Because most epidemiological data supporting metformin's antineoplastic activity was obtained from a diabetic population displaying high rates of hyperinsulinemia and obesity, studies were designed specifically to evaluate the effectiveness of metformin in the two-stage skin chemical carcinogenesis model system in obese mice. Obesity was generated via administration of a high-fat diet (DIO, 60 kcal % fat) that elevated insulin levels and caused dramatic weight gain. The control diet (10 kcal % fat) was considered to cause mice to become modestly overweight. In addition, a dual targeting therapy was designed in which metformin was administered in combination with rapamycin to test for an

additive effect. Ideally, the effectiveness of this combination would be achieved with very low doses of each compound.

#### **4.1 Metformin administered via the drinking water attenuates TPA skin tumor promotion in overweight mice**

To evaluate the effect of oral administration of metformin via the drinking water on skin tumor promotion by TPA in overweight mice, female FVB/N 6-7 weeks of age were initiated with 25 nmol of DMBA. They continued on the overweight/control diet (10 kcal % fat) fed *ad libitum* to generate an overweight phenotype for the duration of the studies. After a 6 week period on diet, metformin was added to the drinking water at doses of 50 mg/kg body weight per day or 250 mg/kg body weight per day. Thus it could be assumed that a 30 g mouse drinking approximately 5 mls of water per day would receive 1.5 mg of metformin administered as 5 mls of a 0.30 mg/ml solution. These doses were chosen based on previous data from the literature that demonstrated doses ranging from 50 mg/kg body weight per day to 350 mg/kg body weight per day in the drinking water or diet was sufficient to demonstrate antineoplastic effects *in vivo* (98-100, 122, 123). Additionally, *in vivo* data also showed that much higher doses used actually had the opposite effect on tumor growth. Phoenix and colleagues reported that metformin administered at 750 mg/kg body weight per day increased tumor growth and angiogenesis in a xenograft model using ER $\alpha$  negative MDA-MB-435 cells (124). This dose is about 45 fold the recommended human dose administered (125). Promotion with 6.8 nmol of TPA applied topically was also begun at this time (Figure 4-1A). Promotion with TPA was continued twice weekly for the duration of the experiment and metformin was replaced fresh in the drinking water twice weekly. Tumor incidence and tumor multiplicity were measured weekly for each diet/treatment group. As shown in figure 4-1B, metformin at both doses significantly attenuated skin tumor promotion in a dose dependent manner.

**Figure 4-1**

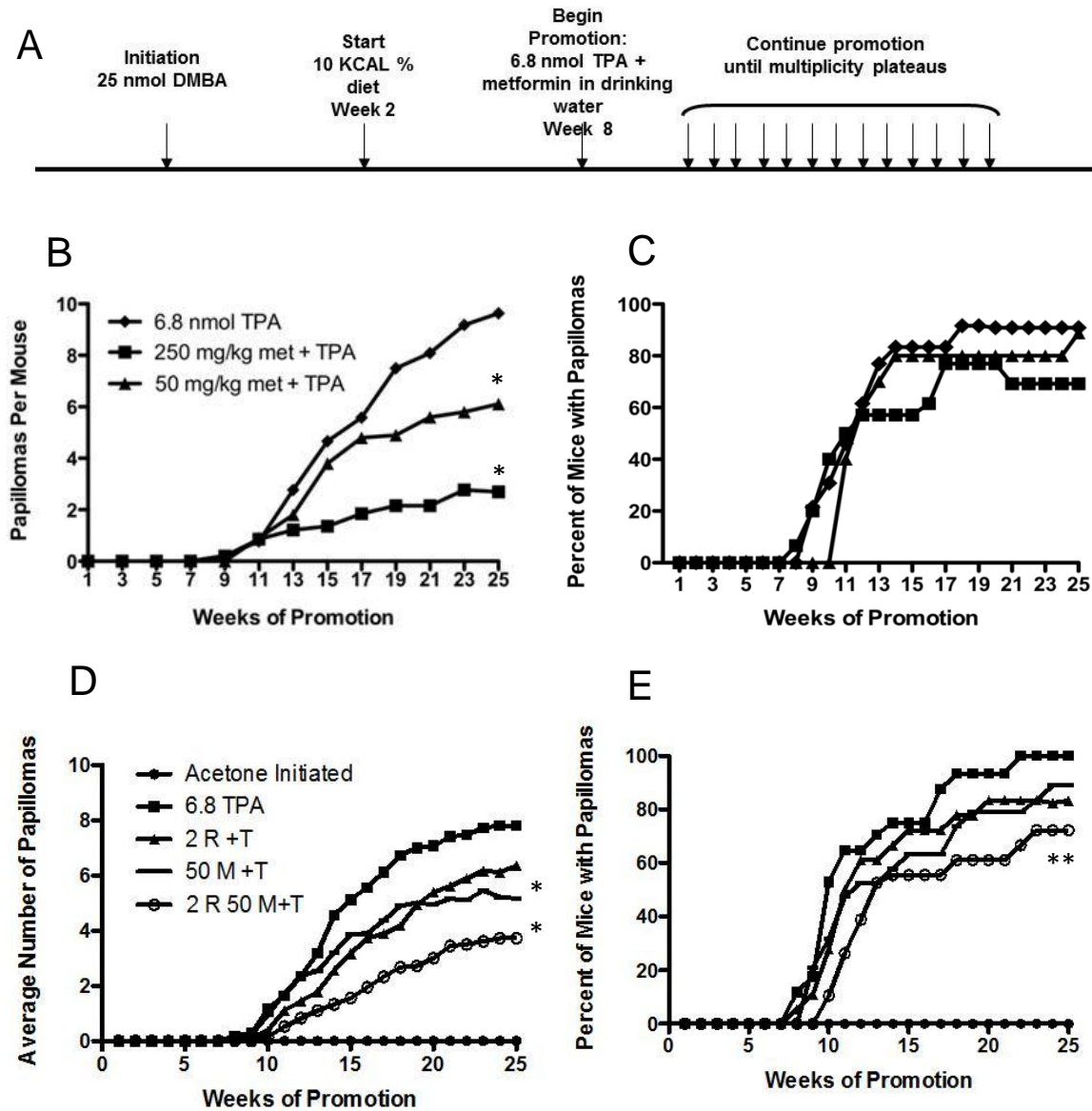


**Figure 4-1 Metformin alone and in combination with rapamycin attenuates skin tumor promotion in overweight mice.** **A)** Female FVB/N mice 7-8 weeks of age were initiated with 25 nmol of DMBA. Mice were then placed on the overweight/control diet (10 kcal % fat). After 6 weeks on diet, mice were administered metformin via the drinking water and promotion began with TPA. In experiments with combination treatments, 2 nmol of rapamycin was applied topically 30 min prior to TPA. **B)** Differences in tumor multiplicity at 25 weeks between the metformin + TPA treated groups and the DMBA-TPA control group were significantly different at both doses (\*,  $P < 0.05$ , Mann-Whitney U). **C)** Differences in tumor incidence at 25 weeks were not statistically significant between any treatment groups. **D)** Both the 50 mg/kg metformin + TPA group (---) and the combination treatment group (o) were statistically significant from the DMBA control group (■) in terms of tumor multiplicity. **E)** Differences in tumor multiplicity between the combination treatment group (o) and the DMBA-TPA (■) control group were statistically significant (\*\*,  $P \leq 0.01$ ,  $\chi^2$ -test).

In this regard, a 72% inhibition of papilloma development in the 250 mg/kg body weight per day dose and a 36% inhibition in tumor development in the 50 mg/kg body weight per day dose were observed after metformin treatment. While tumor latency was not affected with either dose of metformin, there was a modest decrease in tumor incidence at the highest dose used (Figure 4-1C). The DMBA-TPA control group displayed 91% tumor incidence as compared to 69% incidence for the 250 mg/kg dose of metformin and 89 % incidence for the 50 mg/kg dose of metformin. This tumor study was also carried out to carcinomas to evaluate metformin's effect on the conversion of papillomas to carcinomas and conversion ratios. As expected, metformin decreased the number of squamous cell carcinomas in both treatment groups in a dose dependent manner that corresponded to the average number of papillomas recorded. Metformin also had no effect on the malignant conversion ratio (Figure 4-2).

**Figure 4-2**

Treatment Group	Total Number of Mice <sup>1</sup>	Average Papillomas Per Mouse <sup>1</sup>	Carcinoma Incidence (%)	Carcinomas per Mouse	Conversion Ratio <sup>2</sup>
6.8 nmol TPA	11	9.54	100.0	2.44	0.26
50 mg/kg M+T	9	6.22 <sup>a</sup>	75.0	1.75 <sup>a</sup>	0.28
250 mg/kg M+T	10	2.69 <sup>a</sup>	70.0	0.70 <sup>a</sup>	0.26

**Figure 4-2 Metformin decreases the number of SCCs and does not alter the rate of malignant conversion in overweight mice** <sup>1</sup>Data taken at 27 weeks of promotion with 6.8 nmol TPA after which the papilloma response had reached a plateau. <sup>2</sup>Ratio of the average number of SCCs at 49 weeks to average number of papillomas at 27 weeks. <sup>a</sup>Denotes significantly different from the DMBA/TPA control group. (  $P < 0.05$ , Mann Whitney  $U$  )

This study was followed by a repeat two-stage skin carcinogenesis study with the addition of a rapamycin/metformin combination treatment group. For this tumor experiment, the effects of low doses of metformin and rapamycin alone or in combination on skin tumor development were evaluated. There was approximately 52% inhibition of papilloma development with the rapamycin/metformin + TPA combination treatment group compared to the DMBA-TPA control group. This was more effective than either compound alone as 50 mg/kg metformin + TPA, similar to the initial experiment, displayed 34% inhibition, and the 2 nmol rapamycin + TPA displayed 19% inhibition of papilloma development (Figure 4-1D). As in the previous tumor experiment, there were modest effects on tumor incidence with each treatment regimen. There was 82% tumor incidence in the 2 nmol rapamycin + TPA treated group, 89% incidence in the 50 mg/kg metformin + TPA treated group, and 72% incidence in the combination treated group compared to 100% tumor incidence in the DMBA-TPA control group (Figure 4-1E).

#### **4.2 Metformin administered via the drinking water potentially inhibits skin tumor promotion by TPA in obese mice**

During this experiment, a high fat diet group was also included to determine whether metformin was more highly effective in the obese mice. In a similar treatment protocol outlined in figure 4-4A, mice were initiated with 25 nmol of DMBA and then placed on the control diet (10 kcal% fat) for a two week equilibration period. They were then placed on the high fat diet (DIO, 60 kcal% fat) for the duration of the study. Weight distributions of both the control/overweight 10 kcal% diet and the high fat, DIO 60 kcal % diet can be found in Figure 4-3. The differences in average body weight between the two diet groups were statistically significant as expected ( $P \leq 0.05$ , Mann-Whitney  $U$ ). However, within a given diet, neither metformin nor rapamycin caused any significant differences in body weight gain between treatment groups. After 6 weeks on diet, mice began metformin treatment in the drinking water at doses of 250 and 50 mg/kg body weight per day or received a very low

dose of rapamycin (2 nmol) alone or in combination with the low dose of metformin (50 mg/kg). Promotion with 6.8 nmol of TPA was also begun at this same time point and was continued for the duration of the study (25 weeks). In all treatment groups, there was greater inhibition in the DIO group in terms of tumor multiplicity (Figure 4-4B). There was 42% inhibition of papilloma development in the DIO, 2 nmol rapamycin + TPA group compared to just 19% in this same treatment group in the control/overweight mice. The DIO, 50 mg/kg metformin + TPA treatment group displayed 44% inhibition versus 34% in the control/overweight group, and the combination group displayed 62% inhibition as compared to 52% inhibition in the control/overweight group. Tumor multiplicity and percent inhibition in each diet/treatment group are summarized in Figure 4-5. In terms of tumor incidence, there were modest decreases with each treatment group as compared to the DMBA-TPA control group as the 2 nmol rapamycin + TPA treatment group reached 84% incidence, the 50 mg/kg metformin + TPA group reached 93% incidence and the 250 mg/kg metformin + TPA group reached 83% incidence as compared to 100% incidence in the DMBA-TPA control group (Figure 4-4C). In addition, there were differences in tumor latency between the treatment groups and the DMBA-TPA control group. Time to 50% incidence was 13-14 weeks in the single compound treatment groups (i.e. 250 mg/kg or 50 mg/kg met + TPA, 2 nmol rapamycin + TPA) compared to 8-9 weeks in the DMBA-TPA control group. In addition, the combination treatment group did not reach 50% incidence until week 16 (Figure 4-4C).

**Figure 4-3**

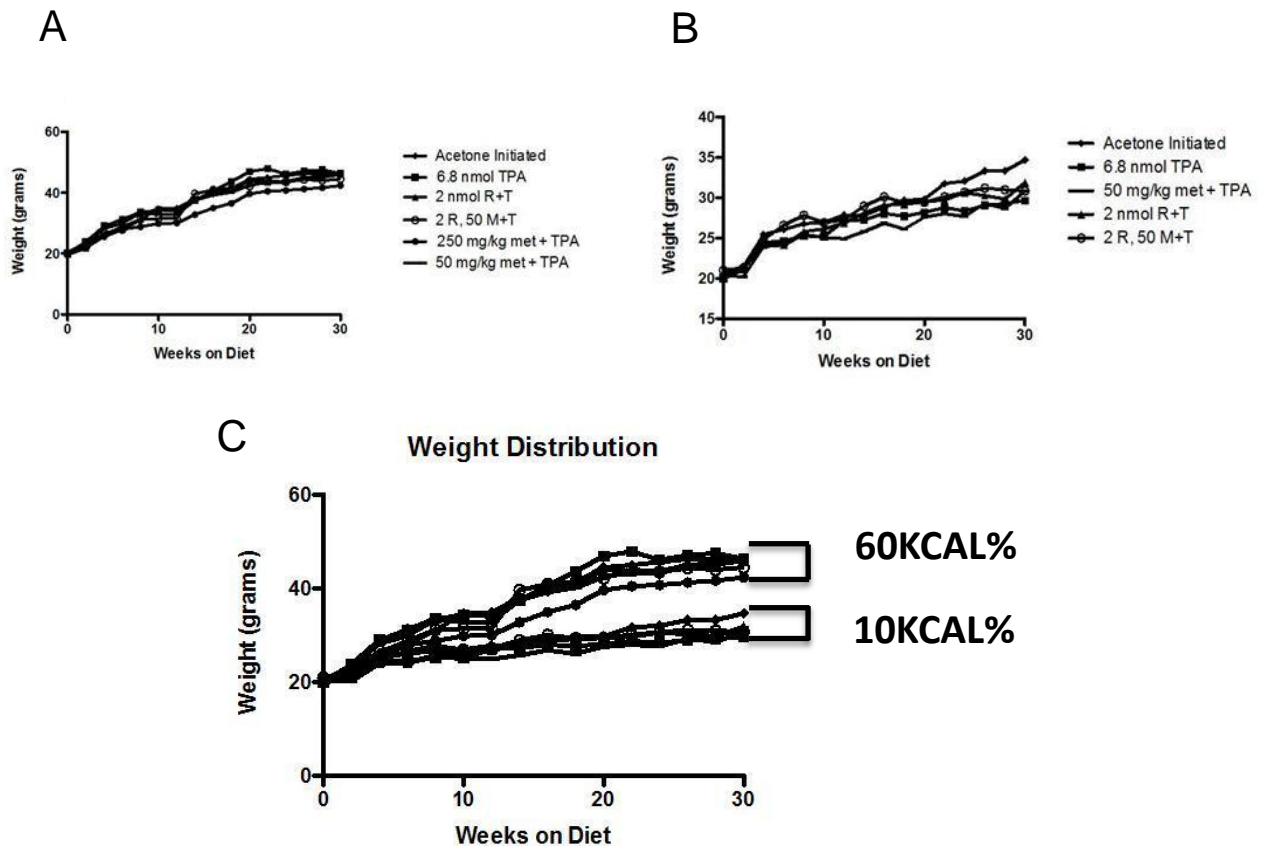


**Figure 4-3 Metformin and rapamycin did not significantly alter weight gain in mice on control (overweight) or obesity inducing diets** **A)** Weight gain throughout 30-week period for mice receiving DIO, high fat diet (60 kcal % fat). Mice were weighed weekly for duration of experiment. Differences in weight between treatment groups were not significant. **B)** Weight gain throughout 30-week period for mice receiving control/overweight diet (10 kcal% fat). Mice were weighed weekly for the duration of experiment. Differences in weight between treatment groups were not significant. **C)** The differences between body weights between the two diet groups were statistically significant ( $31.6 \pm 0.86$  vs.  $45.2 \pm 0.63$ ,  $P \leq 0.05$ , Mann-Whitney  $U$ ).

**Figure 4-4**

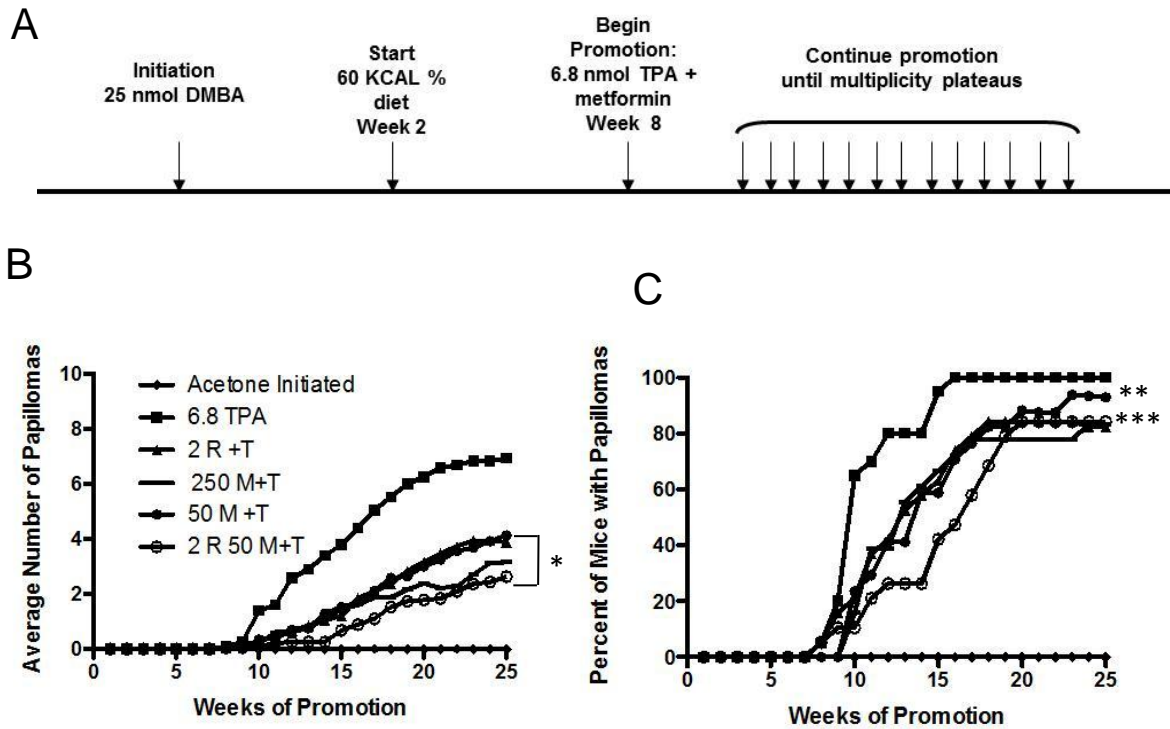


**Figure 4-4 Metformin given in the drinking water is a potent inhibitor of skin tumor promotion by TPA in obese mice. A)** Female FVB/N mice 7-8 weeks of age were initiated with 25 nmol of DMBA. Mice were then placed on the control diet (10 kcal % fat). After a 2 week period to equilibrate, mice were placed on the high fat diet (DIO, 60 kcal % fat). After 6 weeks on diet, mice were administered metformin via the drinking water, and promotion began with 6.8 nmol of TPA. In experiments with combination treatments, 2 nmol of rapamycin was applied topically 30 min prior to TPA. **B)** Differences in tumor multiplicity at 25 weeks between the 250 mg/kg metformin + TPA (--) or 50 mg/kg metformin + TPA (●) and the DMBA-TPA control group (■) were statistically significant. In addition, differences in tumor multiplicity between 2 nmol rapamycin + TPA (▲) or the combination group, 2 nmol rapamycin, 50 mg/kg metformin + TPA (○) were statistically significant (\*,  $P < 0.05$ , Mann-Whitney  $U$ ). **C)** Differences in tumor incidence at 25 weeks between 2 nmol rapamycin + TPA (▲), 250 mg/kg metformin + TPA (--), or 2 nmol rapamycin, 50 mg/kg metformin + TPA (○) and the DMBA-TPA control group (■), were statically significant (\*\*,  $P < 0.01$ , \*\*\*,  $P < 0.001$ ,  $\chi^2$ -test).



**Figure 4-5**

Group Number	Diet Group	Treatment Group	Number of Mice	Avg Papillomas Per Mouse	% Inhibition
1	10 KCAL %	TPA (6.8)	15	7.80	--
2	10 KCAL %	2 R+T	18	6.35	19
3	10 KCAL %	50 M+T	18	5.16	34
4	10 KCAL %	2 R, 50 M+T	18	3.72	52
5	60 KCAL %	TPA (6.8)	18	6.94	--
6	60 KCAL %	2 R+T	19	4.00	42
7	60 KCAL %	50 M+T	15	3.92	44
8	60 KCAL %	250 M+T	18	3.16	54
9	60 KCAL %	2 R, 50 M+T	18	2.64	62

**Figure 4-5 Summary of the effects of metformin and rapamycin on skin tumor promotion in overweight and obese mice.** Figure represents data collected at 27 weeks of tumor promotion with 6.8 nmol of TPA after which papilloma response had reached a plateau. Metformin, rapamycin and combination treatments appeared to be more highly effective in the obese mice (60 kcal % fat).

### 4.3 Metformin and rapamycin reduce skin tumor size in overweight and obese mice

In addition, the impact of diet and metformin or rapamycin treatment on tumor growth was analyzed. As shown in Chapter 3, treatment with rapamycin to existing skin tumors led to decreases in the size of pre-existing papillomas in mice of a normal weight, so a similar effect on tumor growth with rapamycin and possibly metformin in the context of dietary energy balance was expected. During week 23 of the two-stage study, a representative subset of papillomas (approx. 25) from each treatment and diet group was measured to determine average surface area. The DIO, high fat diet DMBA-TPA control group was associated with an increase in tumor growth and overall tumor size as compared to the DMBA/TPA, overweight/control group (tumor size of  $30 \pm 3.2 \text{ mm}^2$  for DIO vs  $20 \pm 2.6 \text{ mm}^2$  for control diet,  $P \leq 0.05$ , Mann-Whitney  $U$ ) (Figure 4-6). In response to treatment with either rapamycin or metformin, tumor size was reduced in both dietary groups. In addition, the effect appeared to be additive with the combination treatment group. While there were reductions in tumor size with each diet and treatment regimen, the effect was more pronounced in the obese mice, with significant differences seen in all treatment groups. In terms of the percent of reduction in tumor size, groups receiving 2 nmol rapamycin + TPA displayed 46% reduction in tumor size in the DIO diet as compared to just 18% in the control/overweight diet. In groups receiving 50 mg/kg metformin + TPA, the DIO group displayed a 60% decrease in tumor size versus 43% decrease in the control/overweight diet group. The combination treatment groups in both diet groups had similar percentages of reductions in tumor growth (69% in DIO group vs. 67% in control/overweight group). This data further shows the inhibitory effects of both rapamycin and metformin on skin tumor promotion during dietary energy balance effects. Furthermore, this data also provides evidence to suggest that each of these compounds may be more highly effective in an obese state.

Figure 4-6

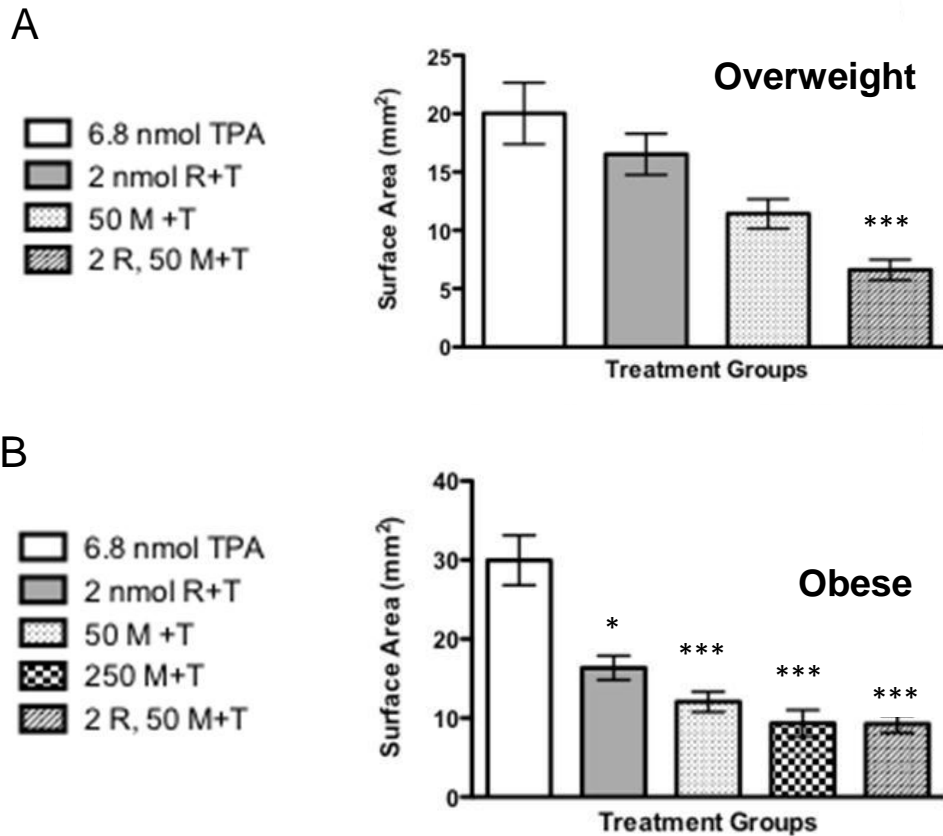


**Figure 4-6 Metformin and rapamycin treatment reduced the size of skin tumors in both overweight and obese mice.** Impact of diet and metformin and/or rapamycin treatment on tumor growth in mice. **A)** Average surface area of a random subset of papillomas taken at week 23 during two-stage study from overweight mice. Graphs represent the average surface area  $\pm$  SEM. The combination treatment group's papilloma size (2 nmol rapamycin, 50 mg/kg metformin + TPA) was significantly smaller than the DMBA-TPA control group papilloma size (\*\*\*,  $P > 0.001$ , Kruskal Wallis Test). **B)** Average surface area of a random subset of papillomas taken at week 23 during two-stage study from obese mice. Graph represents the average surface area  $\pm$  SEM. Differences in tumor size in all treatment groups were statistically significant from the DMBA-TPA control group. (\*,  $P > 0.05$ , \*\*\*,  $P > 0.001$ , Kruskal Wallis Test).

## **Chapter 5: Mechanisms Associated with the Inhibitory Effects of Rapamycin and Metformin on Skin Tumor Promotion by TPA**

After obtaining promising, highly reproducible skin tumor data from two-stage skin carcinogenesis experiments demonstrating the inhibitory effects of both rapamycin and metformin on skin tumor promotion by TPA, the underlying mechanisms behind the efficacy of these chemopreventive agents were explored. The two-stage skin carcinogenesis model has proven very useful in defining various stages of epithelial carcinogenesis as well as biochemical events that are associated with each stage (126). Thus a number of short term markers are available that enable us to study the underlying molecular mechanisms of various modifying factors (i.e. compounds, dietary energy balance manipulation) on tumor response. For instance, the tumor promotion stage is associated with the selective clonal expansion of initiated cells. Furthermore, this stage is characterized by heightened and sustained hyperplasia prior to the development of small exophytic skin tumors referred to as papillomas. Previous, published data has also well characterized the expression of many proteins during both the promotion and progression phases of skin tumorigenesis some of which include  $\gamma$ -glutamyltransferase, keratin-8, keratin-1, E-cadherin and loricrin (101). In addition, tumor promoter activation of several PKC isoforms is critical for the induction of proliferation and inflammation. Particularly, their activation results in the secretion of several pro-inflammatory molecules from keratinocytes which result in further recruitment of macrophages, leukocytes, and lymphocytes involved in the innate immune response into the dermal compartment. These activated cells are then able to further promote cellular proliferation, angiogenesis, and suppression of adaptive immunity through secretion of various cytokines, chemokines and growth factors thus facilitating skin tumor promotion (127).

Furthermore, in the context of dietary energy balance, more recent data has emerged elucidating possible mechanisms through which CR or DIO may affect the

carcinogenic process. In this section, mechanisms associated with the differential effects of these compounds or agents on dietary energy balance manipulation during skin tumor promotion are studied.

### **5-1 Rapamycin inhibits TPA-induced epidermal hyperproliferation**

Sustained cellular proliferation in the epidermis leads to chronic hyperplasia which is a hallmark of skin tumor promotion. In addition, short term markers of this including BrdU incorporation (labeling index) and epidermal thickness have become reliable predictors of tumor promoting capabilities of compounds as well as the effectiveness of inhibitor compounds (126). After the dramatic effects of rapamycin on skin tumor promotion by TPA were witnessed, the effect of rapamycin on TPA-induced epidermal hyperproliferation and hyperplasia in mice of a normal weight was explored.

For these experiments, groups of female FVB/N mice 7-8 weeks of age were treated topically with acetone (vehicle) or various doses of rapamycin (5-200 nmol) followed 30 min later by 6.8 nmol of TPA. This treatment regimen was continued twice-weekly for two weeks (i.e. 4 treatments total), and mice were sacrificed 48 hours after the final treatment. After sacrifice, the skin was removed and processed for histological examination. Whole skin sections were evaluated for epidermal hyperplasia (as measured by epidermal thickness) and epidermal LI (as measured by BrdU incorporation). Figure 5-1A shows representative H&E and BrdU stained sections of dorsal skin after multiple treatments with either acetone, 6.8 nmol TPA, or 200 nmol of rapamycin followed by 6.8 nmol of TPA. Visual inspection of the sections revealed that rapamycin significantly reduced epidermal hyperplasia as well as LI when applied 30 minutes prior to TPA application. Quantitative analyses of the effect of rapamycin on TPA induced epidermal hyperplasia and LI are summarized in Figures 5-1B and 5-1C, respectively. All doses of rapamycin used (200, 100, 50, 20 and 5 nmol) produced statistically significant reductions in epidermal thickness and labeling index (LI) induced by TPA treatment (\*,  $P < 0.05$ , Mann Whitney  $U$ ). These data demonstrate that rapamycin effectively blocked TPA-induced epidermal hyperproliferation and that this effect may explain its ability, at least in part, to inhibit skin tumor promotion by TPA. [Reprinted from (114)]

**Figure 5-1**

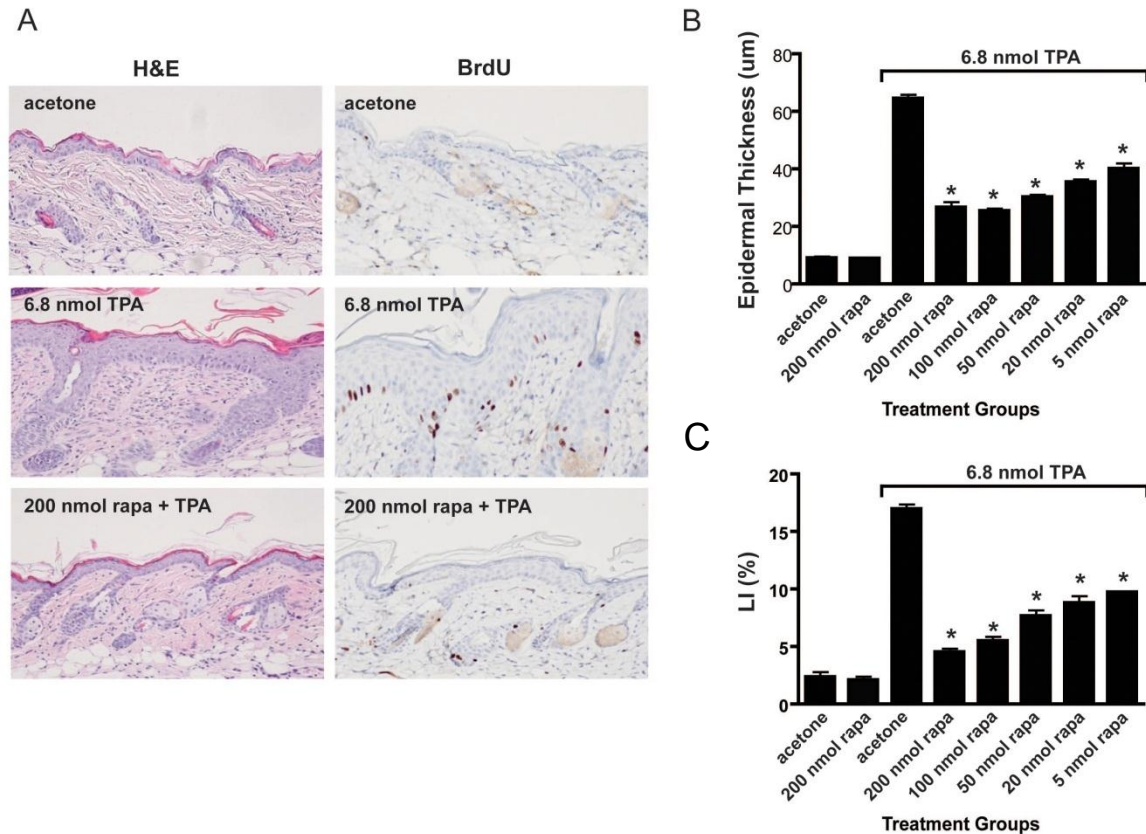


**Figure 5-1 Rapamycin inhibits TPA-induced epidermal hyperplasia in a dose-dependent manner** **A)** Representative sections of H&E and BrdU stains of dorsal skin collected from female FVB mice after multiple treatments with either acetone, 6.8 nmol of TPA, or 200 nmol (rapa) followed by 6.8 nmol of TPA (twice a week for 2 weeks). **B)** Quantitative evaluation of the effects of rapamycin on TPA-induced epidermal hyperplasia (epidermal thickness) **C)** Quantitative evaluation of the effects of rapamycin on TPA – induced epidermal hyperproliferation (labeling index: LI). Values represent the mean  $\pm$  SEM. (\*,  $P < 0.05$ ; Mann-Whitney  $U$ ). [Reprinted from (114)]

## 5-2 Rapamycin reduces TPA-induced inflammation in mouse skin

Another short term marker and chronic feature of skin tumor promotion is inflammatory cell infiltration (101, 127). Hence, the effects of rapamycin on TPA-induced inflammation were studied to provide a potential mechanism by which rapamycin could be exerting its potent inhibitory effects in addition to inhibition of mTORC1 in mice of a normal weight.

During the course of analyzing skin sections from rapamycin-treated mice, a significant decrease in dermal inflammation and dermal inflammatory cell numbers was observed. Therefore, the effect of topical treatments of rapamycin prior to TPA on dermal inflammatory cell infiltration was further examined. For these experiments, groups of female FVB/N mice, 7 to 8 weeks of age, were treated topically with acetone (vehicle) or various doses of rapamycin (5–200 nmol) followed 30 minutes later by 6.8 nmol of TPA. This treatment regimen was continued twice weekly for 2 weeks, and mice were sacrificed 48 hours after the final treatment for histochemical and immunohistochemical analysis of various inflammatory cells. Whole skin sections were processed and stained for the following markers including CD3 (T cells), S100A9 (macrophages), LY6G (neutrophils), and toluidine blue (mast cells). As noted above, visual inspection of skin sections revealed that rapamycin dramatically reduced infiltration of all 4 types of inflammatory cells as seen in Figure 5-2 for the 200 nmol dose of rapamycin (A–D, respectively). Quantitative analyses of each cell type at 2 different doses of rapamycin (200 and 5 nmol) are shown in Figure 5-3. Rapamycin at both doses presented produced statistically significant reductions in the number of all inflammatory cell types examined (\*,  $P < 0.05$ ; Mann–Whitney  $U$ ). [Reprinted from (114)]

**Figure 5-2**

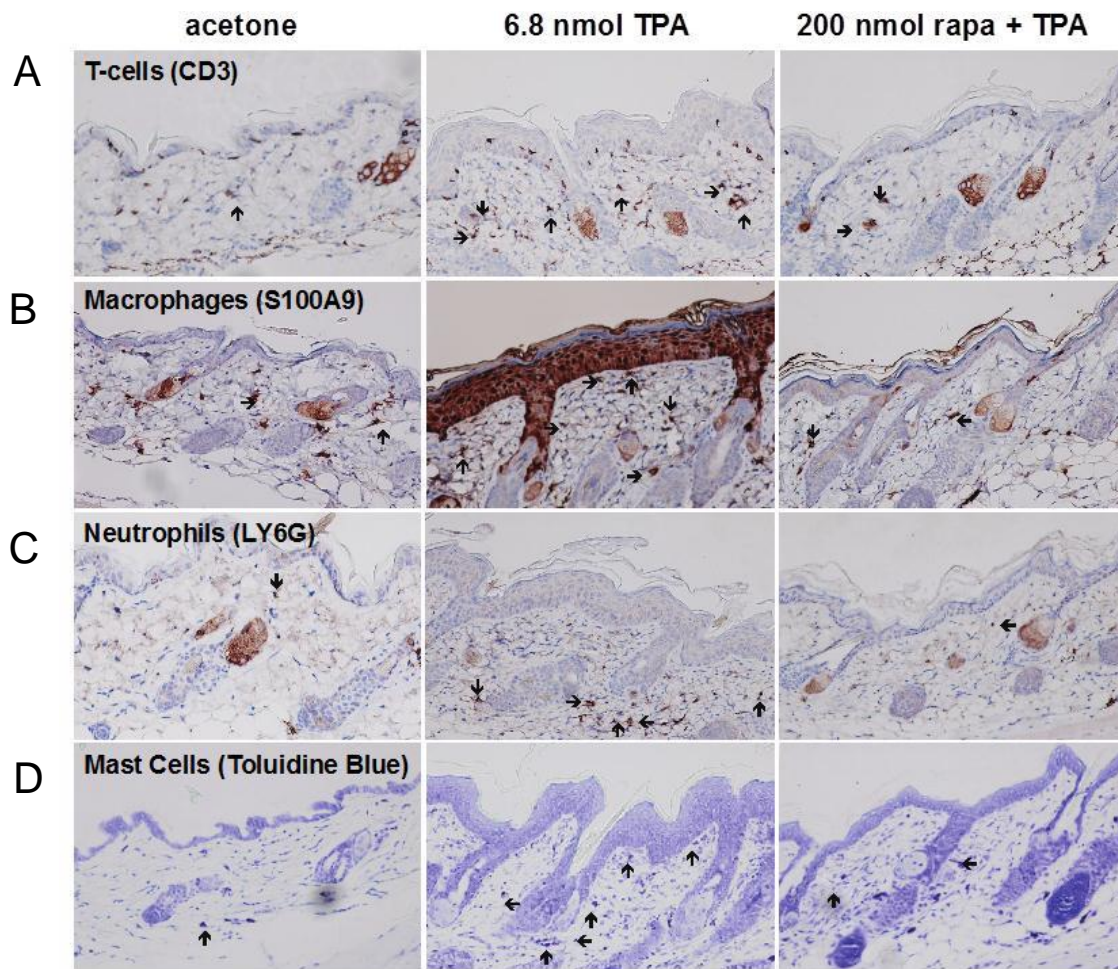


**Figure 5-2 Visual representation of the inhibition of TPA-induced dermal inflammation by rapamycin** **A)** Representative sections of CD3-stained (T cells) dorsal skin sections collected after multiple treatments of acetone, 6.8 nmol of TPA, or 200 nmol rapamycin (rapa) + TPA. **B)** Representative sections of S100A9-stained (macrophages) dorsal skin sections collected after multiple treatments of acetone, 6.8 nmol of TPA, or 200 nmol rapamycin (rapa) + TPA. **C)** Representative sections of LY6G-stained (neutrophils) dorsal skin sections collected after multiple treatments of acetone, 6.8 nmol of TPA, or 200 nmol rapamycin (rapa) + TPA. **D)** Representative sections of toluidine blue-stained (mast cells) dorsal skin sections collected after multiple treatments of acetone, 6.8 nmol of TPA, or 200 nmol rapamycin (rapa) + TPA. [Reprinted from (114)]



**Figure 5-3**

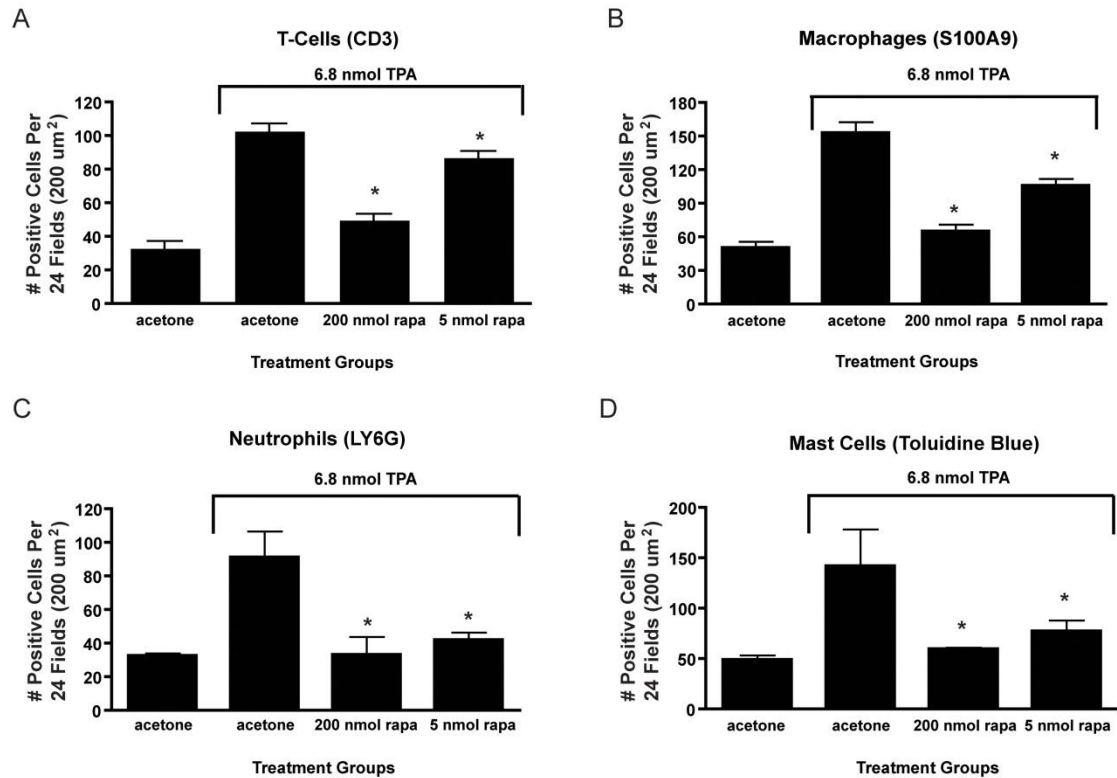


**Figure 5-3 Quantitative analysis of the effect of rapamycin on TPA-induced dermal inflammation** **A)** Average number of positive cells per 24 fields ( $200 \mu\text{m}^2$ ) for CD3-stained sections in acetone, 6.8 nmol TPA, 200 nmol rapamycin + TPA, and 5 nmol rapamycin + TPA treated skins. **B)** Average number of positive cells per 24 fields ( $200 \mu\text{m}^2$ ) for S100A9-stained sections in acetone, 6.8 nmol TPA, 200 nmol rapamycin + TPA, and 5 nmol rapamycin + TPA treated skins. **C)** Average number of positive cells per 24 fields ( $200 \mu\text{m}^2$ ) for LY6G-stained sections in acetone, 6.8 nmol TPA, 200 nmol rapamycin + TPA, and 5 nmol rapamycin + TPA treated skins. **D)** Average number of positive cells per 24 fields ( $200 \mu\text{m}^2$ ) for Toluidine blue-stained sections in acetone, 6.8 nmol TPA, 200 nmol rapamycin + TPA, and 5 nmol rapamycin + TPA treated skins. Values represent the mean  $\pm$  SEM. (\*,  $P < 0.05$ ; Mann-Whitney  $U$ ). [Reprinted from (114)]

Because there were dramatic reductions in dermal inflammatory cell infiltration, the anti-inflammatory effects of rapamycin during skin tumor promotion were further explored. The enzyme cyclooxygenase 2 (COX-2) is a critical mediator of inflammation and serves as the catalyst for the rate limiting step in the conversion of arachidonic acid into prostaglandins (128). It is inducibly expressed in many different tissues by, but not limited to, tumor promoting agents. COX-2 is also induced by various growth factors, oncogenes and pro-inflammatory cytokines (129). As shown in Figure 5-4, TPA applied directly to the skin potently induced COX-2 expression at 6 h post treatment in mouse epidermis. Previous data also support this activation in mouse skin after TPA is topically applied (130).

**Figure 5-4**

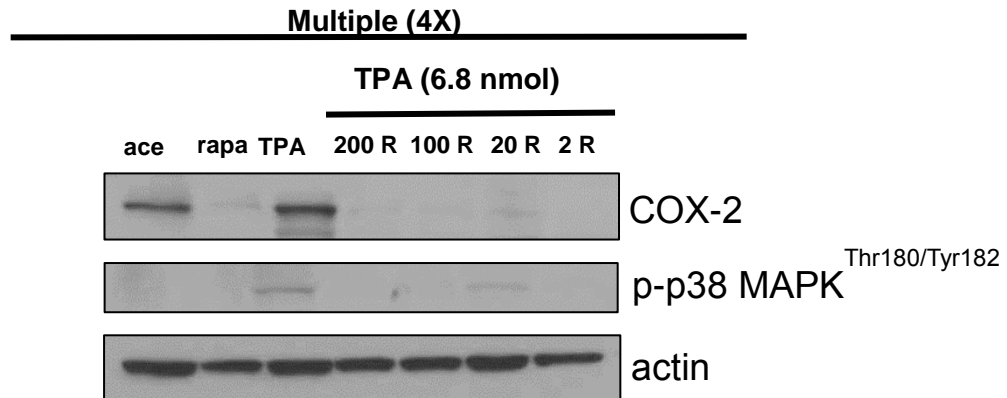


**Figure 5-4 Rapamycin inhibits TPA-induced expression of COX-2 in the epidermis.** Pooled protein lysates were prepared from the epidermal scrapings of female FVB/N mice undergoing a multiple treatment regimen of acetone, 6.8 nmol of TPA, 200 nmol rapamycin (rapa), or various doses of rapamycin (2-200 nmol) prior to 6.8 nmol TPA. Western blot analyses were then conducted to determine the effect of topical rapamycin treatment on inflammatory signaling pathways in the epidermis.

Consistent with the observed reduction in dermal inflammatory cells, topical rapamycin treatment also produced potent decreases in epidermal COX-2 expression after a multiple treatment protocol in which female FVB/N mice 7-8 weeks of ages received treatment with either acetone, 200 nmol rapamycin, 6.8 nmol of TPA, or various doses of rapamycin (2-200 nmol) prior to treatment with 6.8 nmol of TPA (Figure 5-4).

Eukaryotic transcription factor NF $\kappa$ B critically regulates the expression of many genes including COX-2, as the *cox-2* promoter contains an NF $\kappa$ B binding site. Prior to activation, NF $\kappa$ B dimers are retained in the cytoplasm by binding to the members of the I $\kappa$ B (IKK) inhibitory complex. Cellular stimulation of IKK stimulates rapid degradation via polyubiquitination of this complex allowing for the freed NF $\kappa$ B dimers to translocate to the nucleus to coordinate the transcription of hundreds of target genes including COX-2 (131). While the upstream signaling cascade proceeding NF $\kappa$ B activation is quite complex, there is evidence that kinases involved include mitogen-activated protein (MAP) kinases, such as p38, c-Jun and ERK (132). Additional data from our lab has also found that topical application of rapamycin at a dose of 50 nmol decreased TPA-induced activation of NF $\kappa$ B subunit p65 or RelA as indicated by a decrease in phosphorylation of this protein at Ser536 in the epidermis (Data not shown). In addition, in this experiment, there was attenuation of signaling through p38 (Figure 5-4). On a molecular basis, this preliminary signaling data suggest that one facet of rapamycin's anti-tumor action may be through inhibition of TPA-induced inflammation through decreases in expression of COX-2. Specifically, this may occur through suppression of signaling through p38 and subsequent inhibition of NF $\kappa$ B. Further experiments are necessary to confirm the exact mechanism by which rapamycin exerts these potent anti-inflammatory effects.

Overall, these data provide another possible mechanism by which rapamycin might exert its potent inhibition of skin tumor promotion. At the start of this project, the primary hypothesis comprised a situation in which rapamycin exerted its anti-tumor effects primarily

through inhibition of mTORC1 and subsequent downstream signaling to which included many cell cycle regulatory proteins. However, this data provides an interesting scenario by which rapamycin may exhibit dual inhibitory effects. There are however conflicting results in terms of the effect of rapamycin on inflammation in cancer. Previous studies from Granville and colleagues reported that there were no significant changes in macrophage content of skin tumors from mice collected after treatment with rapamycin compared to tumors treated with the control (vehicle treated) (81). Amornphimoltham et al. also reported no change in T-cell or macrophage content in tumors after rapamycin treatment (80). However, in both of these studies, the route of administration of rapamycin was different (IP injection), and each study evaluated the effect of rapamycin on inflammation in pre-existing tumors. In our protocol, rapamycin's effect on skin tumor promotion was evaluated via a short term mechanistic study which represents the early phases of skin tumor promotion before skin tumors developed. Therefore, the current data suggest that the anti-inflammatory effects of rapamycin may have been exerted earlier in the skin carcinogenesis process during the first few weeks of skin tumor promotion thus contributing to its anti-tumorigenic effects.

### **5-3 Rapamycin inhibits TPA-induced activation of mTORC1 and downstream signaling in mouse epidermis**

To further explore the potential mechanisms by which rapamycin inhibited TPA-induced epidermal hyperproliferation and skin tumor promotion, experiments were conducted to evaluate changes in epidermal Akt and mTOR signaling pathways. For these experiments, female FVB/N mice, 7 to 8 weeks of age, were treated topically with either acetone or various doses of rapamycin (5–1,000 nmol) 30 minutes prior to treatment with 6.8 nmol of TPA twice weekly for 2 weeks (total of 4 treatments). Note that a higher dose of rapamycin (1,000 nmol) was used in initial Western blot experiments (Figure 5-5A). However, in subsequent experiments, it was not used, as doses of 50, 100, and 200 nmol rapamycin completely inhibited skin tumor promotion by TPA. Mice were sacrificed 6 hours after final treatment and epidermal protein lysates were prepared for Western blot analyses of Akt, mTOR, and several mTORC1 downstream effector molecules. Topical application of TPA using this protocol led to phosphorylation of mTOR (Ser<sup>2448</sup>), and downstream effectors of mTORC1 including p70S6K (Thr<sup>389</sup>), p4E-BP1 (Thr<sup>37/46</sup> and Ser<sup>65</sup>), and pS6 ribosomal (Ser<sup>240/244</sup>); (Figure 5-5A and B) as well as phosphorylation of Akt (Thr<sup>308</sup> and Ser<sup>473</sup>); Figure 5-5C and D as expected on the basis of previous studies

(106, 113). Although the phosphorylation of mTOR (Ser<sup>2448</sup>) was reduced somewhat at several doses of rapamycin, the most dramatic effects were seen on phosphorylation of p70S6K and S6 ribosomal protein (Figure 5-5A and B). In this regard, phosphorylation of the mTORC1 downstream effectors p70S6K (Thr<sup>389</sup>) and p-S6 ribosomal protein (Ser<sup>240/244</sup>) was decreased in the rapamycin-treated groups in a dose-dependent manner. In addition, at the 1,000-nmol dose, p4E-BP1 (Thr<sup>37/46</sup> and Ser<sup>65</sup>) was decreased as compared with the TPA-treated group. Rapamycin given at a dose of 200 nmol in this multiple treatment regimen appeared to increase Akt phosphorylation at Ser<sup>473</sup> as well as increase phosphorylation at the Thr<sup>308</sup> site (again see Figure 5-5C and D). None of the other doses of rapamycin appeared to affect Akt phosphorylation at either site. Figure 5-5B and D show the quantitation of the Western blot analyses shown in Figure 5-5A and C, respectively. Similar results were obtained in a separate, independent experiment. The Western blot analyses shown in Figure 5-5A and C are representative of both experiments. The quantitation shown in Figure 5-5B and D represent an average from both of these experiments. Collectively, these data suggest that treatment with rapamycin led to inhibition of TPA-induced mTORC1 downstream signaling, particularly through the p70S6K and S6 ribosomal protein pathway. Furthermore, at higher doses ( $\geq 200$  nmol per mouse), rapamycin also appeared to increase Akt phosphorylation at Thr<sup>308</sup>. [Reprinted from (114)]

**Figure 5-5**

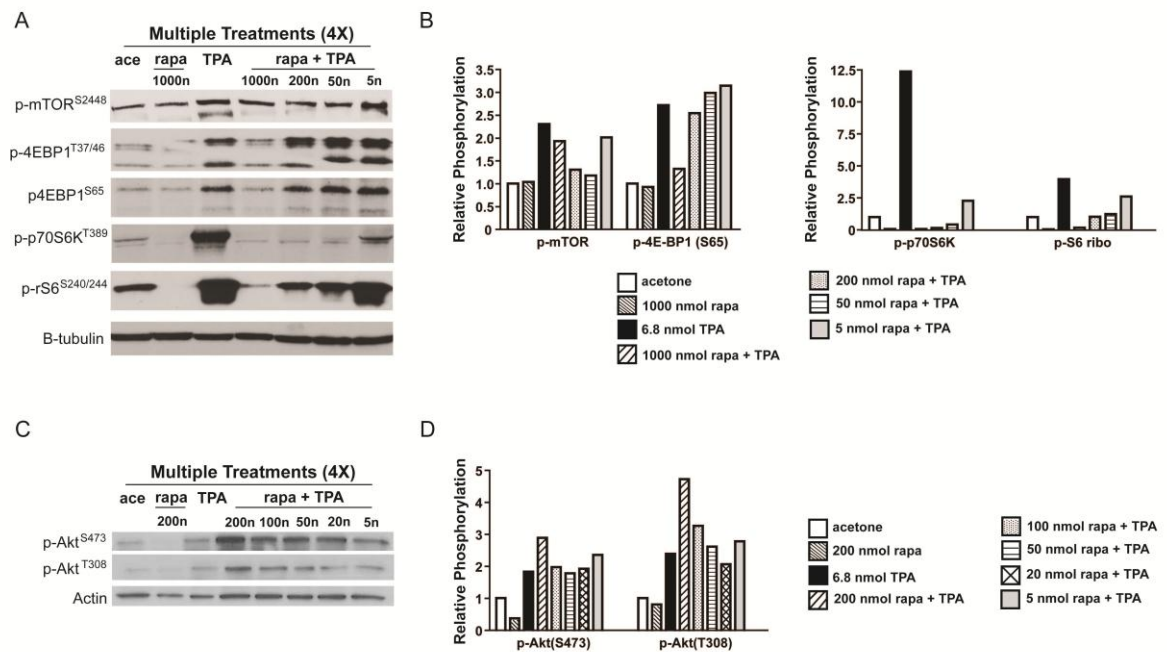


**Figure 5-5 Rapamycin inhibits TPA-induced signaling through mTORC1.** Effect of rapamycin on TPA-induced mTOR signaling in mouse epidermis using a multiple treatment protocol. Pooled protein lysates were prepared from the epidermal scrapings of FVB/N mice undergoing a multiple treatment regimen of acetone, 6.8 nmol TPA, 200 and 1000 nmol rapamycin (rapa), or various doses of rapamycin (5-1000 nmol) prior to 6.8 nmol TPA. Western blot analyses were then conducted to examine activation of Akt and mTOR and downstream targets. **A)** Western blot analysis of mTOR and downstream signaling molecules. **B)** Quantification of Western blot analyses in A. **C)** Western blot analysis of Akt phosphorylation status. **D)** Quantification of Western blot analysis in C. These experiments were repeated with nearly identical results. Note that the quantitation shown in B and D represent an average of the two experiments, whereas the Western blot analysis in A and C are from a single representative experiment. [Reprinted from (114)]

In addition, even after a single topical application of rapamycin to the skin, rapamycin potently inhibited signaling through mTORC1 (data not shown). Furthermore, there was inhibition of mTORC1 and downstream signaling through disruption of mTOR and raptor after topical administration of rapamycin prior to TPA treatment. As shown in figure 5-6, multiple treatments with rapamycin at doses of 1000 and 20 nmol effectively disrupted interactions between raptor and mTOR. This effect also appeared to be dose dependent.

**Figure 5-6**

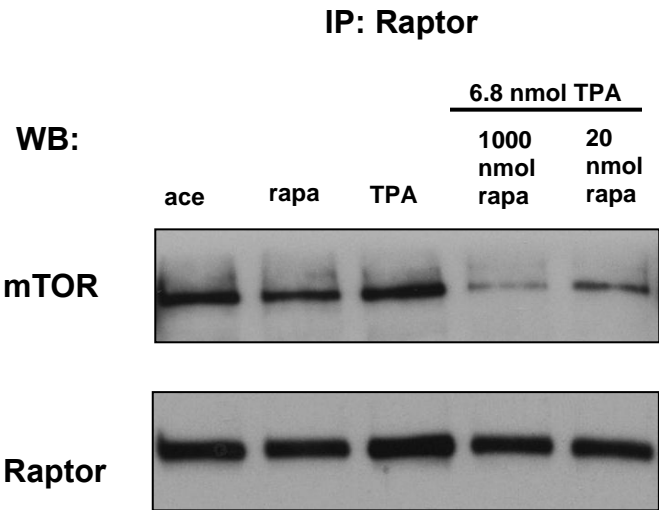


**Figure 5-6 Multiple treatments with rapamycin at higher doses prevent mTOR complex I formation.** Female FVB/N mice were treated topically with either acetone, rapamycin, 6.8 nmol TPA or 1000 nmol or 20 nmol of rapamycin prior to TPA treatment. Epidermal lysates were prepared as previously described. Panel shows co-immunoprecipitation with raptor and subsequent western blot analyses of mTOR and raptor.

Overall, this data is consistent with previous published reports that attribute the anti-tumor effects of rapamycin to its ability to reduce signaling through mTORC1 and further downstream as assessed by levels of pS6 (80). As demonstrated in Figure 5-5A and B, rapamycin applied topically 30 min prior to treatment with 6.8 nmol of TPA, inhibits TPA-induced mTORC1 activation in the epidermis as evidenced by decreased phosphorylation of mTOR (Ser<sup>2448</sup>) and its downstream targets p70S6K (Thr<sup>389</sup>) and pS6 ribosomal protein (Ser<sup>240/244</sup>). In addition, another downstream target of mTORC1, translation repressor 4E-BP1 was evaluated. Interestingly, rapamycin only appeared to effect phosphorylation of 4E-BP1 at the highest dose of rapamycin tested (1000 nmol). At lower doses used, there appeared to be much less inhibition of this protein. As discussed in the Introduction chapter, 4E-BP1, when unphosphorylated, binds to initiation factor eIF4E, and inhibits cap-dependent translation. Our observation is consistent with previous reports that show full inhibition of p70S6K and pS6, but only partial inhibition of 4E-BP1 after rapamycin treatment (133, 134). However, it should be noted that the phosphorylation of 4E-BP1 is quite complex and requires phosphorylation from various other kinases for release from eIF4E to inhibit translational activation. Previously published data showed that phosphorylation at the Thr<sup>37</sup> and Thr<sup>46</sup> sites of 4E-BP1 by mTORC1 did not eliminate its binding to eIF4E and that other kinases are required for eIF4E's release and subsequent translation activation (135). In summary, the current data indicate that the inhibitory effects of rapamycin on mTORC1 signaling appear to be primarily mediated through downstream targets p70S6K and pS6, and effects through downstream target 4E-BP1 appear to be less important in terms of inhibition of skin tumor promotion (114).

In terms of Akt status in the epidermis, interestingly rapamycin at a dose of 200 nmol increased activation of Akt as evaluated by phosphorylation at Thr<sup>308</sup>. This activation was not apparent at the lower doses of rapamycin used (100, 50, 20 and 5 nmol) as shown in Figure 5-5C and D. The increase in activation in this multiple treatment regimen was



attributed to a partial inhibition of the mTORC1-dependent negative feedback loop in which p70S6K and pS6 negatively regulate insulin signaling through phosphorylation of IRS-1 causing subsequent attenuation of signaling through PI3K/Akt. This conclusion is also supported by previous published data that have shown an increase in Akt activity after treatment with mTOR inhibitors due to reductions in feedback inhibition of the PI3K/Akt pathway (121). In addition, phosphorylation of Akt at Ser<sup>473</sup> at a dose of 200 nmol may have also been slightly increased (Figure 5-5C and D). However, further experiments in our lab have demonstrated decreased phosphorylation of PRAS40 at Thr<sup>246</sup> which is the Akt-specific phosphorylation site when rapamycin was applied topically to the skin prior to TPA (data not shown). Consonant with this observation, Sarbassov and colleagues (76) reported that rapamycin inhibited mTORC2 assembly after subsequent Akt activity *in vitro* after prolonged treatment. Further investigations will be necessary to determine whether the mTORC2 complex is disrupted in response to rapamycin at higher dose, multiple treatment regimens. Nonetheless, lower doses of rapamycin (i.e. 100, 50, 20 and 5 nmol) effectively inhibited epidermal mTORC1 signaling and complex formation without any effects on phosphorylation status of Akt at either Ser<sup>473</sup> or Thr<sup>308</sup> and this inhibition appears to be a primary mechanism and biochemical alteration associated with inhibition of murine skin tumor promotion (114).

These initial findings demonstrate the importance of Akt downstream substrate mTORC1 in mediating the effects of rapamycin on skin tumor promotion by TPA via reduction of signaling through p70S6K and pS6 as well as a through reduced TPA-induced inflammation. Next, a possible mechanism through which rapamycin exerts its potent anti-tumor effects via induction of autophagy was explored. It is possible that some of the chemopreventive actions of rapamycin demonstrated in our model are a concerted effort between a reduction in protein synthesis, a reduction in inflammation as well as increases in pro-autophagic pathways. Most pro-autophagic events including initiation and nucleation

converge on the mammalian Target of Rapamycin (mTOR). Activation of these pathways may provide a less hostile microenvironment via reductions in damaged proteins and organelles and subsequent reductions in overall inflammation.

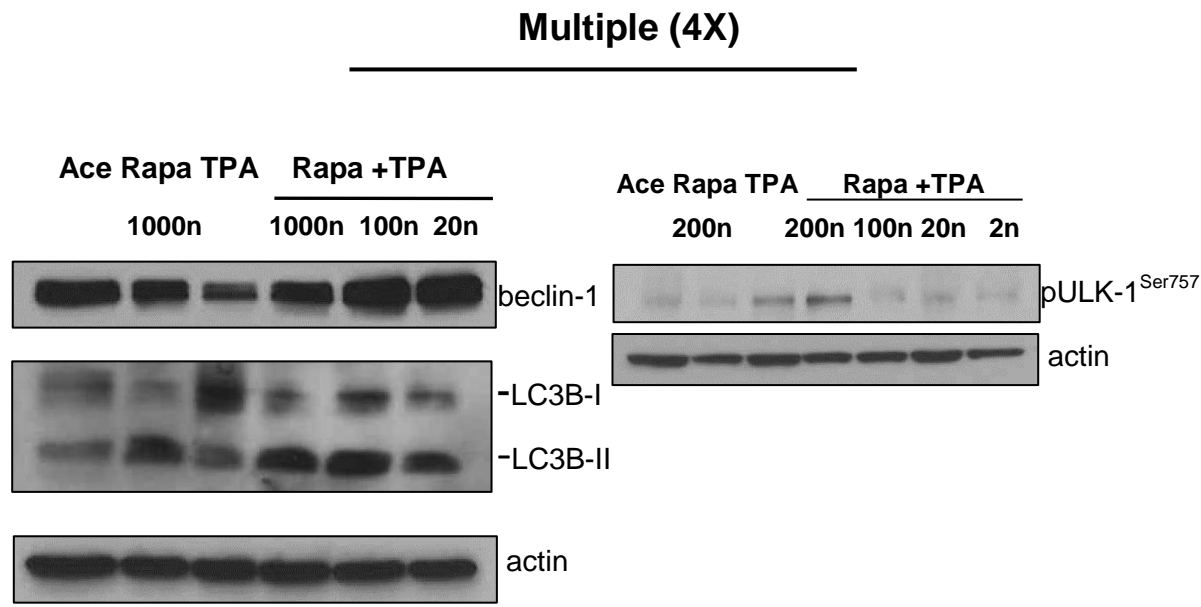
Preliminary data gathered showed that topical application of rapamycin induced pro-autophagic or autophagic proteins in mouse epidermis after TPA treatment. Initial results have demonstrated increases in specific protein markers that have been validated as visual markers for autophagosome formation including LC3B II as well as autophagic initiator beclin-1. Autophagy Marker Light Chain 3 (LC3B) is cleaved at the C-terminal end by Atg5 into a cytoplasmic form of LC3B-I. If autophagy is present, then cytosolic LC3B-I is cleaved into LC3B-II and is then recruited to the autophagosomal membrane (58). Beclin-1 is involved in the initiation step of autophagy and acts as a platform for binding activators such as UVRAG or repressors such as Bcl-2 depending on external signaling and nutrient stimuli, rather than possessing its own enzymatic activity (136).

Consistent with previous data that demonstrated PKC activation to downregulate autophagy (137), topical treatment with 6.8 nmol of TPA down-regulated beclin-1 and LC3B-II (Figure 5-7). Treatment with rapamycin at various doses (1000 nmol, 100 nmol and 20 nmol) prior to TPA treatment reversed the reduction in autophagic markers seen with TPA treatment alone in mouse epidermis. Expression of LC3B-II and beclin-1 was increased in rapamycin treated groups compared to the TPA only treated group which primarily expressed the uncleaved form, LC3B-I (Figure 5-7). Ongoing studies in the lab are also evaluating the effect of rapamycin treatment on autophagy regulators directly downstream of mTORC1, such as ULK1. Preliminary Western blot analyses showed phosphorylation of ULK1 at Ser757, which is the mTORC1 phosphorylation site, after TPA application to the skin (Figure 5-7). Phosphorylation of ULK1 by mTORC1 at this site inactivates the ULK1/FIP200/ATG13 complex, inhibiting its release from mTOR and raptor thus preventing the association between AMPK and ULK1 and the induction of autophagy

(63). However, in skins treated with rapamycin at doses of 100, 20 and 2 nmol prior to treatment with 6.8 nmol of TPA, phosphorylation of ULK1 at this site was abolished (Figure 5-7). Interestingly, the highest dose of rapamycin used caused an increase in phosphorylation at this site comparable to the increases in phosphorylation seen with TPA. We hypothesized that this increase could be due to a novel negative feedback loop involving mTOR, raptor and ULK1 described by Dunlop et al. They provided evidence that ULK1 promotes phosphorylation of raptor at multiple sites thus hindering substrate binding to this complex causing inhibition of mTORC1. Upon overexpression, ULK1 promoted increases in mTORC1 kinase activity through the autophosphorylation site (Ser2481) despite continued inhibition of mTORC1 mediated phosphorylation of p70S6K and 4E-BP1(138). It's probable that higher doses of rapamycin may affect ULK1's interactions with raptor thus altering mTORC1 activity.

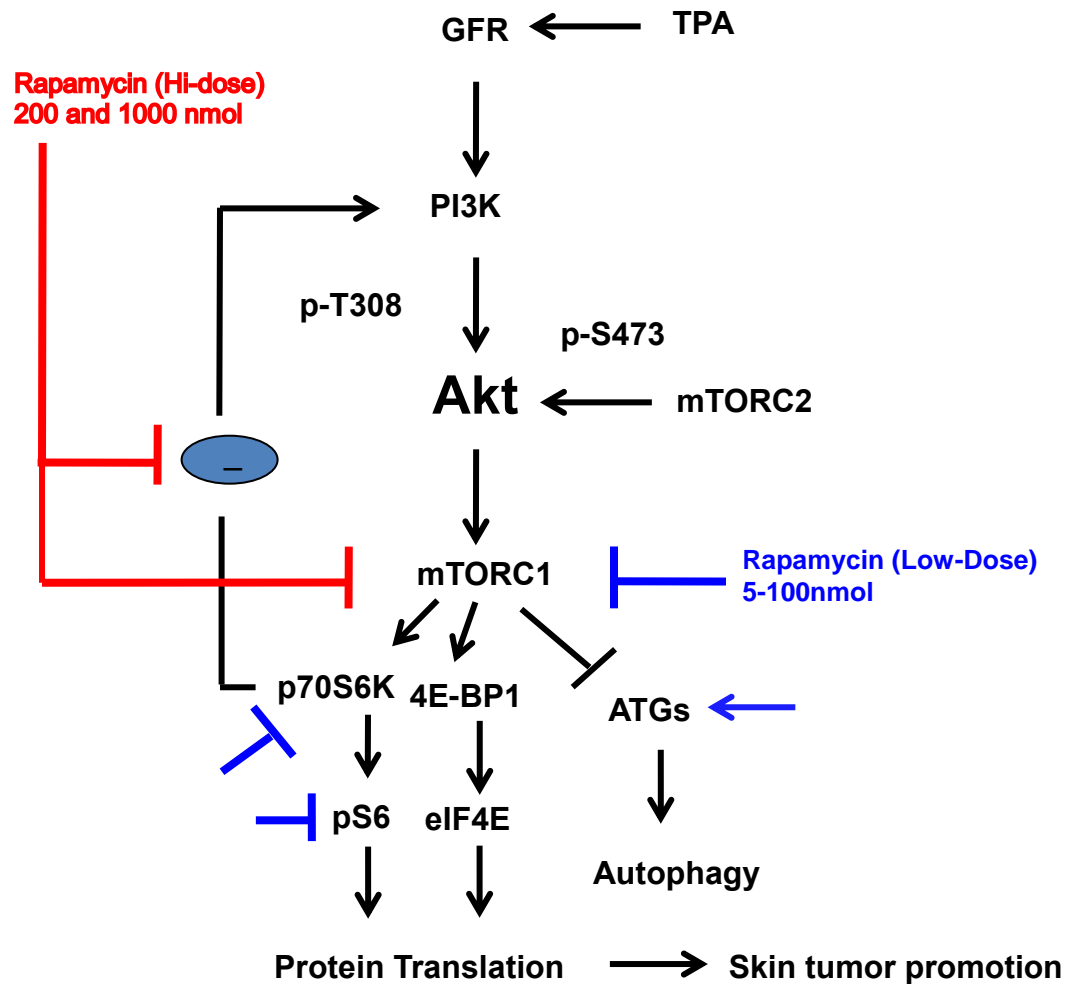
A summary of our findings on the impact of rapamycin on Akt/mTOR phosphorylation and downstream effectors following rapamycin treatment in mouse epidermis can be found in Figure 5-8.

Figure 5-7



**Figure 5-7 Effect of rapamycin on the induction of autophagy in the epidermis using a multiple treatment protocol.** Pooled protein lysates were prepared from the epidermal scrapings of FVB/N mice undergoing a multiple topical treatment regimen of acetone, 6.8 nmol TPA, 1000 nmol or 200nmol of rapamycin, or various other doses of rapamycin (20-1000 nmol) prior to 6.8 nmol of TPA. Western blot analyses were conducted to examine the activation of autophagic markers LC3B, beclin-1 and ULK1.

Figure 5-8



**Figure 5-8 Summary of the impact of rapamycin treatment on Akt/mTOR phosphorylation in mouse epidermis following TPA treatment.** Impact of low dose rapamycin treatment represented in **blue**. Impact of high dose rapamycin treatment represented in **red**. High doses of rapamycin used (200 and 1000 nmol) affected mTORC1-dependent negative feedback inhibition of PI3K/Akt as well as inhibited mTORC1. Rapamycin at low doses (5-100 nmol) that inhibited skin tumor promotion primarily affected downstream targets p70S6K, pS6 and ULK1.

#### **5-4 Metformin attenuates TPA-induced epidermal hyperproliferation**

After obtaining exciting results from two-stage skin carcinogenesis experiments demonstrating anti-carcinogenic effects of metformin during the tumor promotion stage when administered via the drinking water, the potential mechanisms by which this anti-diabetic drug and apparent anti-neoplastic agent was exerting these effects was examined. First, to further examine the ability of metformin to reduce proliferation in the epidermis, short term markers of skin tumor promotion, hyperproliferation (BrdU incorporation) and hyperplasia (epidermal thickness) were evaluated after TPA treatment. For these experiments, groups of normal weight female FVB/N mice 7 to 8 weeks of age were topically treated with either acetone or 6.8 nmol of TPA twice a week for two weeks with or without the addition of metformin in the drinking water at doses of 350, 250 or 50 mg/kg body weight per day for the duration of the study. Mice were sacrificed 48 hours after the final acetone or TPA treatment, and skin sections were removed for histological examination. Figure 5-9A displays representative H&E and BrdU stained skin sections from the acetone, TPA, and 250 mg/kg metformin + TPA treatment group. Visual inspection revealed modest decreases in both epidermal thickness and labeling index in response to metformin administration in the drinking water. Upon quantitative evaluation as shown in Figure 5-9B the range of doses of metformin used significantly reduced each parameter measured compared to the TPA control group. The reductions also appeared to be dose-dependent (\*,  $P < 0.05$ , Mann-Whitney  $U$ ). Overall, this data shows metformin's ability to inhibit, at least partially, TPA-induced hyperproliferation. This may help explain how it inhibits skin tumor promotion.

**Figure 5-9**

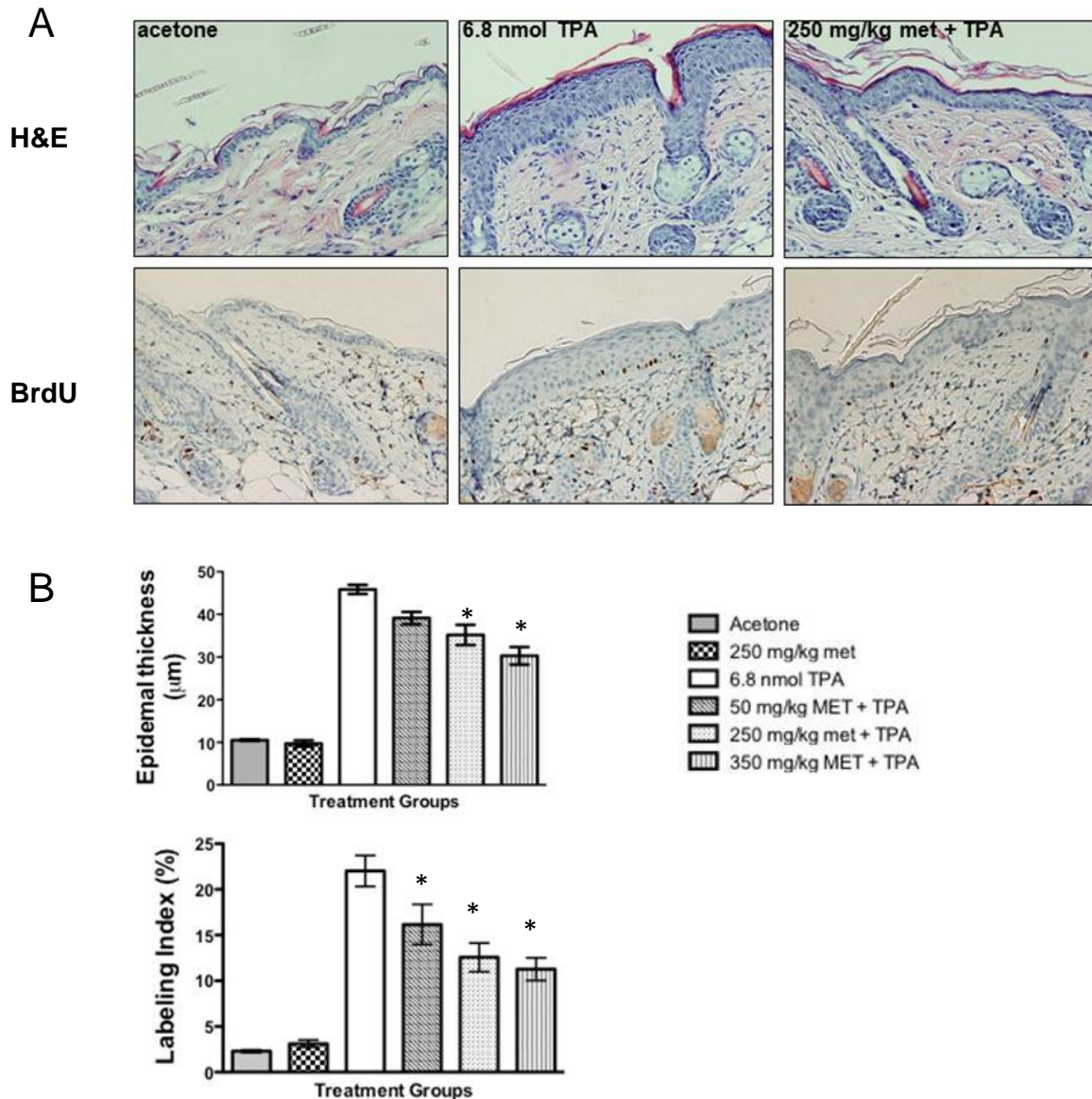


**Figure 5-9 Metformin inhibits TPA-induced hyperplasia and hyperproliferation. A)** Representative sections of H&E and BrdU stains of dorsal skin collected from female FVB/N mice after multiple treatments with either acetone, 6.8 nmol of TPA twice a week for two weeks with or without metformin in the drinking water at the representative dose of 250 mg/kg body weight per day. **B)** Quantitative evaluation of the effects of metformin on TPA-induced epidermal hyperplasia (epidermal thickness and labeling index: LI). Values represent the mean  $\pm$  SEM. (\*,  $P < 0.05$ ; Mann-Whitney  $U$ ).

### **5-5 Metformin activates epidermal AMPK and attenuates TPA-induced signaling through mTORC1**

As discussed in the Introduction, metformin acts by inhibiting oxidative phosphorylation thus increasing intracellular levels of AMP and subsequently activating the LKB1/AMPK pathway (139, 140). This action, when occurring in the liver, impairs gluconeogenesis thus lowering glucose production and subsequent circulating insulin levels. Current data has revealed that this activation of AMPK in neoplastic cells can result in decreased cellular proliferation (141). Thus, the anticancer effects of this drug may be a result of either an indirect insulin lowering effect due to activation of AMPK in the liver, and/or a direct effect by activation of AMPK and further alterations in cell signaling and gene expression in transformed cells. Distinguishing between direct and indirect mechanisms behind the anticancer effects of metformin is important, as most epidemiological data show metformin's anticancer effects in type II diabetes populations which tend to be obese and display chronic hyperinsulinemia. Our initial experiments explored the baseline effects (independent of diet) of short term administration of metformin in the drinking water (two weeks) on AMPK activation and subsequent signaling through mTORC1 and further downstream in female FVB/N mice on a regular chow diet in response to treatment with tumor promoter, TPA. During this period, mice received topical treatments with either acetone (vehicle) or 6.8 nmol of TPA with or without metformin in the drinking water at doses of 250 and 50 mg/kg body weight per day. Mice were sacrificed 6 h after the final acetone or TPA treatment, and epidermal protein lysates were prepared. Activation of AMPK has been shown to inhibit signaling through mTORC1, therefore it was hypothesized that metformin inhibits the growth of skin tumors via activation of AMPK and a subsequent decrease in signaling through mTORC1/p70S6K resulting in limitations in protein synthesis. Western blot analyses showed abundant activation of AMPK in the epidermis in groups receiving both doses of metformin as compared to the TPA-control treated group (Figure 5-10A).



As previously shown, topical TPA treatment to the skin resulted in potent activation of mTORC1 as shown through increases in phosphorylation of p70S6K<sup>T389</sup>, pS6r<sup>S240/244</sup>, pS6r<sup>S235/236</sup>, and p4E-BP1<sup>S37/46</sup>, as well as degradation of mTORC1 downstream target, PDCD4. In treatment groups receiving metformin, there was a dose-dependent reduction in p70S6K<sup>T389</sup> as well as pS6r<sup>S235/236</sup> (Figure 5-10A and B). In addition, translational repressor PDCD4 was partially protected from degradation at the higher dose of metformin used (250 mg/kg). In this short term administration protocol, metformin had no apparent effect on mTORC1 mediated phosphorylation of 4E-BP1. Figure 5-10B shows the quantification of these blots with graphs displaying the mean and SEM from three independent experiments. It should be noted that while there was a dose-dependent response, only the highest dose used (250 mg/kg) had statistically significant differences in protein activation from the TPA-control treated group. Graphs without error bars represent the average from two independent experiments.

The data thus far supports an AMPK dependent mechanism for the inhibition of skin tumor development in the two-stage skin carcinogenesis model. It is well established that one of the primary pharmacological mechanisms of action of metformin is activation of AMPK (142). Activation of the LKB1/AMPK pathway activates a host of downstream effectors that modulate cellular growth and metabolism and helps regulate energy balance in the cell during times of stress (87). In short term mechanistic studies, metformin partially inhibited signaling through mTORC1. Furthermore, this inhibition was confirmed to be associated with AMPK activation as evidenced by increases in phosphorylation of AMPK at activation site Thr<sup>172</sup> in the presence of metformin. Another downstream target of AMPK that might be of interest to explore is Acetyl CoA carboxylase. Acetyl CoA carboxylase, when activated causes the carboxylation of acetyl-CoA to produce malonyl-CoA, which is the rate limiting step in *de novo* fatty acid synthesis (99). This may also represent another downstream mechanism by which metformin exhibits anti-neoplastic effects, as many

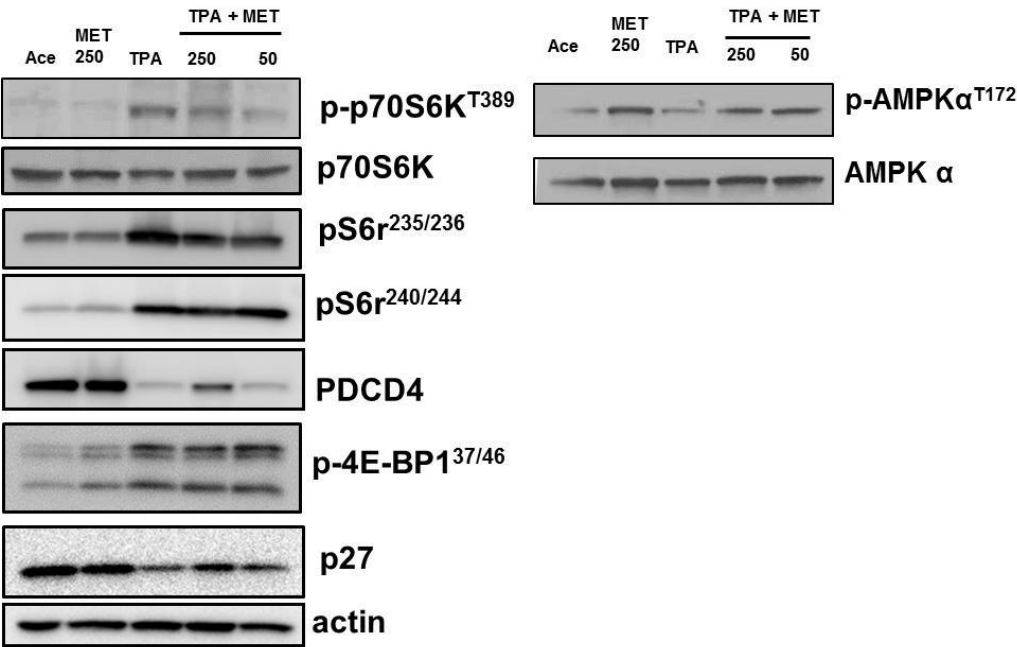
human cancers have been associated with fatty acid synthase (FASN) increases (143). Further work will be necessary to explore these downstream signaling pathways in more detail.

It should also be noted that there is additional evidence that metformin might mediate its anti-cancer effects independently of LKB1 and AMPK. Kalender and colleagues demonstrated metformin to inhibit signaling through mTORC1 independent of the LKB1/AMPK axis by inhibiting Rag GTPase activation of mTOR (144). In addition, metformin induced cell cycle arrest through REDD1 mediated inhibition of mTOR in prostate cancer cell lines (145). Furthermore, the ability of metformin to inhibit gluconeogenesis in the liver was not impaired in the absence of LKB1 and AMPK and instead was initiated in response to flux in energy levels (146). Despite these interesting observations, AMPK activation and subsequent mTORC1 inhibition remain the primary proposed mechanism by which metformin exerts antineoplastic effects.

Figure 5-10

Multiple (4X) Treatment Protocol

A



B

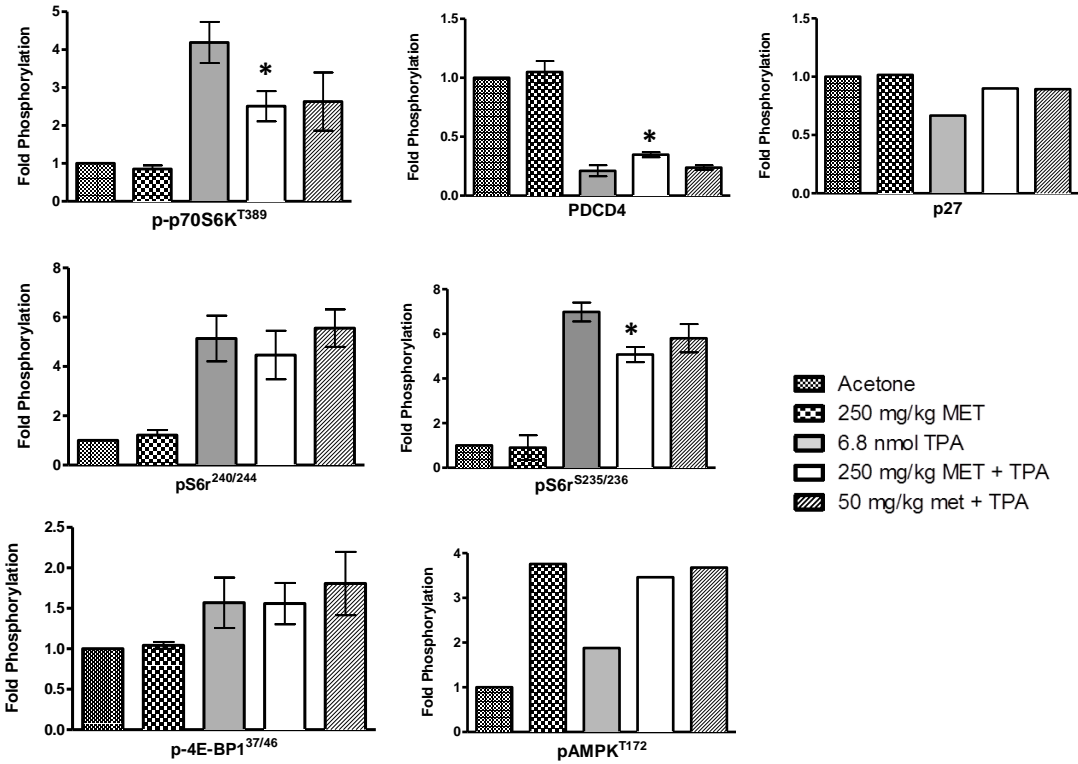


**Figure 5-10 Metformin activates epidermal AMPK and attenuates TPA-induced activation of mTOR and downstream targets.** Pooled protein lysates were prepared from the epidermal scrapings of FVB/N mice undergoing a multiple treatment regimen of either acetone, 6.8 nmol of TPA with or without the addition of metformin in the drinking water at doses of 250 and 50 mg/kg body weight per day. Western blot analyses were conducted to examine activation of AMPK, mTORC1 and downstream targets. **A)** Western blot analyses of AMPK and mTORC1 substrates. **B)** Quantification of Western blot analysis in A. Graphs with error bars represent quantitation from three independent experiments (\*,  $P < 0.05$ , Mann-Whitney  $U$ ).

In preliminary experiments, the effects of low dose combinations of metformin and rapamycin on epidermal mTORC1 signaling were explored to further characterize the mechanisms of the additive effect of these two compounds that were witnessed in the two-stage skin carcinogenesis protocol. As shown in Chapter 4, a combination of 50 mg/kg body weight per day of metformin administered via the drinking water accompanied by topical treatment with 2 nmol of rapamycin prior to promotion with 6.8 nmol of TPA was sufficient in both overweight and obese mice to cause statistically significant reductions in tumor development as compared to either compound alone. An additive effect was also observed through the reduction of phosphorylation of p70S6K (Thr389) in the combination group compared to either single agent alone in mouse epidermis. There was also dramatic inhibition of the degradation of translational repressor PDCD4 in the combination treatment group. (Figure 5-11).

**Figure 5-11**

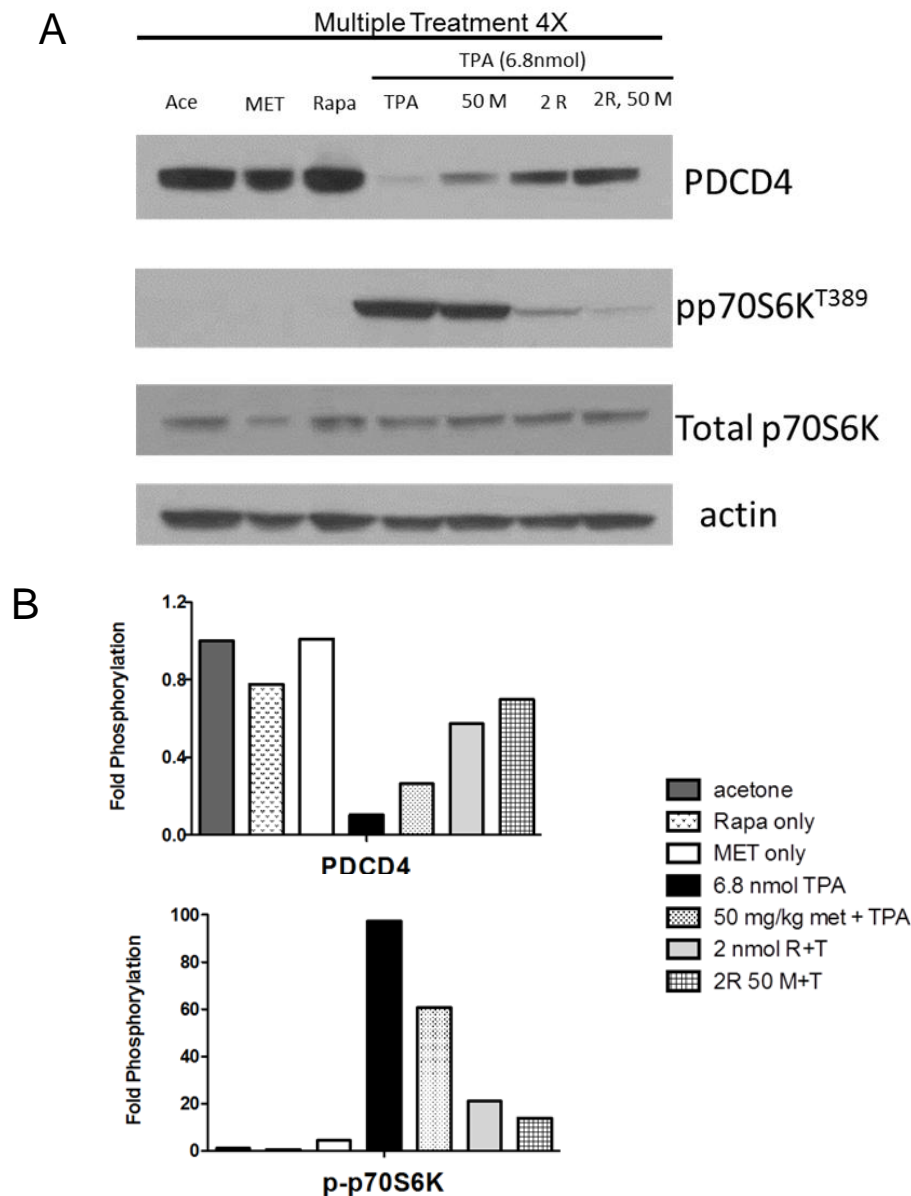


**Figure 5-11 Combination treatments of metformin and rapamycin are more effective than either agent alone at inhibiting TPA-induced mTORC1 signaling in the epidermis.** Pooled protein lysates were prepared from the epidermal scrapings of FVB/ N mice undergoing a multiple topical treatment regimen of acetone, 6.8 nmol TPA, 2 nmol of rapamycin or 50 mg/kg metformin, or these treatments alone or in combination prior to 6.8 nmol of TPA. **A)** Western blot analyses from a single representative experiment **B)** Quantitation from western blots in A

## **5-6 Effect of metformin on body weight, serum hormones, and glucose tolerance**

As previously shown in Chapter 4, dietary intervention via administration of either the 10 kcal % fat, overweight/control diet or the 60 kcal % fat, DIO diet generated two different weight phenotypes. In the last few weeks of the tumor study, after which mice had been on diet for 30 weeks, the mean body weight of the DIO diet group was  $45.2 \pm 0.63$  g and the mean body weight of the overweight/control diet group was  $31.6 \pm 0.86$ , and differences were statistically significant (\*,  $P < 0.05$ , Figure 5-12D). As expected, there were also altered levels of energy balance-related hormones in the overweight mice in the DMBA/TPA control group as compared to the DIO mice in the DMBA/TPA control group as fasting insulin levels on average in the DIO group were approximately 7-fold higher than the overweight control group ( $P < 0.05$ ; Figure 5-12A). Serum leptin levels were approximately 20-fold higher in the DIO DMBA/TPA control group as compared to the overweight DMBA/TPA control group ( $P < 0.05$ ; Figure 5-12B). However, differences in serum adiponectin levels were not statistically significant in these two groups (Figure 5-12C). To determine whether or not metformin exerts its anti-tumor effects in the two-stage model through indirect insulin lowering effects or decreases in various other serum adipokines, serum hormones in the metformin treated mice were evaluated. Metformin at a dose of 50 mg/kg body weight per day in the drinking water reduced the elevated levels in insulin in the DIO, hyperinsulinemic mice but had no effect on the insulin levels of mice receiving the overweight control diet (DIO DMBA-TPA control:  $4,828.9 \pm 1128.3$  pg/ml versus DIO 50 mg/kg MET + TPA:  $1,914.7 \pm 338.8$  pg/ml; \*,  $P < 0.05$ , Mann-Whitney *U*) (Figure 5-12A). In addition, adiponectin levels were modestly higher in the DIO 50 mg/kg MET + TPA group compared to the DIO DMBA-TPA control group, but there were no differences between the metformin and DMBA-TPA treated groups in the overweight/control diet groups (DIO DMBA-TPA control:  $6272.9 \pm 783.2$  pg/ml versus DIO 50 mg/kg MET + TPA:  $8,812.9 \pm 1018.4$  pg/ml; \*,  $P < 0.05$ , Mann-Whitney *U*) (Figure 5-12C). The addition of metformin in the drinking water had

no apparent effect on circulating serum leptin levels (Figure 5-12B). This data is consistent with previous published data that showed that while there were statistically significant increases in leptin levels in mice receiving a high-energy diet vs the control diet, metformin had no significant effects on leptin levels in either diet group (139)

Our findings show that metformin reduced increases in circulating insulin levels in obese mice consuming the high fat diet (60 kcal % fat) suggesting that the antitumor effects of metformin in the skin carcinogenesis model may partially occur via LKB1/AMPK activation in the liver and subsequent inhibition of gluconeogenesis. While there was reduced signaling in the epidermis through mTORC1 via AMPK activation after metformin administration in both diet groups, maximal antitumor effects were seen in the diet-induced obesity group suggesting that the indirect effect of metformin on circulating metabolic hormones may play an important role as well. Genetic approaches will be necessary to absolutely discern whether metformin exerts its effects primarily directly and/or indirectly.

**Figure 5-12**

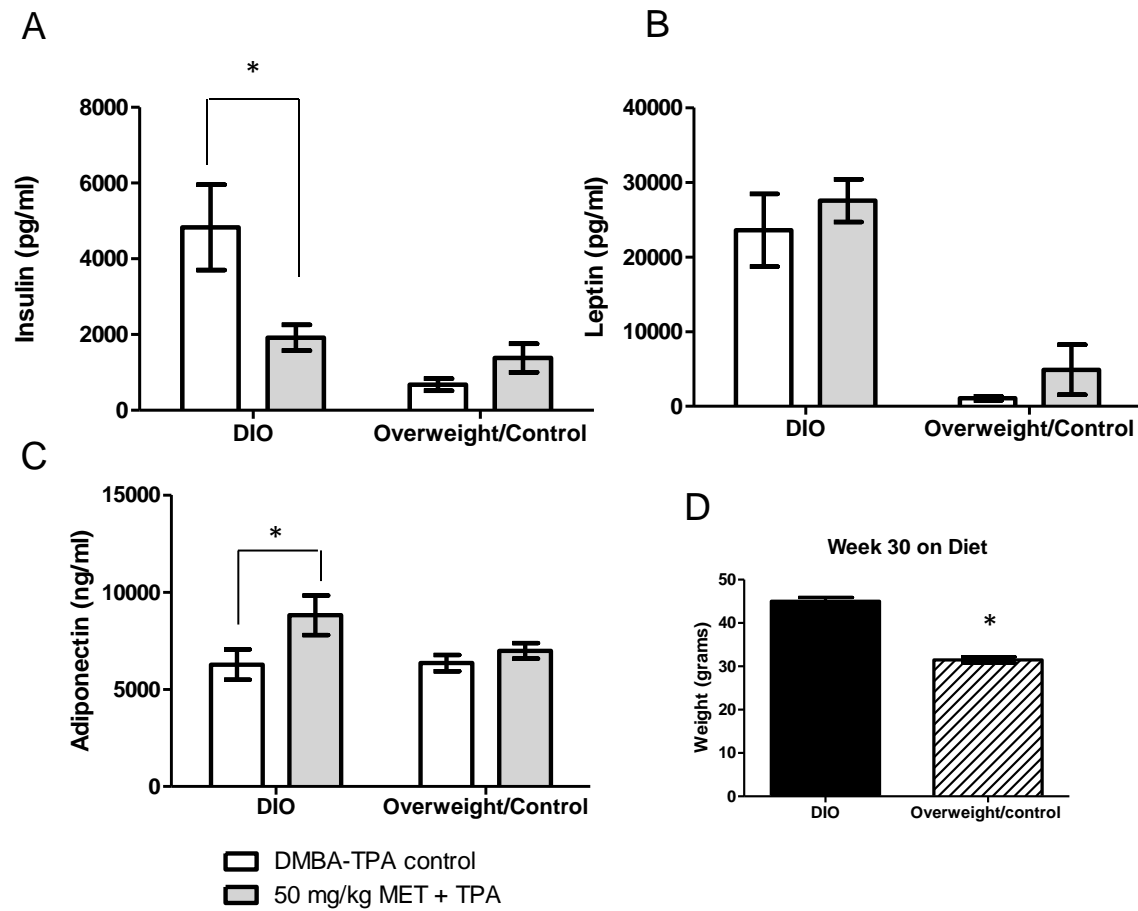


**Figure 5-12 Effect of metformin and diet on energy balance related serum hormones.**

At week 26 of promotion and metformin treatment during a two-stage study, mice were sacrificed and serum was collected via cardiac puncture from a subset of mice from each diet/treatment group (n=7). **A)** Insulin **B)** Leptin **C)** Adiponectin **D)** Average weight of each dietary group (including all treatments) after 30 weeks on each *ad libitum* fed diet. Graphs represent the mean  $\pm$  SEM. (\*,  $P < 0.05$ , Mann-Whitney U)



In addition, the effect of metformin on glucose tolerance was examined. Female FVB/N mice from an ongoing two-stage skin carcinogenesis experiment from a subset of each diet and treatment group were used for glucose tolerance tests at week 20. The DIO group, relative to the overweight/control group, as assessed by the GTT, displayed a modest decrease in glucose tolerance. At 20 weeks of tumor promotion, the DIO DMBA-TPA control group peaked at 30 minutes and averaged  $387.8 \pm 39$  mg/dl versus  $340 \pm 30$  mg/dl for the overweight/control DMBA-TPA control group. After these peaks were achieved, blood glucose levels were consistently lower for the remainder of the time course in the overweight/control group (Figure 5-13). However, metformin did not greatly improve glucose tolerance in either diet group as there were not significant differences between metformin and the DMBA-TPA control groups in either diet administered. It was surprising that there were not significant improvements in glucose tolerance in the DIO mice, however, these mice are not considered diabetic, and the differences between glucose tolerances in the overweight/control versus the DIO are not all that dramatic. It should also be noted that these readings were taken later into the tumor study at week 20 at which time the tumor burden of mice increased as well as stress levels which could have diminished the ability to distinguish differences in tolerance.

**Figure 5-13**

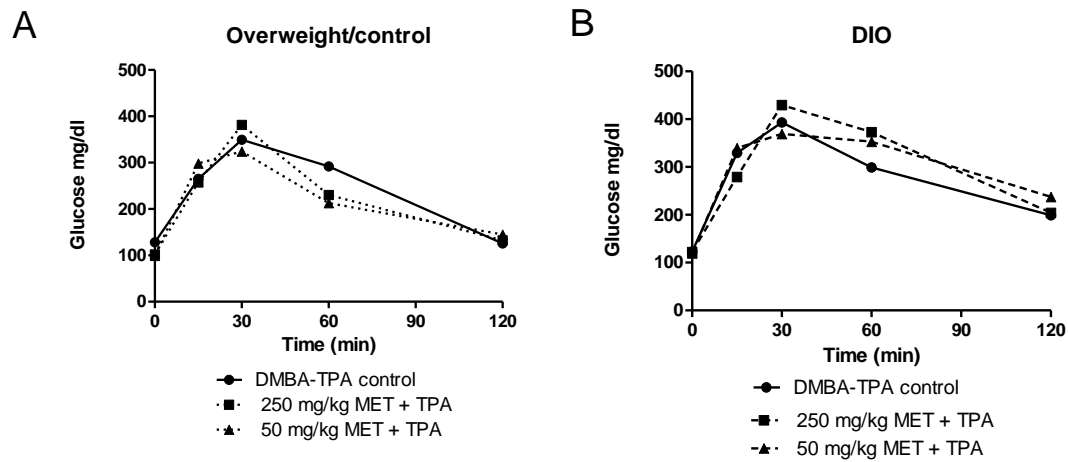


**Figure 5-13 Effect of metformin and diet on glucose tolerance.**

After 20 weeks of tumor promotion and metformin treatment during two-stage skin carcinogenesis experiments, GTTs were performed on a subset of mice from each diet/treatment group (n=10). **A)** Results from GTT performed on mice receiving the 10 kcal % fat, overweight/control diet in each treatment group (DMBA-TPA control, 250 mg/kg MET + TPA, and 50 mg/kg MET + TPA **B)** Results from GTT performed on mice receiving the 60 kcal % fat diet, DIO in each treatment group (DMBA-TPA control, 250 mg/kg MET + TPA, and 50 mg/kg MET + TPA)

## **Chapter 6-Summary, Significance and Future Studies**

### *Summary and Significance*

The prevalence of obesity has drastically increased in the US over the past 30 years and is associated with increases in various cancer risk as well as increased cancer mortality.

While DIO has consistently been shown to increase cancer risk, CR has been shown to be an effective intervention, inhibiting carcinogenesis and increasing lifespan in a variety of animal models. CR acts broadly and potently in chronic disease prevention and strengthens the notion that the identification, development and study of both natural and synthetic compounds mimicking the anticancer effects of CR should be explored. Initial studies in this project found mTORC1 inhibitor rapamycin to be a potent inhibitor of TPA-induced skin tumor promotion. To date, this data demonstrates on a molar basis, rapamycin to be one of the most highly potent inhibitors of skin tumor promotion by phorbol esters (114). In addition, this inhibition by rapamycin was associated with attenuation of mTORC1 and downstream signaling in keratinocytes and inhibition of TPA-induced epidermal hyperproliferation. Rapamycin also inhibited TPA-induced dermal inflammatory cell infiltration as well as reduced signaling through inflammatory pathways in the epidermis. The observed effects of rapamycin on these parameters are very similar to previous observed effects in CR mice during two-stage skin carcinogenesis studies providing support for rapamycin as CR mimetic agent. Furthermore, in the context of dietary energy balance, rapamycin counteracted the effects of overweight and obese states on skin tumor promotion and progression. Mice placed on either a 10 kcal % fat or 60 kcal % fat diet corresponding to overweight and obese phenotypes respectively, displayed highly significant reductions in tumor multiplicity and incidence. In this regard, tumor inhibition was slightly more effective in the obese mice. This project has provided new insights into the therapeutic and preventive potential of rapamycin for a range of weight phenotypes in environmentally induced skin cancer. In addition, these studies provide the first published

evidence for the importance of mTORC1 as a critical mediator of skin tumor promotion by TPA, independent of Akt.

mTORC1 activity can be regulated via Akt or AMPK signaling pathways, and energy balance has been shown to influence both pathways of activation. In addition to high serum levels of IGF-1 and insulin and subsequent increases in cellular signaling through their receptors to PI3K and Akt, obese states are also associated with elevations in amino acids, glucose and ATP levels. Flux in energy metabolism can lead to activation or repression of mTORC1 through the LKB1/AMPK pathway. Additional experiments in this project explored the anti-cancer effects of antidiabetic drug metformin in the context of dietary energy balance. Metformin's primary mechanism of action is through activation of AMPK. Two-stage skin carcinogenesis studies demonstrated that metformin, when administered via the drinking water, partially blocked skin tumor promotion in both overweight and obese mice, though it appeared to be more highly effective in the obese mice. Furthermore, this inhibition was associated with activation of epidermal AMPK and inhibition of mTORC1. Serum analyses also revealed metformin to decrease circulating levels of insulin and increase adiponectin in the obese mice suggesting a dual direct/indirect mechanism of cancer prevention in this model system. However, metformin had no effect on serum hormone levels in the overweight mice lending to a common hypothesis that metformin may be more effective in an obese or diabetic population. Metformin and other biguanides have tolerable associated risks and are already widely used in the treatment of type II diabetes. In these studies, we have provided for the first time, evidence that oral administration of metformin in the drinking water decreases tumor development in a chemically induced model of non-melanoma skin cancer. In addition, we have shown metformin to be slightly more effective in obese mice due to possible dual inhibitory effects of mTORC1 inhibition as well as reduced circulating insulin levels. There are very few studies in the literature to date that have evaluated host metabolic status as a variable to study the anticancer effects of

metformin. Data from this project will help fill a gap in knowledge regarding the effectiveness of metformin in a range of weight phenotypes. These data are highly relevant for future clinical trials as they help define target populations that will benefit most from metformin.

Growing evidence from CR studies throughout the last few decades suggests that the inhibitory effects of CR are multifaceted and clearly, one single pathway is not responsible for all the anticancer effects. In addition to the IGF-1/Akt/mTOR pathway, CR has been shown to effect components of adipokine signaling, inflammatory signaling as well as sirtuin signaling pathways (9). Hence, combination chemoprevention strategies that target multiple pathways are most likely to result in success at preventing cancer with increased efficacy. While there is promise of increased efficacy with dual inhibitor treatments, a risk of toxicity is also a concern as there is evidence of deregulation of carbohydrate metabolism when administering PI3K, Akt, or mTOR inhibitors resulting in hyperinsulinemia and hyperglycemia. Thus using metformin with inhibitors of the IR pathway may prevent dose limiting toxicities. The current study demonstrated that a combination treatment approach with a very low dose of topical rapamycin (2 nmol) and a low dose of metformin in the drinking water resulted in an additive effect that was more effective than either single compound alone at preventing the development of skin tumors. Current data in the literature have not explored the effects of combination treatments with rapamycin and metformin.

Overall, the current data support the hypothesis that elevation of mTORC1 and subsequent activation of downstream signaling pathways is a highly important event during skin tumor promotion and targeting this pathway alone or in combination may be an effective chemoprevention strategy. While this project demonstrates the effectiveness of the compounds in the context of overweight and obesity, mechanistic data obtained provides

strong implications for chemoprevention on a broader spectrum which includes a non-diabetic, normal weight population.

### *Ongoing and Future Studies*

Ongoing experiments in the lab are currently exploring the differential effects of an overweight versus obese phenotype on epidermal signaling through AMPK and mTORC1 and downstream substrates after treatment with inhibitor compounds. Completing these studies will help better elucidate the underlying mechanisms responsible for the increase in efficacy of these inhibitors in the obese mice. In addition, we are exploring activation of other substrates of AMPK in addition to mTORC1. Of particular interest, is AMPK's inhibition of *de novo* fatty acid synthesis and cholesterol synthesis. AMPK was initially identified as a kinase that inhibits acetyl CoA carboxylase through phosphorylation thus preventing the conversion of acetyl CoA to malonyl CoA subsequently inhibiting the synthesis of fatty acids. It also phosphorylates HMG-CoA to inhibit *de novo* cholesterol synthesis (147). These enzymes required for the synthesis of fatty acids and cholesterol are highly expressed in many types of cancer (148). In addition, metformin has also been shown *in vivo* to mediate some of its anticancer effects via activation of AMPK and subsequent inhibition of ACC (100) as well as through decreased expression of FASN (99). Because the effects of metformin in our model system on mTORC1 and p70S6K inhibition in the epidermis are somewhat modest, it is possible that metformin may be exerting its inhibitory effects via AMPK activation and inhibition of fatty acid synthesis or cholesterol synthesis.

In addition, interest lies in further clarifying the effects of rapamycin downstream of mTORC1 on the induction of autophagy in the epidermis. As presented in Chapter 5, preliminary data gathered have presented a potential mechanism by which rapamycin induces autophagy via mTORC1 inhibition. Future planned studies include

immunofluorescence (IF) and immunohistochemical (IHC) staining to identify the formation of LC3B puncta which are indicative of autophagosome formation, after rapamycin treatment. Skin tumor samples from previous two-stage studies in each treatment group will also be evaluated for expression of autophagic markers by western blot analysis as well as IF and IHC.

Future work beyond the scope of this research project would likely entail delving into pharmacokinetic/pharmacodynamic considerations of metformin use in cancer chemoprevention and treatment. Much of the current literature as well as data from this project suggest that some of the anticancer effects of metformin may be due to direct mechanisms on cancer cells whereby AMPK is activated and mTORC1 is inhibited leading to decreases in protein synthesis. Hence, there is a clear need for PK/PD studies to identify optimal doses of metformin to be administered as well as to identify which extrahepatic tissues will respond to treatment and to what extent. In order for metformin to be taken up by cells, the cells have to express organic cation transporter 1 or 2 (OCT 1) (OCT 2) (149). An interesting pharmacokinetics research question would be whether or not keratinocytes isolated from normal epithelial tissue, papillomas, or squamous cell carcinomas express transcripts for genes that encode organic cation transporter 1, 2, and 3. Experiments could be carried out to confirm expression of these genes at various doses of metformin administered via the drinking water to determine the potential for the accumulation of metformin. Experiments could also be done to evaluate whether dietary energy balance modulation has any effects on expression of these transporter genes. Completing these experiments could provide valuable information on the dose of metformin that will result in optimal response in our model system and provide further information about target populations for which metformin should be tested in the clinic. Additionally, pharmacodynamic experiments could be completed to evaluate the expression of metformin's primary target in cells, mitochondrial complex I as long as previous PK data

from metformin ensured metformin uptake is occurring in our target cells. This research plan would be novel, as few studies have specifically evaluated PK/PD. Understanding the pharmacokinetics behind metformin as well as other biguanides will provide valuable biologically based criteria for eligibility in clinical trials.



## References

1. Society, A. C. 2011. Cancer Facts and Figures, 2011. A. C. Society, editor, Atlanta.
2. Ogden, C. L., M. E. Carroll, B. K. Kit, and K. M. Flegal. 2012. Prevalence of obesity in the United States, 2009-2010. NCHS Data Brief:1-8.
3. White, P. B., E. M. True, K. M. Ziegler, S. S. Wang, D. A. Swartz-Basile, H. A. Pitt, and N. J. Zyromski. 2010. Insulin, leptin, and tumoral adipocytes promote murine pancreatic cancer growth. *J Gastrointest Surg* 14:1888-1893; discussion 1893-1884.
4. Yakar, S., N. P. Nunez, P. Pennisi, P. Brodt, H. Sun, L. Fallavollita, H. Zhao, L. Scavo, R. Novosyadlyy, N. Kurshan, B. Stannard, J. East-Palmer, N. C. Smith, S. N. Perkins, R. Fuchs-Young, J. C. Barrett, S. D. Hursting, and D. LeRoith. 2006. Increased tumor growth in mice with diet-induced obesity: impact of ovarian hormones. *Endocrinology* 147:5826-5834.
5. Hill-Baskin, A. E., M. M. Markiewski, D. A. Buchner, H. Shao, D. DeSantis, G. Hsiao, S. Subramaniam, N. A. Berger, C. Croniger, J. D. Lambris, and J. H. Nadeau. 2009. Diet-induced hepatocellular carcinoma in genetically predisposed mice. *Hum Mol Genet* 18:2975-2988.
6. Mai, V., L. H. Colbert, D. Berrigan, S. N. Perkins, R. Pfeiffer, J. A. Lavigne, E. Lanza, D. C. Haines, A. Schatzkin, and S. D. Hursting. 2003. Calorie restriction and diet composition modulate spontaneous intestinal tumorigenesis in *Apc(Min)* mice through different mechanisms. *Cancer Res* 63:1752-1755.
7. Birt, D. F., L. T. White, B. Choi, and J. C. Pelling. 1989. Dietary fat effects on the initiation and promotion of two-stage skin tumorigenesis in the SENCAR mouse. *Cancer Res* 49:4170-4174.

8. Hursting, S. D., J. A. Lavigne, D. Berrigan, S. N. Perkins, and J. C. Barrett. 2003. Calorie restriction, aging, and cancer prevention: mechanisms of action and applicability to humans. *Annu Rev Med* 54:131-152.
9. Hursting, S. D., S. M. Smith, L. M. Lashinger, A. E. Harvey, and S. N. Perkins. 2010. Calories and carcinogenesis: lessons learned from 30 years of calorie restriction research. *Carcinogenesis* 31:83-89.
10. Moore, T., L. A. Checkley, and J. DiGiovanni. 2011. Dietary energy balance modulation of epithelial carcinogenesis: a role for IGF-1 receptor signaling and crosstalk. *Ann N Y Acad Sci* 1229:7-17.
11. Calle, E. E., and R. Kaaks. 2004. Overweight, obesity and cancer: epidemiological evidence and proposed mechanisms. *Nat Rev Cancer* 4:579-591.
12. Saxena, N. K., L. Taliaferro-Smith, B. B. Knight, D. Merlin, F. A. Anania, R. M. O'Regan, and D. Sharma. 2008. Bidirectional crosstalk between leptin and insulin-like growth factor-I signaling promotes invasion and migration of breast cancer cells via transactivation of epidermal growth factor receptor. *Cancer Res* 68:9712-9722.
13. Lanzino, M., C. Morelli, C. Garofalo, M. L. Panno, L. Mauro, S. Ando, and D. Sisci. 2008. Interaction between estrogen receptor alpha and insulin/IGF signaling in breast cancer. *Curr Cancer Drug Targets* 8:597-610.
14. Macaulay, V. M., M. J. Everard, J. D. Teale, P. A. Trott, J. J. Van Wyk, I. E. Smith, and J. L. Millar. 1990. Autocrine function for insulin-like growth factor I in human small cell lung cancer cell lines and fresh tumor cells. *Cancer Res* 50:2511-2517.
15. Hay, N. 2005. The Akt-mTOR tango and its relevance to cancer. *Cancer Cell* 8:179-183.
16. Baserga, R., C. Sell, P. Porcu, and M. Rubini. 1994. The role of the IGF-I receptor in the growth and transformation of mammalian cells. *Cell Prolif* 27:63-71.

17. Lashinger, L. M., L. M. Malone, M. J. McArthur, J. A. Goldberg, E. A. Daniels, A. Pavone, J. K. Colby, N. C. Smith, S. N. Perkins, S. M. Fischer, and S. D. Hursting. 2011. Genetic reduction of insulin-like growth factor-1 mimics the anticancer effects of calorie restriction on cyclooxygenase-2-driven pancreatic neoplasia. *Cancer Prev Res (Phila)* 4:1030-1040.
18. Moore, T., S. Carbajal, L. Beltran, S. N. Perkins, S. Yakar, D. Leroith, S. D. Hursting, and J. Digiovanni. 2008. Reduced susceptibility to two-stage skin carcinogenesis in mice with low circulating insulin-like growth factor I levels. *Cancer Res* 68:3680-3688.
19. Garofalo, C., and E. Surmacz. 2006. Leptin and cancer. *J Cell Physiol* 207:12-22.
20. Woods, S. C., R. J. Seeley, D. Porte, Jr., and M. W. Schwartz. 1998. Signals that regulate food intake and energy homeostasis. *Science* 280:1378-1383.
21. Zhang, Y., M. Olbort, K. Schwarzer, B. Nusslein-Hildesheim, M. Nicolson, E. Murphy, T. J. Kowalski, I. Schmidt, and R. L. Leibel. 1997. The leptin receptor mediates apparent autocrine regulation of leptin gene expression. *Biochem Biophys Res Commun* 240:492-495.
22. Brennan, A. M., and C. S. Mantzoros. 2006. Drug Insight: the role of leptin in human physiology and pathophysiology--emerging clinical applications. *Nat Clin Pract Endocrinol Metab* 2:318-327.
23. Stattin, P., A. Lukanova, C. Biessy, S. Soderberg, R. Palmqvist, R. Kaaks, T. Olsson, and E. Jellum. 2004. Obesity and colon cancer: does leptin provide a link? *Int J Cancer* 109:149-152.
24. Chang, S., S. D. Hursting, J. H. Contois, S. S. Strom, Y. Yamamura, R. J. Babaian, P. Troncoso, P. S. Scardino, T. M. Wheeler, C. I. Amos, and M. R. Spitz. 2001. Leptin and prostate cancer. *Prostate* 46:62-67.

25. Ashizawa, N., T. Yahata, J. Quan, S. Adachi, K. Yoshihara, and K. Tanaka. 2010. Serum leptin-adiponectin ratio and endometrial cancer risk in postmenopausal female subjects. *Gynecol Oncol* 119:65-69.
26. Bouloumie, A., H. C. Drexler, M. Lafontan, and R. Busse. 1998. Leptin, the product of Ob gene, promotes angiogenesis. *Circ Res* 83:1059-1066.
27. Fenton, J. I., N. G. Hord, J. A. Lavigne, S. N. Perkins, and S. D. Hursting. 2005. Leptin, insulin-like growth factor-1, and insulin-like growth factor-2 are mitogens in ApcMin/+ but not Apc+/+ colonic epithelial cell lines. *Cancer Epidemiol Biomarkers Prev* 14:1646-1652.
28. Villanueva, E. C., and M. G. Myers, Jr. 2008. Leptin receptor signaling and the regulation of mammalian physiology. *Int J Obes (Lond)* 32 Suppl 7:S8-12.
29. Grossmann, M. E., A. Ray, S. Dogan, N. K. Mizuno, and M. P. Cleary. 2008. Balance of adiponectin and leptin modulates breast cancer cell growth. *Cell Res* 18:1154-1156.
30. Ray, A., K. J. Nkhata, and M. P. Cleary. 2007. Effects of leptin on human breast cancer cell lines in relationship to estrogen receptor and HER2 status. *Int J Oncol* 30:1499-1509.
31. Kelesidis, I., T. Kelesidis, and C. S. Mantzoros. 2006. Adiponectin and cancer: a systematic review. *Br J Cancer* 94:1221-1225.
32. Jung, C. H., E. J. Rhee, J. H. Choi, J. C. Bae, S. H. Yoo, W. J. Kim, C. Y. Park, J. O. Mok, C. H. Kim, W. Y. Lee, K. W. Oh, S. W. Park, and S. W. Kim. 2010. The relationship of adiponectin/leptin ratio with homeostasis model assessment insulin resistance index and metabolic syndrome in apparently healthy Korean male adults. *Korean Diabetes J* 34:237-243.

33. Otani, K., J. Kitayama, K. Yasuda, Y. Nio, M. Iwabuchi, S. Okudaira, J. Aoki, T. Yamauchi, T. Kadowaki, and H. Nagawa. 2010. Adiponectin suppresses tumorigenesis in Apc(Min)(/+) mice. *Cancer Lett* 288:177-182.
34. Birt, D. F., J. Przybylski, W. Wang, J. Stewart, and Y. Liu. 2004. Identification of molecular targets for dietary energy restriction prevention of skin carcinogenesis: an idea cultivated by Edward Bresnick. *J Cell Biochem* 91:258-264.
35. Jiang, W., Z. Zhu, N. Bhatia, R. Agarwal, and H. J. Thompson. 2002. Mechanisms of energy restriction: effects of corticosterone on cell growth, cell cycle machinery, and apoptosis. *Cancer Res* 62:5280-5287.
36. Pashko, L. L., and A. G. Schwartz. 1992. Reversal of food restriction-induced inhibition of mouse skin tumor promotion by adrenalectomy. *Carcinogenesis* 13:1925-1928.
37. Zhu, Z., W. Jiang, and H. J. Thompson. 2003. Mechanisms by which energy restriction inhibits rat mammary carcinogenesis: in vivo effects of corticosterone on cell cycle machinery in mammary carcinomas. *Carcinogenesis* 24:1225-1231.
38. Coussens, L. M., and Z. Werb. 2002. Inflammation and cancer. *Nature* 420:860-867.
39. Shoelson, S. E., L. Herrero, and A. Naaz. 2007. Obesity, inflammation, and insulin resistance. *Gastroenterology* 132:2169-2180.
40. Park, E. J., J. H. Lee, G. Y. Yu, G. He, S. R. Ali, R. G. Holzer, C. H. Osterreicher, H. Takahashi, and M. Karin. 2010. Dietary and genetic obesity promote liver inflammation and tumorigenesis by enhancing IL-6 and TNF expression. *Cell* 140:197-208.
41. Luo, Z., A. K. Saha, X. Xiang, and N. B. Ruderman. 2005. AMPK, the metabolic syndrome and cancer. *Trends Pharmacol Sci* 26:69-76.
42. Fulco, M., and V. Sartorelli. 2008. Comparing and contrasting the roles of AMPK and SIRT1 in metabolic tissues. *Cell Cycle* 7:3669-3679.

43. Moore, T., L. Beltran, S. Carbajal, S. Strom, J. Traag, S. D. Hursting, and J. DiGiovanni. 2008. Dietary energy balance modulates signaling through the Akt/mammalian target of rapamycin pathways in multiple epithelial tissues. *Cancer Prev Res (Phila)* 1:65-76.
44. Dogan, S., A. C. Johannsen, J. P. Grande, and M. P. Cleary. 2011. Effects of intermittent and chronic calorie restriction on mammalian target of rapamycin (mTOR) and IGF-I signaling pathways in mammary fat pad tissues and mammary tumors. *Nutr Cancer* 63:389-401.
45. Nunez, N. P., W. J. Oh, J. Rozenberg, C. Perella, M. Anver, J. C. Barrett, S. N. Perkins, D. Berrigan, J. Moitra, L. Varticovski, S. D. Hursting, and C. Vinson. 2006. Accelerated tumor formation in a fatless mouse with type 2 diabetes and inflammation. *Cancer Res* 66:5469-5476.
46. Taniguchi, C. M., B. Emanuelli, and C. R. Kahn. 2006. Critical nodes in signalling pathways: insights into insulin action. *Nat Rev Mol Cell Biol* 7:85-96.
47. Siddle, K. 2011. Signalling by insulin and IGF receptors: supporting acts and new players. *J Mol Endocrinol* 47:R1-10.
48. Shaw, R. J., and L. C. Cantley. 2006. Ras, PI(3)K and mTOR signalling controls tumour cell growth. *Nature* 441:424-430.
49. Vivanco, I., and C. L. Sawyers. 2002. The phosphatidylinositol 3-Kinase AKT pathway in human cancer. *Nat Rev Cancer* 2:489-501.
50. Manning, B. D., and L. C. Cantley. 2007. AKT/PKB signaling: navigating downstream. *Cell* 129:1261-1274.
51. Jacinto, E. 2008. What controls TOR? *IUBMB Life* 60:483-496.
52. Wang, X., and C. G. Proud. 2011. mTORC1 signaling: what we still don't know. *J Mol Cell Biol* 3:206-220.

53. Itamochi, H. 2010. Targeted therapies in epithelial ovarian cancer: Molecular mechanisms of action. *World J Biol Chem* 1:209-220.
54. Dowling, R. J., I. Topisirovic, T. Alain, M. Bidinosti, B. D. Fonseca, E. Petroulakis, X. Wang, O. Larsson, A. Selvaraj, Y. Liu, S. C. Kozma, G. Thomas, and N. Sonenberg. 2010. mTORC1-mediated cell proliferation, but not cell growth, controlled by the 4E-BPs. *Science* 328:1172-1176.
55. Lankat-Buttgereit, B., and R. Goke. 2003. Programmed cell death protein 4 (pdc4): a novel target for antineoplastic therapy? *Biol Cell* 95:515-519.
56. Schmid, T., A. P. Jansen, A. R. Baker, G. Hegamyer, J. P. Hagan, and N. H. Colburn. 2008. Translation inhibitor Pdc4 is targeted for degradation during tumor promotion. *Cancer Res* 68:1254-1260.
57. Cuervo, A. M. 2008. Autophagy and aging: keeping that old broom working. *Trends Genet* 24:604-612.
58. Rosenfeldt, M. T., and K. M. Ryan. 2011. The multiple roles of autophagy in cancer. *Carcinogenesis* 32:955-963.
59. Chen, H. Y., and E. White. 2011. Role of autophagy in cancer prevention. *Cancer Prev Res (Phila)* 4:973-983.
60. Steeves, M. A., F. C. Dorsey, and J. L. Cleveland. 2010. Targeting the autophagy pathway for cancer chemoprevention. *Curr Opin Cell Biol* 22:218-225.
61. Hosokawa, N., T. Hara, T. Kaizuka, C. Kishi, A. Takamura, Y. Miura, S. Iemura, T. Natsume, K. Takehana, N. Yamada, J. L. Guan, N. Oshiro, and N. Mizushima. 2009. Nutrient-dependent mTORC1 association with the ULK1-Atg13-FIP200 complex required for autophagy. *Mol Biol Cell* 20:1981-1991.
62. Chan, E. Y. 2009. mTORC1 phosphorylates the ULK1-mAtg13-FIP200 autophagy regulatory complex. *Sci Signal* 2:pe51.

63. Kim, J., M. Kundu, B. Viollet, and K. L. Guan. 2011. AMPK and mTOR regulate autophagy through direct phosphorylation of Ulk1. *Nat Cell Biol* 13:132-141.
64. Vogt, A., R. L. Rice, C. E. Settineri, F. Yokokawa, S. Yokokawa, P. Wipf, and J. S. Lazo. 1998. Disruption of insulin-like growth factor-1 signaling and down-regulation of cdc2 by SC-alphaalphadelta9, a novel small molecule antisiRNA agent identified in a targeted array library. *J Pharmacol Exp Ther* 287:806-813.
65. Scotlandi, K., C. Maini, M. C. Manara, S. Benini, M. Serra, V. Cerisano, R. Strammiello, N. Baldini, P. L. Lollini, P. Nanni, G. Nicoletti, and P. Picci. 2002. Effectiveness of insulin-like growth factor I receptor antisense strategy against Ewing's sarcoma cells. *Cancer Gene Ther* 9:296-307.
66. Granerus, M., and W. Engstrom. 2001. Effects of insulin-like growth factor-binding protein 2 and an IGF-type I receptor-blocking antibody on apoptosis in human teratocarcinoma cells in vitro. *Cell Biol Int* 25:825-828.
67. Decensi, A., H. Johansson, R. Miceli, L. Mariani, T. Camerini, E. Cavadini, M. G. Di Mauro, A. Barreca, A. G. Gonzaga, S. Diani, M. T. Sandri, G. De Palo, and F. Formelli. 2001. Long-term effects of fenretinide, a retinoic acid derivative, on the insulin-like growth factor system in women with early breast cancer. *Cancer Epidemiol Biomarkers Prev* 10:1047-1053.
68. Zujewski, J. 2002. Selective estrogen receptor modulators (SERMs) and retinoids in breast cancer chemoprevention. *Environ Mol Mutagen* 39:264-270.
69. Shojamanesh, H., F. Gibril, A. Louie, J. V. Ojeaburu, S. Bashir, A. Abou-Saif, and R. T. Jensen. 2002. Prospective study of the antitumor efficacy of long-term octreotide treatment in patients with progressive metastatic gastrinoma. *Cancer* 94:331-343.
70. Guertin, D. A., and D. M. Sabatini. 2007. Defining the role of mTOR in cancer. *Cancer Cell* 12:9-22.



71. Crowell, J. A., V. E. Steele, and J. R. Fay. 2007. Targeting the AKT protein kinase for cancer chemoprevention. *Mol Cancer Ther* 6:2139-2148.
72. Anisimov, V. N., M. A. Zabezhinski, I. G. Popovich, T. S. Piskunova, A. V. Semenchenko, M. L. Tyndyk, M. N. Yurova, M. P. Antoch, and M. V. Blagosklonny. 2010. Rapamycin extends maximal lifespan in cancer-prone mice. *Am J Pathol* 176:2092-2097.
73. Kim, W. S., L. Xu, D. Souw, A. Fang, and A. L. Demain. 2002. An unexpected inhibitory effect of rapamycin against germination of spores of *Bacillus brevis* strain Nagano. *J Antibiot (Tokyo)* 55:650-654.
74. Chen, H., S. Sehgal, P. Daloze, and J. Wu. 1995. Pretreatment of donors and grafts with rapamycin: the effect on graft survival and the tissue drug retention. *Clin Immunol Immunopathol* 76:321-323.
75. Choi, J., J. Chen, S. L. Schreiber, and J. Clardy. 1996. Structure of the FKBP12-rapamycin complex interacting with the binding domain of human FRAP. *Science* 273:239-242.
76. Sarbassov, D. D., S. M. Ali, S. Sengupta, J. H. Sheen, P. P. Hsu, A. F. Bagley, A. L. Markhard, and D. M. Sabatini. 2006. Prolonged rapamycin treatment inhibits mTORC2 assembly and Akt/PKB. *Mol Cell* 22:159-168.
77. Namba, R., L. J. Young, C. K. Abbey, L. Kim, P. Damonte, A. D. Borowsky, J. Qi, C. G. Tepper, C. L. MacLeod, R. D. Cardiff, and J. P. Gregg. 2006. Rapamycin inhibits growth of premalignant and malignant mammary lesions in a mouse model of ductal carcinoma in situ. *Clin Cancer Res* 12:2613-2621.
78. Wang, Z., J. Zhou, J. Fan, S. J. Qiu, Y. Yu, X. W. Huang, and Z. Y. Tang. 2008. Effect of rapamycin alone and in combination with sorafenib in an orthotopic model of human hepatocellular carcinoma. *Clin Cancer Res* 14:5124-5130.

79. de Gruijl, F. R., G. E. Koehl, P. Voskamp, A. Strik, H. G. Rebel, A. Gaumann, J. W. de Fijter, C. P. Tensen, J. N. Bavinck, and E. K. Geissler. 2010. Early and late effects of the immunosuppressants rapamycin and mycophenolate mofetil on UV carcinogenesis. *Int J Cancer* 127:796-804.
80. Amornphimoltham, P., K. Leelahavanichkul, A. Molinolo, V. Patel, and J. S. Gutkind. 2008. Inhibition of Mammalian target of rapamycin by rapamycin causes the regression of carcinogen-induced skin tumor lesions. *Clin Cancer Res* 14:8094-8101.
81. Granville, C. A., N. Warfel, J. Tsurutani, M. C. Hollander, M. Robertson, S. D. Fox, T. D. Veenstra, H. J. Issaq, R. I. Linnoila, and P. A. Dennis. 2007. Identification of a highly effective rapamycin schedule that markedly reduces the size, multiplicity, and phenotypic progression of tobacco carcinogen-induced murine lung tumors. *Clin Cancer Res* 13:2281-2289.
82. Yan, Y., Y. Wang, Q. Tan, Y. Hara, T. K. Yun, R. A. Lubet, and M. You. 2006. Efficacy of polyphenon E, red ginseng, and rapamycin on benzo(a)pyrene-induced lung tumorigenesis in A/J mice. *Neoplasia* 8:52-58.
83. Raimondi, A. R., A. Molinolo, and J. S. Gutkind. 2009. Rapamycin prevents early onset of tumorigenesis in an oral-specific K-ras and p53 two-hit carcinogenesis model. *Cancer Res* 69:4159-4166.
84. Liu, M., A. Howes, J. Lesperance, W. B. Stallcup, C. A. Hauser, K. Kadoya, R. G. Oshima, and R. T. Abraham. 2005. Antitumor activity of rapamycin in a transgenic mouse model of ErbB2-dependent human breast cancer. *Cancer Res* 65:5325-5336.
85. Dowling, R. J., P. J. Goodwin, and V. Stambolic. 2011. Understanding the benefit of metformin use in cancer treatment. *BMC Med* 9:33.

86. Owen, M. R., E. Doran, and A. P. Halestrap. 2000. Evidence that metformin exerts its anti-diabetic effects through inhibition of complex 1 of the mitochondrial respiratory chain. *Biochem J* 348 Pt 3:607-614.
87. van Veelen, W., S. E. Korsse, L. van de Laar, and M. P. Peppelenbosch. 2011. The long and winding road to rational treatment of cancer associated with LKB1/AMPK/TSC/mTORC1 signaling. *Oncogene* 30:2289-2303.
88. Jalving, M., J. A. Gietema, J. D. Lefrandt, S. de Jong, A. K. Reyners, R. O. Gans, and E. G. de Vries. 2010. Metformin: taking away the candy for cancer? *Eur J Cancer* 46:2369-2380.
89. Evans, J. M., L. A. Donnelly, A. M. Emslie-Smith, D. R. Alessi, and A. D. Morris. 2005. Metformin and reduced risk of cancer in diabetic patients. *BMJ* 330:1304-1305.
90. Decensi, A., M. Puntoni, P. Goodwin, M. Cazzaniga, A. Gennari, B. Bonanni, and S. Gandini. 2010. Metformin and cancer risk in diabetic patients: a systematic review and meta-analysis. *Cancer Prev Res (Phila)* 3:1451-1461.
91. Lee, J. H., T. I. Kim, S. M. Jeon, S. P. Hong, J. H. Cheon, and W. H. Kim. 2012. The effects of metformin on the survival of colorectal cancer patients with diabetes mellitus. *Int J Cancer* 131:752-759.
92. Sadeghi, N., J. L. Abbruzzese, S. C. Yeung, M. Hassan, and D. Li. 2012. Metformin use is associated with better survival of diabetic patients with pancreatic cancer. *Clin Cancer Res* 18:2905-2912.
93. Jiralerspong, S., S. L. Palla, S. H. Giordano, F. Meric-Bernstam, C. Liedtke, C. M. Barnett, L. Hsu, M. C. Hung, G. N. Hortobagyi, and A. M. Gonzalez-Angulo. 2009. Metformin and pathologic complete responses to neoadjuvant chemotherapy in diabetic patients with breast cancer. *J Clin Oncol* 27:3297-3302.

94. Rattan, R., S. Giri, L. C. Hartmann, and V. Shridhar. 2011. Metformin attenuates ovarian cancer cell growth in an AMP-kinase dispensable manner. *J Cell Mol Med* 15:166-178.
95. Zakikhani, M., R. Dowling, I. G. Fantus, N. Sonenberg, and M. Pollak. 2006. Metformin is an AMP kinase-dependent growth inhibitor for breast cancer cells. *Cancer Res* 66:10269-10273.
96. Memmott, R. M., J. R. Mercado, C. R. Maier, S. Kawabata, S. D. Fox, and P. A. Dennis. 2010. Metformin prevents tobacco carcinogen--induced lung tumorigenesis. *Cancer Prev Res (Phila)* 3:1066-1076.
97. Anisimov, V. N., L. M. Berstein, P. A. Egormin, T. S. Piskunova, I. G. Popovich, M. A. Zabezhinski, I. G. Kovalenko, T. E. Poroshina, A. V. Semenchenko, M. Provinciali, F. Re, and C. Franceschi. 2005. Effect of metformin on life span and on the development of spontaneous mammary tumors in HER-2/neu transgenic mice. *Exp Gerontol* 40:685-693.
98. Tomimoto, A., H. Endo, M. Sugiyama, T. Fujisawa, K. Hosono, H. Takahashi, N. Nakajima, Y. Nagashima, K. Wada, H. Nakagama, and A. Nakajima. 2008. Metformin suppresses intestinal polyp growth in ApcMin/+ mice. *Cancer Sci* 99:2136-2141.
99. Algire, C., L. Amrein, M. Zakikhani, L. Panasci, and M. Pollak. 2010. Metformin blocks the stimulative effect of a high-energy diet on colon carcinoma growth in vivo and is associated with reduced expression of fatty acid synthase. *Endocr Relat Cancer* 17:351-360.
100. Algire, C., M. Zakikhani, M. J. Blouin, J. H. Shuai, and M. Pollak. 2008. Metformin attenuates the stimulatory effect of a high-energy diet on in vivo LLC1 carcinoma growth. *Endocr Relat Cancer* 15:833-839.

101. Abel, E. L., J. M. Angel, K. Kiguchi, and J. DiGiovanni. 2009. Multi-stage chemical carcinogenesis in mouse skin: fundamentals and applications. *Nat Protoc* 4:1350-1362.
102. Morris, R. J. 2004. A perspective on keratinocyte stem cells as targets for skin carcinogenesis. *Differentiation* 72:381-386.
103. Kangsamaksin, T., H. J. Park, C. S. Trempus, and R. J. Morris. 2007. A perspective on murine keratinocyte stem cells as targets of chemically induced skin cancer. *Mol Carcinog* 46:579-584.
104. Karen, J., Y. Wang, A. Javaherian, M. Vaccariello, N. E. Fusenig, and J. A. Garlick. 1999. 12-O-tetradecanoylphorbol-13-acetate induces clonal expansion of potentially malignant keratinocytes in a tissue model of early neoplastic progression. *Cancer Res* 59:474-481.
105. Yuspa, S. H., T. Ben, H. Hennings, and U. Lichti. 1982. Divergent responses in epidermal basal cells exposed to the tumor promoter 12-O-tetradecanoylphorbol-13-acetate. *Cancer Res* 42:2344-2349.
106. Lu, J., O. Rho, E. Wilker, L. Beltran, and J. Digiovanni. 2007. Activation of epidermal akt by diverse mouse skin tumor promoters. *Mol Cancer Res* 5:1342-1352.
107. Benjamin, C. L., and H. N. Ananthaswamy. 2007. p53 and the pathogenesis of skin cancer. *Toxicol Appl Pharmacol* 224:241-248.
108. Bos, J. L. 1989. ras oncogenes in human cancer: a review. *Cancer Res* 49:4682-4689.
109. Hennings, H., E. F. Spangler, R. Shores, P. Mitchell, D. Devor, A. K. Shamsuddin, K. M. Elgjo, and S. H. Yuspa. 1986. Malignant conversion and metastasis of mouse skin tumors: a comparison of SENCAR and CD-1 mice. *Environ Health Perspect* 68:69-74.

110. Wilker, E., J. Lu, O. Rho, S. Carbajal, L. Beltran, and J. DiGiovanni. 2005. Role of PI3K/Akt signaling in insulin-like growth factor-1 (IGF-1) skin tumor promotion. *Mol Carcinog* 44:137-145.
111. DiGiovanni, J., D. K. Bol, E. Wilker, L. Beltran, S. Carbajal, S. Moats, A. Ramirez, J. Jorcano, and K. Kiguchi. 2000. Constitutive expression of insulin-like growth factor-1 in epidermal basal cells of transgenic mice leads to spontaneous tumor promotion. *Cancer Res* 60:1561-1570.
112. Segrelles, C., S. Ruiz, P. Perez, C. Murga, M. Santos, I. V. Budunova, J. Martinez, F. Larcher, T. J. Slaga, J. S. Gutkind, J. L. Jorcano, and J. M. Paramio. 2002. Functional roles of Akt signaling in mouse skin tumorigenesis. *Oncogene* 21:53-64.
113. Segrelles, C., J. Lu, B. Hammann, M. Santos, M. Moral, J. L. Cascallana, M. F. Lara, O. Rho, S. Carbajal, J. Traag, L. Beltran, A. B. Martinez-Cruz, R. Garcia-Escudero, C. Lorz, S. Ruiz, A. Bravo, J. M. Paramio, and J. DiGiovanni. 2007. Deregulated activity of Akt in epithelial basal cells induces spontaneous tumors and heightened sensitivity to skin carcinogenesis. *Cancer Res* 67:10879-10888.
114. Checkley, L. A., O. Rho, T. Moore, S. Hursting, and J. DiGiovanni. 2011. Rapamycin is a potent inhibitor of skin tumor promotion by 12-O-tetradecanoylphorbol-13-acetate. *Cancer Prev Res (Phila)* 4:1011-1020.
115. Bol, D. K., K. Kiguchi, I. Gimenez-Conti, T. Rupp, and J. DiGiovanni. 1997. Overexpression of insulin-like growth factor-1 induces hyperplasia, dermal abnormalities, and spontaneous tumor formation in transgenic mice. *Oncogene* 14:1725-1734.
116. Matsumoto, T., J. Jiang, K. Kiguchi, L. Ruffino, S. Carbajal, L. Beltran, D. K. Bol, M. P. Rosenberg, and J. DiGiovanni. 2003. Targeted expression of c-Src in epidermal basal cells leads to enhanced skin tumor promotion, malignant progression, and metastasis. *Cancer Res* 63:4819-4828.

117. Nunez, N. P., C. L. Carpenter, S. N. Perkins, D. Berrigan, S. V. Jaque, S. A. Ingles, L. Bernstein, M. R. Forman, J. C. Barrett, and S. D. Hursting. 2007. Extreme obesity reduces bone mineral density: complementary evidence from mice and women. *Obesity (Silver Spring)* 15:1980-1987.
118. Wilker, E., D. Bol, K. Kiguchi, T. Rupp, L. Beltran, and J. DiGiovanni. 1999. Enhancement of susceptibility to diverse skin tumor promoters by activation of the insulin-like growth factor-1 receptor in the epidermis of transgenic mice. *Mol Carcinog* 25:122-131.
119. Lu, Z. H., M. B. Shvartsman, A. Y. Lee, J. M. Shao, M. M. Murray, R. D. Kladney, D. Fan, S. Krajewski, G. G. Chiang, G. B. Mills, and J. M. Arbeit. 2010. Mammalian target of rapamycin activator RHEB is frequently overexpressed in human carcinomas and is critical and sufficient for skin epithelial carcinogenesis. *Cancer Res* 70:3287-3298.
120. Pollak, M. 2012. The insulin and insulin-like growth factor receptor family in neoplasia: an update. *Nat Rev Cancer* 12:159-169.
121. O'Reilly, K. E., F. Rojo, Q. B. She, D. Solit, G. B. Mills, D. Smith, H. Lane, F. Hofmann, D. J. Hicklin, D. L. Ludwig, J. Baselga, and N. Rosen. 2006. mTOR inhibition induces upstream receptor tyrosine kinase signaling and activates Akt. *Cancer Res* 66:1500-1508.
122. Ben Sahra, I., K. Laurent, A. Loubat, S. Giorgetti-Peraldi, P. Colosetti, P. Auberger, J. F. Tanti, Y. Le Marchand-Brustel, and F. Bost. 2008. The antidiabetic drug metformin exerts an antitumoral effect in vitro and in vivo through a decrease of cyclin D1 level. *Oncogene* 27:3576-3586.
123. Schneider, M. B., H. Matsuzaki, J. Haorah, A. Ulrich, J. Standop, X. Z. Ding, T. E. Adrian, and P. M. Pour. 2001. Prevention of pancreatic cancer induction in hamsters by metformin. *Gastroenterology* 120:1263-1270.

124. Phoenix, K. N., F. Vumbaca, and K. P. Claffey. 2009. Therapeutic metformin/AMPK activation promotes the angiogenic phenotype in the ERalpha negative MDA-MB-435 breast cancer model. *Breast Cancer Res Treat* 113:101-111.
125. Ben Sahra, I., Y. Le Marchand-Brustel, J. F. Tanti, and F. Bost. 2010. Metformin in cancer therapy: a new perspective for an old antidiabetic drug? *Mol Cancer Ther* 9:1092-1099.
126. DiGiovanni, J. 1992. Multistage carcinogenesis in mouse skin. *Pharmacol Ther* 54:63-128.
127. Rundhaug, J. E., I. Gimenez-Conti, M. C. Stern, I. V. Budunova, K. Kiguchi, D. K. Bol, L. G. Coghlan, C. J. Conti, J. DiGiovanni, S. M. Fischer, L. D. Winberg, and T. J. Slaga. 1997. Changes in protein expression during multistage mouse skin carcinogenesis. *Mol Carcinog* 20:125-136.
128. Wu, A. W., J. Gu, J. F. Ji, Z. F. Li, and G. W. Xu. 2003. Role of COX-2 in carcinogenesis of colorectal cancer and its relationship with tumor biological characteristics and patients' prognosis. *World J Gastroenterol* 9:1990-1994.
129. Prescott, S. M. 2000. Is cyclooxygenase-2 the alpha and the omega in cancer? *The Journal of clinical investigation* 105:1511-1513.
130. Chun, K. S., Y. S. Keum, S. S. Han, Y. S. Song, S. H. Kim, and Y. J. Surh. 2003. Curcumin inhibits phorbol ester-induced expression of cyclooxygenase-2 in mouse skin through suppression of extracellular signal-regulated kinase activity and NF-kappaB activation. *Carcinogenesis* 24:1515-1524.
131. Karin, M. 2006. Nuclear factor-kappaB in cancer development and progression. *Nature* 441:431-436.
132. Schulze-Osthoff, K., D. Ferrari, K. Riehemann, and S. Wesselborg. 1997. Regulation of NF-kappa B activation by MAP kinase cascades. *Immunobiology* 198:35-49.



133. Feldman, M. E., B. Apsel, A. Uotila, R. Loewith, Z. A. Knight, D. Ruggero, and K. M. Shokat. 2009. Active-site inhibitors of mTOR target rapamycin-resistant outputs of mTORC1 and mTORC2. *PLoS Biol* 7:e38.
134. McMahon, L. P., K. M. Choi, T. A. Lin, R. T. Abraham, and J. C. Lawrence, Jr. 2002. The rapamycin-binding domain governs substrate selectivity by the mammalian target of rapamycin. *Mol Cell Biol* 22:7428-7438.
135. Gingras, A. C., S. P. Gygi, B. Raught, R. D. Polakiewicz, R. T. Abraham, M. F. Hoekstra, R. Aebersold, and N. Sonenberg. 1999. Regulation of 4E-BP1 phosphorylation: a novel two-step mechanism. *Genes Dev* 13:1422-1437.
136. Pattingre, S., L. Espert, M. Biard-Piechaczyk, and P. Codogno. 2008. Regulation of macroautophagy by mTOR and Beclin 1 complexes. *Biochimie* 90:313-323.
137. Jiang, H., D. Cheng, W. Liu, J. Peng, and J. Feng. 2010. Protein kinase C inhibits autophagy and phosphorylates LC3. *Biochem Biophys Res Commun* 395:471-476.
138. Dunlop, E. A., D. K. Hunt, H. A. Acosta-Jaquez, D. C. Fingar, and A. R. Tee. 2011. ULK1 inhibits mTORC1 signaling, promotes multisite Raptor phosphorylation and hinders substrate binding. *Autophagy* 7:737-747.
139. Algire, C., O. Moiseeva, X. Deschenes-Simard, L. Amrein, L. Petrucci, E. Birman, B. Viollet, G. Ferbeyre, and M. N. Pollak. 2012. Metformin reduces endogenous reactive oxygen species and associated DNA damage. *Cancer Prev Res (Phila)* 5:536-543.
140. Buzzai, M., R. G. Jones, R. K. Amaravadi, J. J. Lum, R. J. DeBerardinis, F. Zhao, B. Viollet, and C. B. Thompson. 2007. Systemic treatment with the antidiabetic drug metformin selectively impairs p53-deficient tumor cell growth. *Cancer Res* 67:6745-6752.
141. Wang, W., and K. L. Guan. 2009. AMP-activated protein kinase and cancer. *Acta Physiol (Oxf)* 196:55-63.

142. Zhou, G., R. Myers, Y. Li, Y. Chen, X. Shen, J. Fenyk-Melody, M. Wu, J. Ventre, T. Doebber, N. Fujii, N. Musi, M. F. Hirshman, L. J. Goodyear, and D. E. Moller. 2001. Role of AMP-activated protein kinase in mechanism of metformin action. *The Journal of clinical investigation* 108:1167-1174.
143. Menendez, J. A., and R. Lupu. 2007. Fatty acid synthase and the lipogenic phenotype in cancer pathogenesis. *Nat Rev Cancer* 7:763-777.
144. Kalender, A., A. Selvaraj, S. Y. Kim, P. Gulati, S. Brule, B. Viollet, B. E. Kemp, N. Bardeesy, P. Dennis, J. J. Schlager, A. Marette, S. C. Kozma, and G. Thomas. 2010. Metformin, independent of AMPK, inhibits mTORC1 in a rag GTPase-dependent manner. *Cell Metab* 11:390-401.
145. Ben Sahra, I., C. Regazzetti, G. Robert, K. Laurent, Y. Le Marchand-Brustel, P. Auberger, J. F. Tanti, S. Giorgetti-Peraldi, and F. Bost. 2011. Metformin, independent of AMPK, induces mTOR inhibition and cell-cycle arrest through REDD1. *Cancer Res* 71:4366-4372.
146. Foretz, M., S. Hebrard, J. Leclerc, E. Zarrinpashneh, M. Soty, G. Mithieux, K. Sakamoto, F. Andreelli, and B. Viollet. 2010. Metformin inhibits hepatic gluconeogenesis in mice independently of the LKB1/AMPK pathway via a decrease in hepatic energy state. *The Journal of clinical investigation* 120:2355-2369.
147. Luo, Z., M. Zang, and W. Guo. 2010. AMPK as a metabolic tumor suppressor: control of metabolism and cell growth. *Future Oncol* 6:457-470.
148. Kuhajda, F. P. 2000. Fatty-acid synthase and human cancer: new perspectives on its role in tumor biology. *Nutrition* 16:202-208.
149. Reitman, M. L., and E. E. Schadt. 2007. Pharmacogenetics of metformin response: a step in the path toward personalized medicine. *The Journal of clinical investigation* 117:1226-1229.

## Vita

Laura Allyson Checkley was born on September 8, 1984 in Shreveport, LA to Dave and Charmaine Sandifer. After graduating from Airline High School in Bossier City, LA in 2003, she earned her Bachelor of Science degree in Biology from Centenary College of Louisiana in May of 2007. During her time at Centenary College, she worked as a student researcher at Louisiana State University Health Science Center Shreveport in the Dept. of Cellular and Molecular Physiology under the mentorship of Dr. Chantal Rivera. During this time, she investigated the inflammatory state that accompanies chronic obesity and assisted in characterizing the inflammatory phenotypes associated with the microvasculature of adipose tissue. After graduating from Centenary College, she entered the University of Texas Health Science Center at Houston Graduate School of Biomedical Sciences in August of 2007. Allyson promptly affiliated with the Molecular Carcinogenesis program at the MD Anderson Cancer Center Science Park in Smithville, TX. She completed tutorial rotations under Drs. John DiGiovanni, Robin Fuchs-Young, and Marcelo Aldaz before joining Dr. DiGiovanni's lab in Summer of 2008 to carry out her dissertation research. Allyson's work thus far targeting the mTORC1 pathway in murine two-stage skin carcinogenesis for cancer prevention has led to first authorship of the following publication: Checkley, L. A., O. Rho, T. Moore, S. Hursting, and J. DiGiovanni. 2011. Rapamycin is a potent inhibitor of skin tumor promotion by 12-O-tetradecanoylphorbol-13-acetate. *Cancer prevention research* 4:1011-1020.